'EMERGING THEMES IN FUNDAMENTAL AND APPLIED SCIENCES'

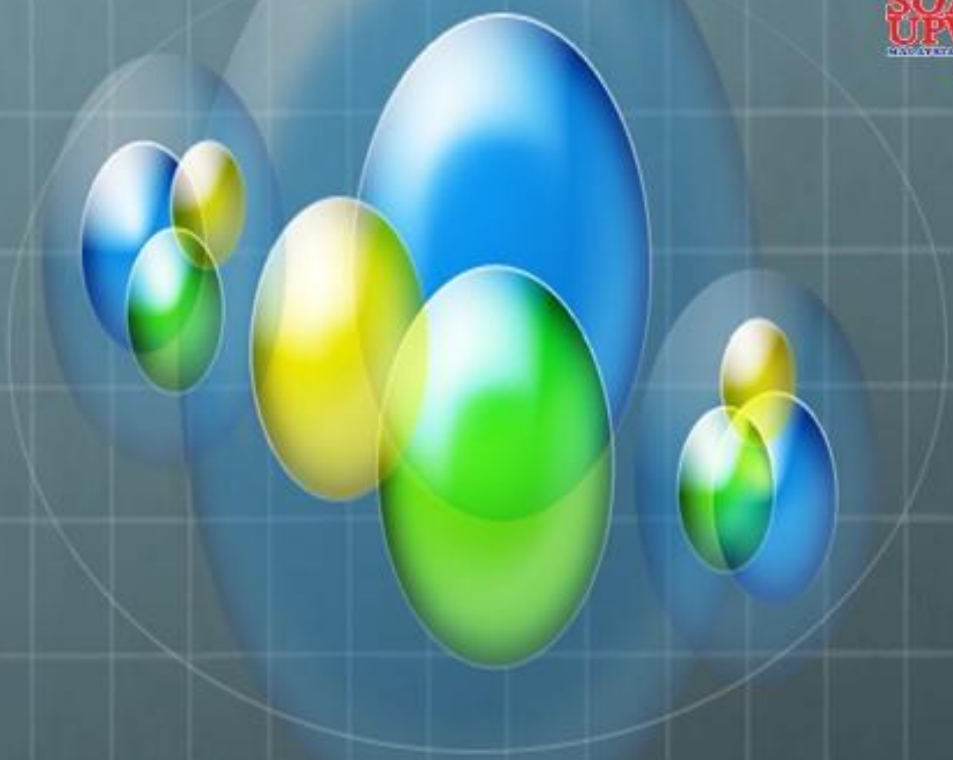

# MATHEMATICS

## VOLUME 1

EDITOR

ATHIRAH NAWAWI

Universiti Putra Malaysia Press
Serdang • 2018

First Print 2018



UPM Press is a member of the Malaysian Book Publishers Association (MABOPA) Membership No.: 9802 and a member of Majlis Penerbitan Ilmiah Malaysia (MAPIM)

Perpustakaan Negara Malaysia Cataloguing-in-Publication Data

'EMERGING THEMES IN FUNDAMENTAL AND APPLIED SCIENCES' :
MATHEMATICS. VOLUME 1 / EDITOR: ATHIRAH NAWAWI.
Mode of access: Internet
eISBN 978-967-344-889-0
1. Mathematics--Research.
2. Education, Higher--Research.
3. Government publications--Malaysia.
4. Electronic books.
I. Athirah Nawawi.
519.072

URL: http://science.upm.edu.my/ebook-3213

E-mail: penerbit@upm.edu.my
Web: www.penerbit.upm.edu.my

# EMERGING THEMES IN FUNDAMENTAL AND APPLIED SCIENCES

**Edited by**

**Athirah Nawawi**

**Faculty of Science**
**Universiti Putra Malaysia**
**Serdang**
**Selangor**
**Malaysia**

**UPM Press**
**Universiti Putra Malaysia**
**Serdang**
**Selangor**
**Malaysia**

# CONTENTS

# PREFACE

This book is the first volume of research papers presented at the Fundamental Science Congress 2017 at Universiti Putra Malaysia on November 21-22, 2017.The congress served as a platform for researchers from different parts of Malaysia to share their knowledge and initiate collaboration among themselves. This book presents the latest findings in various fields of applied mathematics generally and numerical analysis and fluid dynamics specifically.

Chapter 2 comprises paper on the new four-stage third-order trigonometrically fitted explicit modified Runge-Kutta type (MRKT) methods which are called TFRKTGG3. TFRKTGG3 trigonometrically-fitted explicit MRKT method is used to solve general $y'''(x) = f(x, y, y', y'')$ with oscillating solutions involving trigonometric functions.

Chapter 3 presented paper related to the four-stage fourth-order Runge–Kutta–Nyström method (RKN) for solving second-order two-point boundary value problem (BVP) with Dirichlet condition. Numerical results are compared with the existing Runge-Kutta (RK) method and have clearly shown the advantage and the efficiency of the RKN.

Chapter 4 consists of a paper on 2-point diagonally implicit multistep block method of order four for solving first order ordinary differential equations. The stability region of the proposed method will be discussed and numerical examples are given to demonstrate the performance of the method.

In Chapter 5, numerical method for volterra integro-differential equation (VIDE) with implicit multistep block method (IMBM) is discussed. Preliminary results from the application of the implicit multistep block method are given and the comparisons are made with the existing methods in order to test the efficiency of the proposed method.

Chapter 6 contains paper related to numerical computation for solving boundary value problems with robin conditions. The numerical results are presented and compared with the exact solutions, and also with the solutions of the establish Runge-Kutta order four method.

Chapter 7 discusses on hybrid one–step block method with one-off step for solving first order volterra integro-differential equations (VIDE). The hybrid one-step block method together with numerical quadrature rules are applied for solving the second kind of VIDE using constant step size.

Chapter 8 comprises paper on the development new two derivative Runge-Kutta-Nyström (TDRKN) method for solving $y'' = f(x, y, y')$. The results obtained of numerical

calculations showed that the new TDRKN method is more efficient than the standard explicit RKN methods for the general second order ordinary differential equations of the same algebraic order.

Chapter 9 presented paper related to MHD boundary layer flow of carreau fluid over a stretching surface with suction and thermal radiation. The effect of non-dimensional parameters such as the suction parameter, the Prandtl number and the Biot number on velocity, temperature, local skin friction and local Nusselt number are discussed.

Chapter 10 consists of a paper on heat transfer characteristics of MHD stagnation-point flow of carreau fluid over a shrinking sheet. Numerical results for different values of governing parameters on the heat transfer characteristics are presented and discussed.

# CONTRIBUTORS

## Preface

Athirah Nawawi, Department of Mathematics, Faculty of Science, Universiti Putra Malaysia, 43400 Serdang,Selangor, Malaysia.

## Chapter 1 Introduction

Athirah Nawawi, Department of Mathematics, Faculty of Science, Universiti Putra Malaysia, 43400 Serdang, Selangor, Malaysia.

## Chapter 2 An Explicit Trigonometrically-Fitted Modified Runge-Kutta Type Method for Solving $y'''(x) = f(x, y, y', y'')$ with Oscillating Solutions

**N. Ghawadri[a], N. Senu[a,b], F. Ismail[a,b], Z.B. Ibrahim[a,b]**
[a]Institute for Mathematical Research, Universiti Putra Malaysia, 43400 UPM Serdang, Selangor, Malaysia.
[b]Department of Mathematics, Universiti Putra Malaysia, 43400 UPM Serdang, Selangor, Malaysia.
Email: norazak@upm.edu.my

## Chapter 3 Runge-Kutta-NystrÖM Methods for Directly Solving Second Order Linear Boundary Value Problems with Dirichlet Condition

**A. A. Salam[1,3], N. Senu[1,2] and Z. A. Majid[1,2]**
[1] Department of Mathematics, Universiti Putra Malaysia, 43400 UPM Serdang, Selangor, Malaysia.
[2] Institute for Mathematical Research, Universiti Putra Malaysia, 43400 UPM Serdang,Selangor, Malaysia.
**[3]** Department of Mathematics, University of Baghdad, Al-Jadrriya, Baghdad, Iraq.
Email: azraasalam55@gmail.com

## Chapter 4 2-Point Diagonally Implicit Multistep Block Method of Order Four for Solving First Order Ordinary Differential Equations

**S. Isa[1,3] and Z. A. Majid[1,2]**
[1]Institute for Mathematical Research, Universiti Putra Malaysia, 43400, Serdang, Selangor, Malaysia.
[2]Department of Mathematics, Faculty of Science, Universiti Putra Malaysia, 43400, Serdang, Selangor, Malaysia.
[3]Department of Mathematics and Statistics, Faculty of Applied Science and Technology, Universiti Tun Hussein Onn Malaysia (Pagoh Campus), 84000, Muar, Johor, Malaysia.
Email: syahir@uthm.edu.my

## Chapter 5 Numerical Method for Volterra Integro-Differential Equation with Implicit Multistep Block Method

**N. A. Baharum[1], Z. A. Majid[1,2] and N. Senu[1,2]**
[1]Institute for Mathematical Research, Universiti Putra Malaysia, 43400 UPM Serdang, Selangor Darul Ehsan, Malaysia.

[2]Department of Mathematics, Faculty of Science, Universiti Putra Malaysia, 43400 UPM Serdang, Selangor Darul Ehsan, Malaysia.
Email: am_zana@upm.edu.my

## Chapter 6 Numerical Computation for Solving Boundary Value Problems with Robin Conditions

**N.M. Nasir[1,3] and Z.A. Majid[1,2]**
[1]Institute for Mathematical Research, Universiti Putra Malaysia, 43400, UPM Serdang, Selangor, Malaysia.
[2]Department of Mathematics, Faculty of Science, University Putra Malaysia, 43400, UPM Serdang, Selangor, Malaysia.
[3]Faculty of Industrial Sciences & Technology (FIST), Universiti Malaysia Pahang, 26300, Gambang, Pahang, Malaysia.
Email: am_zana@upm.edu.my

## Chapter 7 Hybrid One–Step Block Method with One-Off Step for Solving First Order Volterra Integro-Differential Equations

**Janodi, M. R.[1], Majid, Z. A.[1,2], Ismail, F[2]. and Senu, N.[2]**
[1] Institute for Mathematical Research, Universiti Putra Malaysia, 43400 Serdang, Selangor, Malaysia.
[2] Department of Mathematics, Faculty of Science, Universiti Putra Malaysia, 43400 Serdang, Selangor, Malaysia.
Email: am_zana@upm.edu.my

## Chapter 8 Development New Two Derivative Runge-Kutta-Nyström Method for Solving $y'' = f(x, y, y')$

**T.S.Mohamed[1, 2], N.Senu [1,3], Z.B.Ibrahim [1,3], N. M. A. Nik Long [1,3]**
[1]Institute for Mathematical Research, Universiti Putra Malaysia, 43400 UPM Serdang, Selangor, Malaysia.
[2]Department of Mathematics, Faculty of Science, Misurata University, Misurata, Libya.
[3]Department of Mathematics, Faculty of Science, Universiti Putra Malaysia, 43400 UPM Serdang, Selangor, Malaysia.
Email: t.salama06@gmail.com

## Chapter 9 MHD Boundary Layer Flow of Carreau Fluid over a Stretching Surface with Suction and Thermal Radiation

**Rusya Iryanti Yahaya[1], Norihan Md Arifin[1,2] and Siti Suzilliana Putri Mohamed Isa[1,3]**
[1]Institute for Mathematical Research, Universiti Putra Malaysia, 43400 UPM Serdang Selangor, Malaysia.
[2]Department of Mathematics, Universiti Putra Malaysia, 43400 UPM Serdang Selangor, Malaysia.
[3]Centre of Foundation Studies for Agricultural Science, Universiti Putra Malaysia, 43400 UPM Serdang Selangor, Malaysia.
Email: norihana@upm.edu.my

## Chapter 10 Heat Transfer Characteristics of MHD Stagnation-Point Flow of Carreau Fluid over a Shrinking Sheet

**F. M. Ali[1,2] and N. Ratanam [1]**
[1]Department of Mathematics, Faculty of Science, Universiti Putra Malaysia, 43400 UPM Serdang, Selangor, Malaysia.
[2]Institute for Mathematical Research, Universiti Putra Malaysia, 43400 UPM Serdang, Selangor, Malaysia.
Email: fadzilahma@upm.edu.my

# CHAPTER 1

# INTRODUCTION

This multidisciplinary book on latest discoveries in various fields of applied mathematics ranges from numerical analysis to fluid dynamics.

Numerical analysis is one of important branch of mathematics which creates or modifies, analyzes and implements algorithms with numerical approximation for solving problems of mathematical analysis. This field of research comprises many subdisciplines such as solving systems of equations whether linear or not, solving differential equations whether ordinary or partial, solving eigenvalues or singular value problems, and many more. Our choice of topics is governed by what is most needed in science and engineering, as well as in applied physical science. Mathematical models are then central, with differential equations constituting the most frequent type of models. Consequently, the numerical focus in this book is on differential equations. There is also a chapter on solving boundary value problems and volterra integro-differential equation. We remark that the book is deliberately brief on numerical analysis. This is because our focus is on analysing stability, convergence of the method, implementing numerical algorithms, and also the readers must be confident about the basic ideas of the numerical approximations involved. Among the famous methods covered in this book include one-step block method, multistep block method, Runge-Kutta type method and Runge-Kutta-Nyström method for solving numerous mathematical problems.

Whilst fluid dynamics which is a subdiscipline of fluid mechanics offers a methodical practical structure. It describes the flow of fluids ie. liquids and gases. The deduction of the boundary layer equations is one of the most important advances in fluid dynamics. Using an order of magnitude analysis, the well-known governing Navier–Stokes equations of viscous fluid flow can be greatly simplified within the boundary layer. Notably, the characteristic of the partial differential equations (PDE) becomes parabolic, rather than the elliptical form of the full Navier–Stokes equations. This greatly simplifies the solution of the equations. By making the boundary layer approximation, the flow is divided into an inviscid portion (which is easy to solve by a number of methods) and the boundary layer, which is governed by an easier to solve PDE. The continuity and Navier–Stokes equations for a two-dimensional steady incompressible flow in Cartesian coordinates. The governing partial differential equations are reduced into a system of ordinary differential equations using a similarity transformation, which are then solved numerically.

The solution to a fluid dynamics problem commonly involves the computation of several properties of fluid such as flow velocity, mass and temperature. Non-dimensional governing parameters such as the stretching/shrinking parameter, the suction parameter, the radiation parameter, the magnetic parameter, and the power law index will usually affect on certain fluid properties. Some findings show that the presence of magnetic field causes the fluid velocity to decrease and the temperature to increase, the power law index

enhances the boundary layer separation, whilst the suction parameter delays the boundary layer separation and many other interesting observations.

These fields under applied mathematics naturally find application in all fields of engineering, the physical sciences, the life sciences, social sciences, medicine, business and even the arts have adopted elements of scientific computations. Hence, this book will be of interest to not only practitioners in the fields of mathematics but to all other experts from other fields.

## CHAPTER 2

## AN EXPLICIT TRIGONOMETRICALLY-FITTED MODIFIED RUNGE-KUTTA TYPE METHOD FOR SOLVING $y'''(x) = f(x, y, y', y'')$ WITH OSCILLATING SOLUTIONS

**Abstract:**
In this paper , we derive TFRKTGG3 trigonometrically-fitted explicit modified Runge-Kutta type (MRKT) method for solving general $y'''(x) = f(x, y, y', y'')$ with oscillating solutions. These methods are constructed which exactly integrates initial value problems whose solutions are linear combinations of the set functions $exp(wx)$ and $exp(-wx)$ for exponentially-fitted and sin($w$x) and cos($w$x) for trigonometrically fitted with $w \in R$ the principal frequency of the problem and the frequency will be used to raise the accuracy of the methods. The new four-stage third-order trigonometrically fitted explicit MRKT methods are called TFRKTGG3 for solving initial value problems whose solutions involving trigonometric functions. The numerical results indicate that trigonometrically fitted explicit modified Runge-Kutta type methods are more efficient than existing methods in the literature.

**Keywords**: Exponentially-fitted method, Trigonometrically-fitted method, Modified Runge-Kutta type methods, Initial value problems, Third-order ODEs.

### 1. Introduction

This study deals with trigonometrically-fitted modified Runge-Kutta type methods for solving general third-order ordinary differential equations (ODEs) with oscillating solutions

$$y'''(x) = f\big(x, y(x), y'(x), y''(x)\big),$$
$$y(x_0) = y_0, \quad y'(x_0) = y_0' \ , \quad y''(x_0) = y_0'' \ , \qquad x \geq x_0 \tag{1}$$

Many researchers construct an explicit trigonometrically fitted Runge-Kutta methods for solving first-order and second-order ordinary differential equations with oscillating solutions. Such as, Sakas et al. [3] develop a fifth algebraic order trigonometrically-fitted modified Runge-Kutta Zonneveld method for the numerical solution of orbital problems. Vanden Berghe et al. [4] construct an exponentially-fitted Runge-Kutta methods. Yang et al. [5] construct a trigonometrically-fitted ARKN methods for perturbed oscillators and Demba et al. [6] construct an explicit trigonometrically-fitted Runge-Kutta-Nystrom (ETFRKN) method using Simos technique. In addition, Yanwei Zhang et al. [7] develop a new trigonometrically-fitted two-derivative Runge-Kutta method. While, Simos [8] extend an exponentially-fitted Runge-Kutta methods for the numerical solution of the Schrodinger equation and related problems. Kalogiratou et al. [9] construct a trigonometrically- and exponentially-fitted Runge-Kutta-Nystrom methods for the numerical solution of the Schrodinger equation and related problems a method of eighth algebraic order.

In this paper, we construct trigonometrically-fitted explicit modified Runge-Kutta type three-stage third-order TFRKG3 method. Section 2 provides exponentially-fitted and trigonometrically-fitted modified Runge-Kutta type method. In section 3, The effectiveness of the new method to compared with existing method. The conclusion is given in Section 4.

## 2. Exponentially-fitted and trigonometrically-fitted modified Runge-Kutta (MRKT) type method

In this Section, we construct exponentially-fitted and trigonometrically-fitted MRKT methods. In this case, it is absolutely necessary to insert the extra parameter $\hat{\gamma}_i$ of produce the MRKT method.

In order to construct the exponentially-fitted and trigonometrically-fitted MRKT method we introduce an extra $\gamma_i$ at each stage and the modified Runge-Kutta (MRKT) type method is

$$y_{n+1} = y_n + hy'_n + \frac{h^2}{2} y''_n + h^3 \sum_{i=1}^{s} b_i \, k_i, \tag{2}$$

$$y'_{n+1} = y'_n + hy''_n + h^2 \sum_{i=1}^{s} b'_i \, k_i, \tag{3}$$

$$y''_{n+1} = y''_n + h \sum_{i=1}^{s} b''_i \, k_i. \tag{4}$$

where

$$k_1 = f(x_n, y_n, y'_n, y''_n), \tag{5}$$

$$k_i = f(x_n + c_i h, y_n + hc_i y'_n + \frac{h^2}{2} c_i^2 y''_n + h^3 \sum_{j=1}^{i-1} a_{ij} \, k_j,$$

$$y'_n + hc_i y''_n + h^2 \sum_{j=1}^{i-1} \hat{a}_{ij} \, k_j, \hat{\gamma}_i y''_n + h \sum_{j=1}^{i-1} \bar{a}_{ij} \, k_j) \tag{6}$$

for $i = 2,3,\ldots,s$.

The parameters $c_i, a_{ij}, \hat{a}_{ij},, \bar{a}_{ij}, b_i, b'_i, b''_i$ and $\gamma_i$ for $i = 1,2,\ldots,s$ and $j = 1,2,\ldots,s$ are assumed to be real. If $a_{ij} = 0$ , $\hat{a}_{ij} = 0$ and $\bar{a}_{ij} = 0$ for $i \leq j$, it is an explicit method otherwise it is an implicit method.

For the exponentially-fitted method we want to integrate $exp(wx)$, $exp(-wx)$ exactly at each stage as follows:

$$e^{\pm v} = \hat{\gamma}_i \pm h \sum_{j=1}^{s} \bar{a}_{ij} \, e^{\pm c_j v}, \tag{7}$$

and the following that corresponds to y , $y'$ and $y''$:

$$e^{\pm v} = 1 \pm v + \frac{1}{2}v^2 \pm v^3 \sum_{i=1}^{s} b_i\, e^{\pm c_i v}, \tag{8}$$

$$e^{\pm v} = 1 \pm v + v^2 \sum_{i=1}^{s} b_i'\, e^{\pm c_i v}, \tag{9}$$

$$e^{\pm v} = 1 \pm v \sum_{i=1}^{s} b_i''\, e^{\pm c_i v}. \tag{10}$$

For the trigonometrically-fitted method we want to integrate exactly $\sin(wx), \cos(wx)$, at each stage to have:

$$cos\,(vc_i) = \widehat{\gamma_i} - v \sum_{j=1}^{i-1} \bar{a}_{ij}\, sin\,(vc_j), \tag{11}$$

$$sin\,(vc_i) = v \sum_{j=1}^{i-1} \bar{a}_{ij}\, cos\left(vc_j\right),\ i = 1, \ldots, s, \tag{12}$$

and the following that corresponds to y , $y'$ and $y''$:

$$cos\,(v) = 1 - \frac{1}{2}\,v^2 + v^3 \sum_{i=1}^{s} b_i\, sin\,(vc_i), \tag{13}$$

$$sin\,(v) = v - v^3 \sum_{i=1}^{s} b_i\, cos\,(vc_i), \tag{14}$$

$$cos\,(v) = 1 - v^2 \sum_{i=1}^{s} b_i'\, cos\,(vc_i), \tag{15}$$

$$sin\,(v) = v - v^2 \sum_{i=1}^{s} b_i'\, sin\,(vc_i), \tag{16}$$

$$cos\,(v) = 1 - v \sum_{i=1}^{s} b_i''\, sin\,(vc_i), \tag{17}$$

$$sin\,(v) = v \sum_{i=1}^{s} b_i''\, cos\,(vc_i). \tag{18}$$

Then, solving Equatios (11) into (12), we have:

$$\bar{a}_{i,i-1} = \frac{sin\,(vc_i) - v \sum_{j=1}^{i-2} \bar{a}_{i,j}\, cos\left(vc_j\right)}{v\, cos\,(vc_{i-1})}, \tag{19}$$

$$\widehat{\gamma_i} = cos\,(vc_i) + v \sum_{j=1}^{i-1} \bar{a}_{i,j}\, sin\left(vc_j\right). \tag{20}$$

For $i = 2, \ldots, s$.

Referring to the following the third-order with three stages method developed by Fawzi et al. [11]

$c_1 = 0, c_2 = \frac{2}{3}, c_3 = \frac{2}{3}, a_{21} = \frac{7}{10}, a_{31} = \frac{28}{25},\ a_{32} = \frac{28}{25}, \bar{a}_{21} = \frac{17}{100}, \bar{a}_{31} = \frac{53}{225}, \bar{a}_{32} = -\frac{17}{100},$
$b_3 = 0, b_3' = 0, b_3'' = -\frac{3}{8}.$

Solving Equations (19)-(20) with the above coefficients and leting $\hat{a}_{21}$ , $\hat{a}_{32}$ , $\hat{\gamma}_2$ and $\hat{\gamma}_3$ as free parameters yields:

$\hat{a}_{21} = \frac{sin\left(\frac{2v}{3}\right)}{v}, \hat{a}_{32} = \frac{sin\left(\frac{2v}{3}\right) - \frac{4v}{3}}{v\, cos\left(\frac{2v}{3}\right)}, \hat{\gamma}_2 = cos\left(\frac{2v}{3}\right), \widehat{\gamma_1} = 1, \hat{\gamma}_3 = cos\left(\frac{2v}{3}\right) - \frac{2v}{3} sin\left(\frac{2v}{3}\right).$

Then, solving Equations (15)-(18) with the above coefficients yields:

$$b_1 = -\frac{1}{2} \frac{2\ cos\left(\frac{2v}{3}\right) cos\,(v) - 2\ cos\left(\frac{2v}{3}\right) + cos\left(\frac{2v}{3}\right) v^2 + 2\ sin\,(v)\, sin\left(\frac{2v}{3}\right) - 2\, v\, sin\left(\frac{2v}{3}\right)}{v^3\, sin\left(\frac{2v}{3}\right)},$$

$$b_2 = -\frac{sin\,(v) - v}{v^2\, sin\left(\left(\frac{2v}{3}\right)\right.},$$

$$b_1' = \frac{cos\left(\frac{2v}{3}\right) sin\,(v) - v\, cos\left(\frac{2v}{3}\right) - cos\,(v)\, sin\left(\frac{2v}{3}\right) + sin\left(\frac{2v}{3}\right)}{v^2\, sin\left(\frac{2v}{3}\right)},$$

$$b_2' = -\frac{sin\,(v) - v}{v^2\, sin\left(\left(\frac{2v}{3}\right)\right.},$$

$$b_1'' = \frac{cos\left(\frac{2v}{3}\right) cos\,(v) - cos\left(\frac{2v}{3}\right) + sin\,(v)\, sin\left(\frac{2v}{3}\right)}{v\, sin\left(\frac{2v}{3}\right)},$$

$$b_2'' = -\frac{-1 - \frac{2v}{8} v\, sin\left(\frac{2v}{3}\right) + cos\,(v)}{v\, sin\left(\frac{2v}{3}\right)}.$$

This leads to our proposed method explicit trigonometrically-fitted TFRKGG3 given by the corresponding Taylor series expansion of the solution as follows:

$$b_1 = \frac{5}{48} + \frac{13}{4320} v^2 + \frac{829}{6531840} v^4 + \frac{9941}{1763596800} v^6 + \frac{25243}{99769190400} v^8 + \frac{586059827}{51477909170688000} v^{10} + \cdots,$$
$$b_2 = \frac{1}{16} + \frac{11}{4320} v^2 + \frac{803}{6531840} v^4 + \frac{9859}{1763596800} v^6 + \frac{176339}{698384332800} v^8 + \frac{53250863}{4679809924608000} v^{10} + \cdots,$$
$$b_1' = \frac{1}{4} + \frac{17}{2160} v^2 + \frac{55}{163296} v^4 + \frac{13231}{881798400} v^6 + \frac{117673}{174596083200} v^8 + \frac{780698467}{25738954585344000} v^{10} + \cdots,$$
$$b_2' = \frac{1}{4} + \frac{13}{2160} v^2 + \frac{271}{816480} v^4 + \frac{1877}{125971200} v^6 + \frac{23497}{34919216640} v^8 + \frac{780383783}{25738954585344000} v^{10} + \cdots,$$

$$b_1'' = \frac{1}{4} + \frac{1}{144} v^2 + \frac{11}{38880} v^4 + \frac{731}{58786560} v^6 + \frac{589}{1058158080} v^8 + \frac{471953}{18856376985600} v^{10} + \cdots,$$

$$b_2'' = \frac{9}{8} - \frac{1}{144} v^2 + \frac{13}{38880} v^4 + \frac{709}{58786560} v^6 + \frac{587}{1058158080} v^8 + \frac{471487}{18856376985600} v^{10} + \cdots,$$

$$\hat{a}_{21} = \frac{2}{3} - \frac{4}{81}\,v^2 + \frac{4}{3645}\,v^4 - \frac{8}{688905}\,v^6 + \frac{4}{55801305}\,v^8 - \frac{8}{27621645975}\,v^{10} + \cdots,$$

$$\hat{a}_{32} = -\frac{2}{3} - \frac{16}{81}\,v^2 - \frac{136}{3645}\,v^4 - \frac{1552}{229635}\,v^6 - \frac{67976}{55801305}\,v^8 - \frac{1212272}{5524329195}\,v^{10} + \cdots,$$

$$\hat{\gamma}_2 = 1 - \frac{2}{9}\,v^2 + \frac{2}{243}\,v^4 - \frac{4}{32805}\,v^6 + \frac{2}{2066715}\,v^8 - \frac{4}{837019575}\,v^{10} + \cdots,$$

$$\hat{\gamma}_3 = 1 - \frac{2}{3}\,v^2 + \frac{10}{243}\,v^4 - \frac{28}{32805}\,v^6 + \frac{2}{229635}\,v^8 - \frac{44}{837019575}\,v^{10} + \cdots.$$

## 3. Numerical Results

In this Section, we apply the proposed method to $y''' = f(x, y, y', y'')$ ordinary differential equations (ODEs) problems. The numerical results of our third-order four-stages TFRKTGG method is tabulated in table 1. The numerical results for TFRKTGG3 is compared with other existing RK methods of the same order. The methods chosen in the numerical experiments are as follows:

- TFRKTGG3: the four-stage third-order TFRKTGG method derived in this paper.
- RKTGG3: the three-stage third-order RKTGG type method given by Fawzi in [11].
- RK3: the three-stage third-order RK method given by Dormand [13].
- RK3M: the six-stage third-order RK method given in Dormand [13].

The problem tested is given as follows:

$$y_1'''(x) = -\frac{1}{8}y_1''(x) + sin\,(2x),\ y_1(0) = \frac{32}{257}\,, y'_1(0) = -\frac{4}{257}\,, y''_1(0) = -\frac{128}{257},$$

$$y_2'''(x) = -\frac{1}{64}y_2''(x) - cos\,(2x), y_2(0) = \frac{16}{16385},\ \ y'_2(0) = \frac{4096}{16385}\,,$$

$$y''_2(0) = -\frac{64}{16385}.$$

$$y_3'''(x) = -\frac{1}{27}y_3''(x) - sin\,(2x), y_3(0) = -\frac{729}{5834}\,, y'_3(0) = \frac{27}{5834}\,, y''_3(0) = \frac{1458}{2917}.$$

Hence, the exact solution are

$$y_1(x) = \frac{32}{257}\,cos\,(2x) - \frac{2}{257}\,sin\,(2x),$$

$$y_2(x) = \frac{16}{16385}\,cos\,(2x) + \frac{2048}{16385}\,sin\,(2x),$$

$y_3(x) = -\frac{729}{5834}\,cos\,(2x) + \frac{27}{11668}\,sin\,(2x)$, Estimated frequency, $w = 2$.

Table 1: Numerical results for the problem for TFRKTGG3 method

| *h* | methods | $x$ =100 | $x$ =1000 | $x$ =10000 |
|---|---|---|---|---|
| 0.01 | TFRKTGG3 | 9.761996(−8) | 1.893467(−6) | 1.665407(−5) |
| | RKTGG3 | 5.859742(−5) | 1.109357(−3) | 1.177915(−2) |

| | | | | |
|---|---|---|---|---|
| | Rk3<br>RK3M | 4.393693(−5)<br>1.586735(−3) | 8.319551(−4)<br>1.586735(−3) | 8.835066(−3)<br>2.403712(−3) |
| 0.025 | TFRKTGG3<br>RKTGG3<br>Rk3<br>RK3M | 3.812524(−6)<br>9.156610(−4)<br>6.865244(−4)<br>4.762779(−3) | 7.223868(−5)<br>1.733571(−2)<br>1.300085(−2)<br>4.776506(−3) | 7.697985(−4)<br>1.840108(−1)<br>1.380068(−1)<br>3.192964(−2) |
| 0.05 | TRKTGG3<br>RKTGG3<br>Rk3<br>RK3M | 6.105092(−5)<br>1.835273(−3)<br>5.497772(−3)<br>1.356709(−2) | 1.156301(−3)<br>3.467555(−2)<br>1.040294(−1)<br>1.617916(−2) | 1.227456(−2)<br>3.680322(−1)<br>1.104297(0)<br>2.562791(−1) |
| 0.075 | TFRKTGG3<br>RKTGG3<br>Rk3<br>RK3M | 3.091299(−4)<br>6.194845(−3)<br>1.855978(−2)<br>2.543279(−2) | 5.857133(−3)<br>1.170405(−1)<br>3.512124(−1)<br>6.152245(−2) | 6.217701(−2)<br>1.242222(0)<br>3.728214(0)<br>8.722326(−1) |

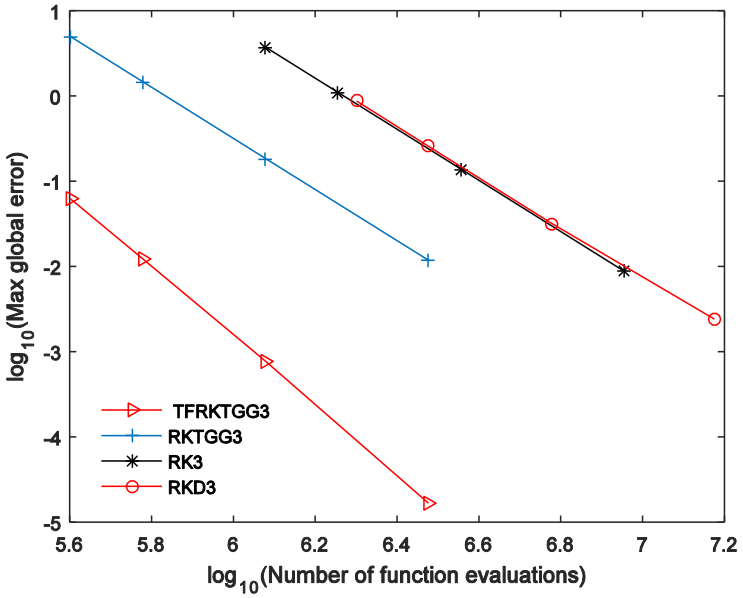


The efficiency curve for TFRKTGG3 method with $x_{end} = 10000$ *and* $h = 0.01, 0.025, 0.05, 0.075$.

## 4. Conclusion

In this studies,we present trigonometrically-fitted explicit modified Runge-Kutta type method for solving general $y'''(x) = f(x, y, y', y'')$ with oscillating solutions. So, we constructed a three-stage third-order method denoted asTFRKTGG3 method. The results show the typical properties of the new trigonometrically-fitted explicit modified Runge-

Kutta type TFRKTGG method. In addition, the efficiency and accuracy of the methods depend on the step size, $h$ and the frequency, $w$. The global error and efficiency of the method over a long period of integration are plotted. The Figure represents the efficiency and accuracy of the method developed by plotting the graph of the logarithm of the maximum global error against the logarithm of function evaluations for a longer periods of computations.The numerical results show that the maximum global error of the proposed method is smaller than that of the other existing methods. The TFRKTGG3 method is much more effcient than the other existing methods.

## References


1. T. E. Simos, Exponentially-fitted Runge-Kutta-Nystr$\ddot{o}$m method for the numerical solution of initial-value problems with oscillating solutions, Applied Mathematics Letters 15 (2) (2002) 217–225.
2. G. V. Berghe, H. De Meyer, M. Van Daele, T. Van Hecke, Exponentially-fitted Runge–Kutta methods, Journal of Computational and Applied Mathematics 125 (1) (2000) 107–115.
3. D. Sakas, T. E. Simos, A fifth algebraic order trigonometrically-fitted modified Runge-Kutta zonneveld method for the numerical solution of orbital problems, Mathematical and computer modelling 42 (7-8) (2005) 903–920.
4. G. V. Berghe, H. De Meyer, M. Van Daele, T. Van Hecke, Exponentially-fitted explicit Runge–Kutta methods supported by the bilateral scientific135 and technological cooperation 1998, flanders-romania, grant bil 98/47.1, Computer Physics Communications 123 (1-3) (1999) 7–15.
5. H. Yang, X. Wu, Trigonometrically-fitted ARKN methods for perturbed oscillators, Applied Numerical Mathematics 58 (9) (2008) 1375–1395.
6. M. Demba, N. Senu, F. Ismail, Trigonometrically-fitted explicit four-stage fourth-order Runge–Kutta$-$Nystr$\ddot{o}$m method for the solution of initial value problems with oscillatory behavior, Global Journal of Pure and Applied Mathematics 12 (1) (2016) 67–80.
7. Y. Zhang, H. Che, Y. Fang, X. You, A new trigonometrically fitted two derivative Runge-Kutta method for the numerical solution of the schr$\ddot{o}$dinger equation and related problems, Journal of Applied Mathematics 2013.
8. T. Simos, exponentially fitted Runge–Kutta methods for the numerical solution of the schr$\ddot{o}$dinger equation and related problems, Computational Materials Science 18 (3) (2000) 315–332.
9. Z. Kalogiratou, T. Simos, Construction of trigonometrically and exponentially fitted Runge–Kutta–Nystr$\ddot{o}$m methods for the numerical solution of the schr$\ddot{o}$dinger equation and related problems–a method of 8th algebraic order, Journal of mathematical chemistry 31 (2) (2002) 211–232.
10. Z. Kalogiratou, T. Monovasilis, T. E. Simos, Computation of the eigen values of the schr$\ddot{o}$dinger equation by exponentially-fitted Runge–Kutta–methods, Computer Physics Communications 180 (2) (2009) 167– 176.
11. F. Fawzi, Runge–Kutta type methods for solving third-order ordinary differential

equations and first-order oscillatory problems, Ph.D. thesis, Department of Mathematics, Faculty of Science, 43400 UPM Serdang, Malaysia(2017).
12. J. R. Dormand, Numerical methods for differential equations: a computational approach, Vol. 3, CRC Press, 1996.

# CHAPTER 3

# RUNGE-KUTTA-NYSTRÖM METHODS FOR DIRECTLY SOLVING SECOND ORDER LINEAR BOUNDARY VALUE PROBLEMS WITH DIRICHLET CONDITION

**Abstract.** In this paper, the four-stage fourth-order Runge–Kutta–Nyström method (RKN) is used for solving second-order two-point boundary value problem (BVP) with Dirichlet condition. The method obtained the solution of the second-order boundary value problem directly without reducing it to first-order equations. The method is implemented using constant step size via shooting technique. Numerical results are compared with the existing Runge-Kutta (RK) method and have clearly shown the advantage and the efficiency of the RKN.

## 1. Introduction

Consider the simplest form of the second-order two-point boundary value problems as follows:

$$y'' = f(x, y), \qquad a \le x \le b \tag{1}$$

with boundary conditions

$$y(a) = \alpha, \quad y(b) = \beta$$

where a, b,$\alpha$, $\beta$ are the given constants. In the past decades, BVPs have played an important role in modeling the real issues, such as of chemical reactions, heat power transmission theory and many physical systems and so forth. These problems can be presented in several types of boundary conditions: e.g. Dirichlet, Neumann, and mixed. Dirichlet boundary condition is the common boundary condition and has been solved by many researchers such as Hamid et al. [6] , Phang et al. [8] , Khan [11] and Jang [12]. Phang et al. [7] and Liu [10] studied on Neumann-type boundary value problems and Lang [14] studied on mixed-type and Han and Wang [15] proved the existence of order two-point BVP subjected to solutions to mixed two-point BVP for impulsive differential equations by variational methods.

In this study we are concerned with Dirichlet type of BVPs. There are many analytical and numerical techniques available to solve BVP with Dirichlet condition including several well-known methods, such as Adomian decomposition method, finite difference method, and collocation method. Hamid et al. [6] solved the Dirichlet type BVPs by using extended cubic B-spline interpolation method. Phang et al. [8] used cubic B-spline method to solve non-Linear BVPs. Ha [9] used Runge-Kutta via shooting method to solve BVPs. Jang [12] solved Linear and non-Linear BVPs by using the Adomian decomposition method.

The purpose of this paper is to use the special RKN method via shooting technique for solving the linear second-order two-point BVPs subjected to Dirichlet boundary condition directly. The approach for solving higher order ordinary differential equation directly has been suggested by NystrÖm 1925. In Section 2 we define linear two-point BVP, Section 3 and 4 deal with materials and the methods. In Section 5 we present the numerical results and the last Section deals with the conclusion.

## 2. Two-Point linear Boundary Value Problem Statement

Two-point BVPs are problems in which, for a set of possibly linear ordinary differential equations, some boundary conditions are specified at the initial value of the independent variable, while the remainder of boundary conditions is specified at the terminal value of the independent variable. The boundary conditions are therefore split between the two points, the initial and terminal values of the independent variable. Consider the simplest form of the second-order linear two-point BVPs as follows:

$$y'' = p(x)y'(x) + q(x)y(x) + r(x) \quad \text{with } y(a) = \alpha, \;\; y(b) = \beta \qquad (2)$$

where a, b,$\alpha$, $\beta$ are the given constants. The following theorem gives the general conditions which ensure that the solution to a second-order BVP exists and is unique.

**Theorem1**. Suppose the function $f$ in the boundary value problem

$$y'' = f(x, y, y'), \qquad a \le x \le b \quad y(a) = \alpha, \quad y(b) = \beta,$$

is continues on the set

$$D = \{(x, y, y') | a \le x \le b, -\infty < y' < \infty\},$$

and $\frac{df}{dy}$ and $\frac{df}{dy'}$ are also continuous on $D$. If

(1) $\frac{df}{dy}(x, y, y') > 0$ for all $(x, y, y') \in D$, and

(2) $\left|\frac{df}{dy'}(x, y, y')\right| < M$ for all $(x, y, y') \in D$,

then the boundary value problem has a unique solution.

**Proof.** See [4].

## 3. Shooting Method for Linear Boundary Value Problem

Shooting technique used to convert the BVP into initial value problems. The idea in shooting technique is to obtain the missing initial value until the boundary condition at the other end converges to its correct value. When we use the shooting method, we transform (1) into the Cauchy-problem of the form

$$y'' = f(x, y, y'), \quad a \le x \le b \qquad with \qquad y(a) = \alpha, \quad y'(a) = \gamma, \tag{3}$$

where $\gamma$ is any number. Then the resulting IVP will be solved using Runge-Kutta method.

**Reduction to Two IVPs:**

The solution of a linear two-point BVP is associated by forming a linear combination of the solutions to two IVPs. The form of the IVPs are as follows:
Suppose that $u(x)$ is the unique solution to the IVP

$$u'' = p(x)u'(x) + q(x)u(x) + r(x) \quad \text{with} \quad u(a) = \alpha \quad \text{and} \quad u'(a) = 0. \tag{4}$$

Furthermore, suppose that $v(x)$ is the unique solution to the IVP

$$v'' = p(x)v'(x) + q(x)v(x) \quad \text{with} \quad v(a) = 0 \quad \text{and} \quad v'(a) = 1. \tag{5}$$

Then the linear combination

$$y(x) = C_1 u(x) + C_2 v(x) \tag{6}$$

is a solution to the linear BVP

$$y'' = p(x)y'(x) + q(x)y(x) + r(x). \tag{7}$$

Let $C_1 = 1$, to find $C_2$, the solution $y(x)$ in equation (6) takes on the boundary values

$$\begin{aligned} y(a) &= u(a) + C_2 v(a) = \alpha, \\ y(b) &= u(b) + C_2 v(b). \end{aligned} \tag{8}$$

Imposing the boundary condition $y(b) = \beta$ in (8) produces $C_2 = \frac{\beta - u(b)}{v(b)}$. Therefore, if $v(b) \neq 0$, the unique solution of the original two-point BVP is given by:

$$y(x) = u(x) + \frac{\beta - u(b)}{v(b)} v(x).$$

## 4. Special Runge-Kutta-NystrÖm Method

The system of $m$ second-order IVP (1) can be written as follows:

$$y'' = f(x, y), \qquad y(a) = \mu$$

where $y(x) = [y_1(x), y_2(x), \dots, y_m(x)]^T$,
$f(x, y) = [f_1(x, y), f_2(x, y), \dots, f_m(x, y)]^T$, $x \in [a, b]$
and $\mu = [\mu_1, \mu_2, \dots, \mu_m]^T$ is the initial conditions.

The s-stage RKN method for solving the system of second-order IVPs is defined as

$$y_{n+1} = y_n + hy'_n + h^2 \sum_{i=1}^{s} b_i k_i$$

$$y'_{n+1} = y'_n + h \sum_{i=1}^{s} \bar{b}_i k_i$$

$$k_i = f\left( x_n + c_i h, y_n + c_i h y'_n + h^2 \sum_{j=1}^{i-1} a_{ij} k_j \right) \quad (9)$$

for $i = 2,3, \dots, i-1$. The Butcher tableau of scheme (9) can be written as follows:

| $C$ | $A$ |
|---|---|
| | $b^T$ |
| | $\bar{b}^T$ |

where $A$ is a matrix$\left(a_{ij}\right)_{sxs}$ , $C = [c_1, c_2, \dots, c_s]^T$ , b $= [b_1, b_2, \dots, b_s]^T$ and $\bar{b} = [\bar{b}_1 , \bar{b}_2 , \dots, \bar{b}_s]^T$. A RKN method (9) is said to be explicit if $a_{ij} = 0$, for $i \leq j$.
In this study, we used the four-stage fourth-order dispersive of order eight RKN method as given in [16]. The coefficients of the method are given in Table below (see Table 1):

Table 1: The RKN4(4,8,5)M Method [16]

| | | | | |
|---|---|---|---|---|
| 0 | | | | |
| $\frac{1}{4}$ | $\frac{1}{32}$ | | | |
| $\frac{7}{10}$ | $\frac{19}{600}$ | $\frac{16}{75}$ | | |
| 1 | $\frac{32}{315}$ | $\frac{58}{315}$ | $\frac{3}{14}$ | |
| | $\frac{1}{21}$ | $\frac{28}{81}$ | $\frac{50}{567}$ | $\frac{1}{54}$ |
| | $\frac{1}{14}$ | $\frac{32}{81}$ | $\frac{250}{567}$ | $\frac{5}{54}$ |

**Algorithm 1: Special Runge-Kutta-Nyström Method via Linear Shooting Technique:**

To approximate the solution of the BVP

$$y'' = p(x)y'(x) + q(x)y(x) + r(x) \qquad \text{with} \quad y(a) = \alpha \quad \text{and} \quad y(b) = \beta$$

INPUT: endpoints $a, b$; boundary conditions $\alpha, \beta$; number of subintervals $N$.
OUTPUT: approximations $w_{1,i}$ to $y(x_i)$ ; $w_{2,i}$ to $y'(x_i)$ for each $i = 0, 1, \ldots, N$.
Step 1: Set $h = (b - a)/N$;

$u_{1,0} = \alpha$;
$u_{2,0} = 0$;
$v_{1,0} = 0$;
$v_{2,0} = 1$.

Step 2: For $i = 0, \ldots, N - 1$ do Steps 3 and 4.
(The special RKN method is used in Steps 3 and 4.)
Step 3: Set $x = a + ih$.
*Step 4:* Set $k_1 = u_{1,i}$;

$k_2 = u_{1,i} + c_2 h u_{2,i} - h^2 a_{21} k_1$;
$k_3 = u_{1,i} + c_3 h u_{2,i} + h^2[-a_{31}k_1 - a_{32}k_2]$;
$k_4 = u_{1,i} + c_4 h u_{2,i} + h^2[-a_{41}k_1 - a_{24}k_2 - a_{43}k_3]$;
$u_{1,i+1} = u_{1,i} + h u_{2,i} + h^2[b_1 k_1 + b_2 k_2 + b_3 k_3 + b_4 k_4]$;
$u_{2,i+1} = u_{2,i} + h\left[\bar{b}_1 k_1 + \bar{b}_2 k_2 + \bar{b}_3 k_3 + \bar{b}_4 k_4\right]$;
$\bar{k}_1 = v_{1,i}$;
$\bar{k}_2 = v_{1,i} + c_2 h v_{2,i} - h^2 a_{21} \bar{k}_1$;
$\bar{k}_3 = v_{1,i} + c_3 h v_{2,i} + h^2[-a_{31}\bar{k}_1 - a_{32}\bar{k}_2]$;
$\bar{k}_4 = v_{1,i} + c_4 h v_{2,i} + h^2[-a_{41}\bar{k}_1 - a_{24}\bar{k}_2 - a_{43}\bar{k}_3]$;
$v_{1,i+1} = v_{1,i} + h v_{2,i} + h^2\left[b_1 \bar{k}_1 + b_2 \bar{k}_2 + b_3 \bar{k}_3 + b_4 \bar{k}_4\right]$;
$v_{2,i+1} = v_{2,i} + h\left[\bar{b}_1 \bar{k}_1 + \bar{b}_2 \bar{k}_2 + \bar{b}_3 \bar{k}_3 + \bar{b}_4 \bar{k}_4\right]$;

Step 5: Set $w_{1,0} = \alpha$;

$w_{2,0} = \frac{\beta - u_{1,N}}{v_{1,N}}$;

OUTPUT $(a, w_{1,0}, w_{2,0})$.
Step 6: For $i = 1, \ldots, N$

set $W1 = u_{1,i} + w_{2,0} v_{1,i}$;
$W2 = u_{2,i} + w_{2,0} v_{2,i}$;
$x = a + ih$;
OUTPUT $(x, W1, W2)$. $(Output\ is\ x_i, w_{1,i}, w_{2,i}.)$

Step 7: Complete.

Burden and Faires, (2001).
This algorithm was developed in C language

## 5. Numerical Results

In this section, we applied RKN method derived by Senu [16] to $y'' = f(x, y)$ ODEs problem. The numerical result is compared with the existing RK of the same order when the same problem is reduced to a system of first-order equations for four different subintervals, N: 4, 8,16 and 32. The following notations are used in the tables:

| | |
|---|---|
| $h = \frac{b-a}{N}$ | Step size |
| NFC | Number of function call |
| RKN4 | Four-stage fourth order dispersive of order eight RKN method derived by Senu [16] |
| RK | Existing RK |

**Problem 1:**

$y'' + 25y = 0, \qquad x \in \left[0, \frac{\pi}{2}\right], \qquad y(0) = 1, \quad y\left(\frac{\pi}{2}\right) = -1,$

The exact solution is: $y(x) = \cos(5x) - \sin(5x)$.

**Numerical results**

Applying Algorithm 1 to this problem requires approximation the solutions to the IVPs

$u'' + 25u = 0, \qquad x \in \left[0, \frac{\pi}{2}\right], \qquad u(0) = 1, \quad u'(0) = 0,$

and

$v'' + 25v = 0, \qquad x \in \left[0, \frac{\pi}{2}\right], \qquad v(0) = 0, \quad v'(0) = 1,$

Table 2: Numerical results for RKN4 with $N = 8$ and $NFC = 32$

| $x_i$ | Method | $u_{1,i}$ | $v_{1,i}$ | $w_i$ | $y(x_i)$ | $\lvert y(x_i) - w_i \rvert$ |
|---|---|---|---|---|---|---|
| 0.0 | RKN4 | 1.00000000 | 0.00000000 | 1.00000000 | 1.00000000 | 0.000000000(0) |
| | RK4 | 1.00000000 | 0.00000000 | 1.00000000 | 1.00000000 | 0.000000000(0) |
| 0.2 | RKN4 | 0.55532318 | 0.16629113 | -0.27573911 | -0.27589938 | 1.602705762(-4) |
| | RK4 | 0.55679262 | 0.16480833 | -0.33915756 | -0.27589938 | 6.325817582(-2) |
| 0.4 | RKN4 | -0.38299271 | 0.18477744 | -1.30644279 | -1.30656297 | 1.201756105(-4) |
| | RK4 | -0.36902658 | 0.18352812 | -1.36674347 | -1.30656297 | 6.018050110(-2) |
| 0.6 | RKN4 | -0.98092043 | 0.03901935 | -1.17592488 | -1.17587560 | 4.927661341(-5) |
| | RK4 | -0.96164532 | 0.04136845 | -1.18653728 | -1.17587560 | 1.066168185(-2) |
| 0.8 | RKN4 | -0.70695576 | -0.14142965 | -0.00014206 | 0.00000000 | 1.420619637(-4) |
| | RK4 | -0.70588363 | -0.13545351 | 0.03048447 | 0.00000000 | 3.048447241(-2) |
| 1.0 | RKN4 | 0.19542286 | -0.19617346 | 1.17582609 | 1.17587560 | 4.951438768(-5) |
| | RK4 | 0.16506585 | -0.19175501 | 1.20750673 | 1.17587560 | 3.163113122(-2) |
| 1.2 | RKN4 | 0.92413896 | -0.07654498 | 1.30668277 | 1.30656296 | 1.198013606(-4) |

| | | | | | | |
|---|---|---|---|---|---|---|
| | RK4 | 0.88197801 | -0.07956355 | 1.31451062 | 1.30656296 | 7.947653276(-3) |
| 1.4 | RKN4<br>RK4 | 0.83144126<br>0.81889722 | 0.11112896<br>0.10105692 | 0.27605934<br>0.26951984 | 0.27589938<br>0.27589938 | 1.599661247(-4)<br>6.379536844(-3) |

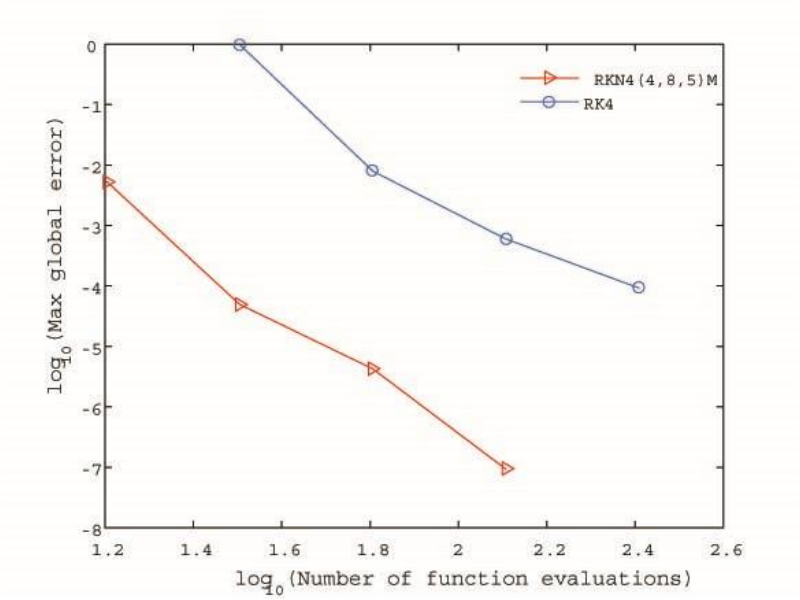


## 6. Conclusion

In this research, we conclude that fourth-order Runge-Kutta-Nystr*Ö*m method with shooting technique using constant step size is suitable for solving directly second-order linear boundary value problems with Dirichlet condition. Numerical results are show that RKN method is more efficient in terms of maximum global error and number of function evaluations compared to the existing RK method**.**

## REFERENCES


[1] Burden, R. L., & Faires, J. D. (2001). Numerical analysis. 2001. Brooks/Cole, USA.
[2] Dormand, J. R. (1996). Numerical methods for differential equations: a computational approach (Vol. 3). CRC Press.
[3] Alexander, R. (1990). Solving ordinary differential equations I: Nonstiff problems (E. Hairer, SP Norsett, and G. Wanner). SIAM Review, 32(3), 485.
[4] Greenspan, D., & Casulli, V. (1988). Numerical analysis for applied mathematics, science and engineering. Addison-Wesley.
[5] Lambert, J. D. (1991). Numerical methods for ordinary differential systems: the initial value problem. John Wiley & Sons, Inc..
[6] Hamid, N. N. A., Majid, A. A., & Ismail, A. I. M. (2011). Extended cubic B-spline method for linear two-point boundary value problems. Sains Malaysiana, 40(11), 1285-1290.
[7] Phang, P. S., Majid, Z. A., Suleiman, M., & Ismail, F. (2013). Solving Boundary Value Problems With Neumann Conditions Using Direct Method.

[8] Phang, P. S., Majid, Z. A., & Suleiman, M. (2011). Solving nonlinear two point boundary value problem using two step direct method (Menyelesaikan masalah nilai sempadan dua titik tak linear menggunakan kaedah langsung dua langkah). *Journal of Quality Measurement and Analysis*, *7*(1), 129-140.

[9] Ha, S. N. (2001). A nonlinear shooting method for two-point boundary value problems. Computers & Mathematics with Applications, 42(10), 1411-1420.

[10] Liu, L. B., Liu, H. W., & Chen, Y. (2011). Polynomial spline approach for solving second-order boundary value problems with Neumann conditions. Applied Mathematics and Computation, 217(16), 6872-6882.

[11] Khan, A. (2004). Parametric cubic spline solution of two point boundary value problems. Applied Mathematics and Computation, 154(1), 175-182.

[12] Jang, B. (2008). Two-point boundary value problems by the extended Adomian decomposition method. Journal of Computational and Applied Mathematics, 219(1), 253-262.

[13] Keller, H. B. (1976). Numerical solution of two point boundary value problems. Society for industrial and applied mathematics.

[14] Lang, F. G., & Xu, X. P. (2012). Quintic B-spline collocation method for second order mixed boundary value problem. Computer Physics Communications, 183(4), 913-921.

[15] Han, Z., & Wang, S. (2011). Mixed two-point boundary-value problems for impulsive differential equations. *Electronic Journal of Differential Equations (EJDE)[electronic only]*, *2011*, Paper-No.

[16] Senu, N. (2010). Runge–Kutta–Nyström methods for solving oscillatory problems, PhD. Thesis, Department of Mathematics, Faculty of Science, 43400 UPM Serdang, Malaysia).

# CHAPTER 4

# 2-POINT DIAGONALLY IMPLICIT MULTISTEP BLOCK METHOD OF ORDER FOUR FOR SOLVING FIRST ORDER ORDINARY DIFFERENTIAL EQUATIONS


## Abstract

This paper presents a new 2-point diagonally implicit block method for solving system of first order ordinary differential equations. The formulae of the method will be derived by using Lagrange interpolation polynomial. This method will approximate the solution of initial value problems at two points simultaneously within a block. Predictor corrector mode will be implemented in this method with variable step size strategy. The stability region of the proposed method will be discussed. Numerical examples are given to demonstrate the performance of the method



*Keywords: Block method, ordinary differential equation, predictor-corrector, variable step size*


## Introduction

Consider the initial value problems (IVPs) for first order ordinary differential equations (ODEs) of the form

$$y' = f(x, y), \quad y(x_0) = y_0, \quad x \in [a, b]. \tag{1}$$

where $a$ and $b$ are finite. The solution of (1) has been discussed by various researchers by using various methods. Block method is one of numerical method with an advantage can obtain approximate solution at more than one point. The number of points is depending on the constructed method.

Shampine and Watts (1969) are among the earliest researchers that discovered block method for solving ODEs. Several researchers proposed block method for solving ODEs such as Mehrkanoon et al. (2010) which introduced various 2-point 2-step method for solving first order ODEs and Majid and Suleiman (2011) introduced 2-point fully implicit multistep block.

The 3-point block method for solving ODEs was presented by Majid et al. (2006) and Mehrkanoon et al. (2012). Nasir et al. (2011) and Zawawi et al. (2012) used block backward differentiation formulas for the solution of ODEs. Hybrid block method was implemented by Sagir (2014) while Odekunle et al. (2012) used 4-point block method for solving ODEs. Fatunla (1991) and Adegboye and Ahmed (2014) solved higher order ODEs by using block method.

The aim of this paper is to investigate the performance of 2-point diagonally implicit block method of order four (2PDO4). This new diagonally implicit method will consider the same order formula for first and second point.

**Formulation of 2PDO4 method**

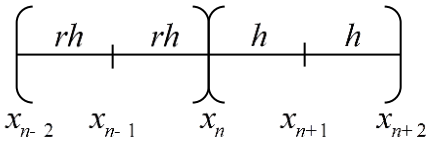


Figure 1: 2PDO4 method

The solution of $y_{n+1}$ and $y_{n+2}$ at the points $x_{n+1}$ and $x_{n+2}$ respectively were computed simultaneously in a block with the step size $h$ as in Figure 1. Three back values at the points $x_n, x_{n-1}$ and $x_{n-2}$ were used to form the corrector formula $y_{n+1}$ while two back values at the points $x_n$ and $x_{n-1}$ were used to form the corrector formula $y_{n+2}$ where each interval has step size $rh$.

Lagrange interpolation polynomial was implemented to derive predictor and corrector formulas. The sets of interpolation points involved for obtaining the corrector formula to approximate the solutions of $y_{n+1}$ and $y_{n+2}$ are $\{(x_{n-2}, f_{n-2}), (x_{n-1}, f_{n-1}), (x_n, f_n), (x_{n+1}, f_{n+1})\}$ and $\{(x_{n-1}, f_{n-1}), (x_n, f_n), (x_{n+1}, f_{n+1}), (x_{n+2}, f_{n+2})\}$ respectively. The first point $y_{n+1}$ and second point $y_{n+2}$ are derived by integrating (1) such that

$$\int y' dx = \int f(x, y) dx \qquad (2)$$

where the interval of integration for $y_{n+1}$ and $y_{n+2}$ are $[x_n, x_{n+1}]$ and $[x_n, x_{n+2}]$ respectively.

The function $f(x, y)$ in (2) is replaced by the Lagrange polynomial which interpolates the set of corresponding mentioned points. Evaluating the integral using MAPLE gives the formula for the first and second point in terms of $r$ as follows:

The first point

$$y_{n+1} = y_n + \frac{h}{2r^2(r+1)(2r+1)}\left[2r^2\left(r^2 + r + \frac{1}{4}\right) f_{n+1} + \left(r^2 + \frac{1}{2}r + \frac{1}{12}\right)(r+1)(2r+1) f_n - 2\left(\frac{1}{3}r + \frac{1}{12}\right)(2r+1) f_{n-1} + \left(\frac{1}{6}r + \frac{1}{12}\right)(r+1) f_{n-2}\right] \qquad (3)$$

and the second point,

$$y_{n+2} = y_n + \frac{h}{2r(r+1)(r+2)}\left[r\left(\frac{2}{3}r + \frac{4}{3}\right)(r+1) f_{n+2} + 2r\left(\frac{4}{3}r + \frac{4}{3}\right)(r+2) f_{n+1} + \frac{2}{3}r(r+1)(r+2) f_n\right]. \qquad (4)$$

The step size strategy in the implementation of the method is the choice for next successful step size will be restricted to double $\left(r = \frac{1}{2}\right)$ or the same as the current step

size $(r = 1)$ and when then step size failure it will be restricted to half $(r = 2)$. This is to minimize the number of formulas required to be stored.

Taking $r = 1,\ r = 2$ and $r = \frac{1}{2}$ in formula (3) and (4) yield the following first and second point of the corrector formulas for the 2PDO4 method:

For $r = 1$

$$y_{n+1} = y_n + \frac{h}{24}(9f_{n+1} + 19f_n - 5f_{n-1} + f_{n-2}) ,$$
$$y_{n+2} = y_n + \frac{h}{3}(f_{n+2} + 4f_{n+1} + f_n) . \quad (5)$$

For $r = 2$

$$y_{n+1} = y_n + \frac{h}{96}(40f_{n+1} + 61f_n - 6f_{n-1} + f_{n-2}) ,$$
$$y_{n+2} = y_n + \frac{h}{3}(f_{n+2} + 4f_{n+1} + f_n) . \quad (6)$$

For $r = \frac{1}{2}$

$$y_{n+1} = y_n + \frac{h}{6}(2f_{n+1} + 7f_n - 4f_{n-1} + f_{n-2}),$$
$$y_{n+2} = y_n + \frac{h}{3}(f_{n+2} + 4f_{n+1} + f_n). \quad (7)$$

The predictor formulas were derived similarly but with set of interpolation points $\{(x_{n-2}, f_{n-2}), (x_{n-1}, f_{n-1}), (x_n, f_n)\}$. The order of predictor formulas are one less than the corrector formulas.

**Implementation**

The choice for the next step size is important in the implementation of the method. By adopting Mehrkanoon et al. (2010), the local error estimate $LErr_k$ will be performed in a process to determine whether the next step is successful or failure. Given

$$LErr_k = |y_{n+1}^c(k+1) - y_{n+1}^c(k)|$$

where $y_{n+1}^c(k+1)$ and $y_{n+1}^c(k)$ denote the first corrector formulas of order $k+1$ and $k$ respectively. The step is said to be successful if the value of $LErr_k$ less than tolerance $TOL$ and failure otherwise. After each successful step, the next step size prediction is given by

$$h_{new} = C \times h_{old} \times \left(\frac{TOL}{LErr_k}\right)^{\frac{1}{p}}$$

where $C$ is a safety factor. To reduce the risk of rejected step, $C = 0.8$ is used. The next step size is doubled if $h_{new} > 2 \times h_{old}$, otherwise it will remain constant. If the step failure occurs, the next step size is halved.

**Order and stability region**

As referred in Fatunla (1991) and Nasir (2011), given

$$\sum_{k=0}^{j} A_k Y_{n+k} = h \sum_{k=0}^{j} B_k F_{n+k} \qquad (8)$$

as the general matrix form of linear multistep method where $A_k$ and $B_k$ are $r$ by $r$ matrices with elements $a_{lm}$ and $b_{lm}$ for $l, m = 1,2, \dots, r$ . The associated difference operator $L$ as follows

$$L[z(x); h] = \sum_{k=0}^{j} [A_k z(x+h) - hB_k z'(x+kh)] \qquad (9)$$

where $z(x)$ is the exact solution and assume to be sufficiently differentiable. $L$ is order $p$ if $C_0 = C_1 = \cdots = C_p = 0, C_{p+1} \neq 0$ . $C_{p+1}$ is called the error constant.

The general form of constant $C_q$ is defined as

$$\begin{aligned} C_0 &= \sum_{k=0}^{j} A_k \ , \\ C_1 &= \sum_{k=0}^{j} [kA_k - B_k] \ , \\ &\vdots \\ C_q &= \sum_{k=0}^{j} \left[ \frac{1}{q!} k^q A_k - \frac{1}{(q-1)!} k^{q-1} B_k \right], \quad q = 2,3, \dots, p+1 \end{aligned} \qquad (10)$$

Formula $y_{n+1}$ and $y_{n+2}$ when $r = 1$ will be considered. Hence, to obtain the order of the method, (5) is written in matrix form as follows

$$\begin{bmatrix} 1 & 0 \\ 0 & 1 \end{bmatrix} \begin{bmatrix} y_{n+1} \\ y_{n+2} \end{bmatrix} = \begin{bmatrix} 0 & 1 \\ 0 & 1 \end{bmatrix} \begin{bmatrix} y_{n-1} \\ y_n \end{bmatrix} + h \left\{ \begin{bmatrix} \frac{9}{24} & 0 \\ \frac{4}{3} & \frac{1}{3} \end{bmatrix} \begin{bmatrix} f_{n+1} \\ f_{n+2} \end{bmatrix} + \begin{bmatrix} -\frac{5}{24} & \frac{19}{24} \\ 0 & \frac{1}{3} \end{bmatrix} \begin{bmatrix} f_{n-1} \\ f_n \end{bmatrix} + \begin{bmatrix} 0 & \frac{1}{24} \\ 0 & 0 \end{bmatrix} \begin{bmatrix} f_{n-3} \\ f_{n-2} \end{bmatrix} \right\} . \qquad (11)$$

By applying (10), $C_0 = C_1 = C_2 = C_3 = C_4 = \begin{bmatrix} 0 \\ 0 \end{bmatrix}$ and $C_5 = \begin{bmatrix} -\frac{19}{720} \\ -\frac{1}{90} \end{bmatrix}$. Therefore, the method is of order four.

In order to analyzed the method stability, we consider a linear first order test problem

$$y' = f = \lambda y \ . \qquad (12)$$

The test equation (12) is substituted into the corrector formulas of 2PDO4 method (5), (6) and (7). The formulas then written in matrix form and setting the determinant to zero will give the stability polynomial. The stability polynomial of 2PDO4 method at $r = 1, r = 2$ and $r = \frac{1}{2}$ are as follows:

At $r = 1$,

$$\left( \frac{1}{8}\overline{h}^2 - \frac{17}{24}\overline{h} + 1 \right) t^4 + \left( -\overline{h}^2 - \frac{13}{12}\overline{h} - 1 \right) t^3 + \left( -\frac{1}{8}\overline{h}^2 - \frac{5}{24}\overline{h} \right) t^2 = 0, \qquad (13)$$

at $r = 2$,

$$\left(\frac{5}{36}\overline{h}^2 - \frac{3}{4}\overline{h} + 1\right)t^4 + \left(-\frac{35}{8}\overline{h}^2 - \frac{19}{16}\overline{h} - 1\right)t^3 + \left(-\frac{5}{144}\overline{h}^2 - \frac{1}{16}\overline{h}\right)t^2 = 0, \tag{14}$$

at $r = \frac{1}{2}$,

$$\left(\frac{1}{9}\overline{h}^2 - \frac{2}{3}\overline{h} + 1\right)t^4 + \left(-\frac{5}{3}\overline{h}^2 - \frac{2}{3}\overline{h} - 1\right)t^3 + \left(-\frac{4}{9}\overline{h}^2 - \frac{2}{3}\overline{h}\right)t^2 = 0 \tag{15}$$

where $\overline{h} = h\lambda$ and the stability region plotted is shown in Figure 2.

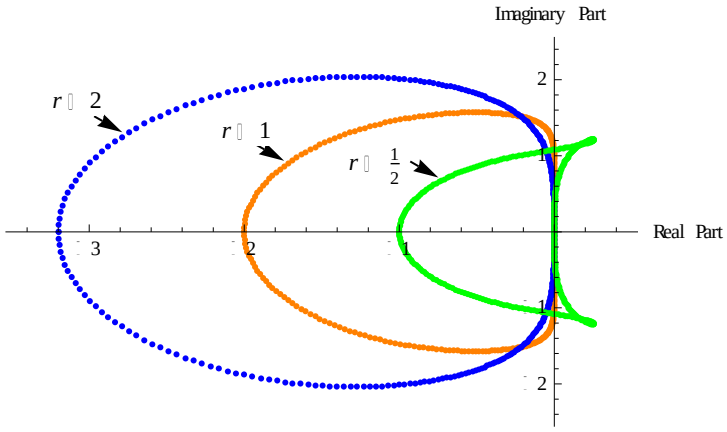


Figure 2: Stability region of 2PDO4 method

Note that in Figure 2, the stability region lies inside the boundary of dotted points. It is clear that as the step size is increased, the region of stability is getting smaller. The largest region is when the step size is halved ($r = 2$).

**Results and Discussion**

The following problems were tested to show the performance of the proposed method:

**Problem 1** (Majid (2004))

$y'_1 = y_2,\ y'_2 = 2y_2 - y_1,\ \ y_1(0) = 0, y_2(0) = 1,\ \ [0,50]$ .

**Exact solution**: $y_1(x) = xe^x, y_2(x) = (1+x)e^x$.

**Problem 2** (Majid (2004))

$y'_1 = y_2,\ y'_2 = -y_3,\ y'_3 = y_4, y'_4 = y_2 + 2e^x,$

$y_1(0) = 0, y_2(0) = -2, y_3(0) = 0, y_4(0) = 2,\ \ [0,10]$ .

**Exact solution**:

$y_1(x) = -e^x + e^{-x},\ y_2(x) = -e^x - e^{-x},\ y_3(x) = e^x - e^{-x},$

$y_4(x) = e^x + e^{-x}$ .

**Problem 3** (Majid (2004))

$y'_1 = y_2,\ y'_2 = -2y_2 - 5y_3 + 3,\ \ y'_3 = y_2 + 2y_3,$

$y_1(0) = 0,\ y_2(0) = 0, y_3(0) = 1,\ \ [0,4\pi].$

**Exact solution**:

$y_1(x) = 2\cos x + 6\sin x - 6x - 2,\ y_2(x) = -2\sin x + 6\cos x - 6 \qquad y_3(x) = 2\sin x -$

$2\cos x + 3.$

The following notations are used in the tables:

| | |
|---|---|
| TOL | Tolerance |
| MTD | Method employed |
| TS | Total steps taken |
| FS | Total failure step |
| MAXE | Magnitude of the maximum error of the computed solution |
| AVERR | Average error |
| FCN | Total function calls |
| 2PDO4 | The implementation of the 2-point diagonally implicit multistep block method of order four |
| 2P1D1 | The implementation of the 2-point 1 block diagonally implicit method (Majid (2004)) |

As referred to Mehrkanoon et al. (2010) the error calculated is defined as

$$(err_i)_t = \left| \frac{(y_i)_t - (y(x_i))_t}{A + B(y(x_i))_t} \right|$$

where $(y)_t$ is the $t$-th component of $y$. Three types of error test that resulted from the formula is absolute error test (when $A = 1, B = 0$), relative error test (when $A = 0, B = 1$) and mixed error test (when $A = 1, B = 1$). The relative error test is used for Problem 1 while absolute error test is used for Problem 2 and 3.

The maximum error and average error are defined as follows:

$$MAXE = \max_{1 \ll t \ll SSTEP} \left( \max_{1 \ll t \ll N} (err_t)_t \right)$$

and

$$AVERR = \frac{\sum_{t=1}^{SSTEP} \sum_{t=1}^{N} (err_t)_t}{(P)(N)(SSTEP)}$$

where $N$ is the number of equations in the system, $SSTEP$ is the number of successful steps and $P$ is the number of points in the block. In the code, we iterate the corrector to converge using the convergence criteria:

$$|y_{n+1}^{t+1} - y_{n+1}^{t}| < 0.1 \times TOL$$

where $t$ here is the number of iterations.

The code is written in C language. The numerical results of the tested problems are tabulated in Table 1-3. From Table 1-2 it can be seen that the maximum errors and the average errors of 2PDO4 method is still within the tolerances even though not as accurate as 2P1D1 method. We must take note that 2P1D1 method has order four formula at the first point and order five formula at the second point while 2PDO4 method has order four formula for both points. However, it is obvious that 2PDO4 is better than 2P1D1 method in term of total number of function evaluations. From Table 3, the maximum errors and

the average errors of 2PDO4 method and 2P1D1 method is comparable with 2PDO4 method is better in term of total number of function evaluations.

Table 1: Numerical results of 2P1D1 and 2PDO4 methods for solving Problem 1

| TOL | MTD | TS | FS | MAXE | AVERR | FCN |
|---|---|---|---|---|---|---|
| $10^{-2}$ | 2PDO4 | 61 | 0 | 4.32962(-2) | 1.06586(-2) | 447 |
| | 2P1D1 | 90 | 0 | 1.06814(-3) | 4.37546(-4) | 639 |
| $10^{-4}$ | 2PDO4 | 198 | 0 | 4.90948(-4) | 1.75571(-4) | 1211 |
| | 2P1D1 | 197 | 0 | 3.22407(-5) | 1.56496(-5) | 1489 |
| $10^{-6}$ | 2PDO4 | 487 | 0 | 2.09039(-6) | 7.53002(-7) | 3211 |
| | 2P1D1 | 464 | 0 | 1.32582(-6) | 3.18242(-6) | 3601 |

Table 2: Numerical results of 2P1D1 and 2PDO4 methods for solving Problem 2

| TOL | MTD | TS | FS | MAXE | AVERR | FCN |
|---|---|---|---|---|---|---|
| $10^{-2}$ | 2PDO4 | 29 | 0 | 8.69604(-3) | 6.87976(-4) | 157 |
| | 2P1D1 | 34 | 0 | 3.98536(-4) | 6.22530(-5) | 191 |
| $10^{-4}$ | 2PDO4 | 59 | 0 | 2.91545(-5) | 6.12691(-6) | 309 |
| | 2P1D1 | 59 | 0 | 4.22637(-6) | 1.04006(-6) | 373 |
| $10^{-6}$ | 2PDO4 | 115 | 0 | 3.69912(-7) | 1.09294(-7) | 639 |
| | 2P1D1 | 117 | 0 | 4.63772(-8) | 1.35866(-8) | 813 |

Table 3: Numerical results of 2P1D1 and 2PDO4 methods for solving Problem 3

| TOL | MTD | TS | FS | MAXE | AVERR | FCN |
|---|---|---|---|---|---|---|
| $10^{-2}$ | 2PDO4 | 34 | 1 | 7.66411(-2) | 2.52185(-3) | 203 |
| | 2P1D1 | 38 | 0 | 1.07756(-2) | 1.30399(-3) | 255 |
| $10^{-4}$ | 2PDO4 | 73 | 3 | 8.22941(-4) | 4.78136(-5) | 421 |
| | 2P1D1 | 68 | 0 | 1.16140(-4) | 1.91641(-5) | 529 |
| $10^{-6}$ | 2PDO4 | 167 | 2 | 9.25550(-6) | 7.14873(-7) | 987 |
| | 2P1D1 | 137 | 0 | 1.24590(-6) | 2.63405(-7) | 987 |

## Conclusion

In this paper, 2PDO4 method that has order four for first and second point approximation formulas is proposed. The maximum errors and average errors of the method are comparable or one decimal places larger than 2P1D1 method but it still within the tolerances. It can be concluded that 2PDO4 method is better in terms of function evaluations than 2P1D1 method.


## Acknowledgements

The authors acknowledge the Ministry of Higher Education Malaysia for the financial support from scholarship of Bumiputra Academic Training Scheme.


## References


Adegboye, Z. A. & Ahmed, U. I. (2014). Modification of Simpson's block hybrid multistep method for general second order ODEs. *International Journal of Science and Technology, 3(1)*, 73-77.

Fatunla, S. O. (1991). Block methods for second order ODEs. *Intern. J. of Computer Math.*, *41*, 55-63.

Majid, Z. A. (2004). *Parallel Block Methods for Solving Ordinary Differential Equations.* (Thesis). Universiti Putra Malaysia, Selangor, Malaysia.

Majid, Z. A. & Suleiman, M. (2011). Predictor-corrector block iteration method for solving ordinary differential equations. *Sains Malaysiana*, *40(6)*, 659-664.

Majid, Z. A., Suleiman, M. & Omar, Z. (2006). 3-Point Implicit Block Method for Solving Ordinary Differential Equations. *Bulletin of the Malaysian Mathematical Science Society*, *29(1)*, 23-31.

Mehrkanoon, S., Majid, Z. A. & Suleiman, M. (2010). Implementation of 2-Point 2-Step Methods for the Solution of First Order ODEs. *Applied Mathematical Science*, *4(7)*, 305-316.

Mehrkanoon, S., Majid, Z. A., Suleiman, M., Othman, K. I. & Ibrahim, Z. B. (2012). 3-Point Implicit Block Multistep Method for the Solution of First Order ODEs. *Bulletin of the Malaysian Mathematical Science Society*, *35(2A)*, 547-555.

Nasir, N. A. A. M., Ibrahim, Z. B., Suleiman, M. B. & Othman, K. I. (2011). Fifth order two-point block backward differentiation formulas for solving ordinary differential equations. *Applied Mathematical Sciences*, *5(71),* 3505-3519.

Odekunle, M. R., Adesenya, A. O., & Sunday, J. (2012). 4-point block method for direct integration of first-order ordinary differential equations. *Internatonal Journal of Engineering Research and Applictions, 2(5)*, 1182-1187.

Sagir, A. M. (2014). Numerical Treatment of Block Method for the solution of Ordinary Differential Equations. *International Journal of Mathematical, Computational, Natural and Physical Engineering*, *8(2),* 259-263.

Shampine, L. F. & Watts, H. A. (1969). Block implicit one-step methods. *Mathematics of Computation*, *23(108)*, 731-740.

Zawawi, S. M, Ibrahim, Z. B., Ismail, F & Majid, Z. A. (2012). Diagonally Implicit Block Backward Differentiation Formulas for Solving Ordinary Differential Equations. *International Journal of Mathematics and Mathematical Science*, *2012*, 1-8.

# CHAPTER 5

# NUMERICAL METHOD FOR VOLTERRA INTEGRO-DIFFERENTIAL EQUATION WITH IMPLICIT MULTISTEP BLOCK METHOD

**Abstract:**
The numerical solution of the second kind of Volterra integro-differential equation (VIDE) implementation of the implicit multistep block method is discussed in this paper. This method will approximate the solutions for the ordinary differential equation part of the VIDE at two points simultaneously using constant step size. The appropriate quadrature rule is chosen to be adapted into the implicit multistep block method for solving the integral part of VIDE. The stability region is plotted to prove the behavior of A-stable. Preliminary results from the application of the implicit multistep block method (IMBM) are given and the comparisons are made with the existing methods in order to test the efficiency of the proposed method.

*Keywords: Volterra integro-differential equation, multistep method, block method, Simpson's rule.*

## Introduction

Integro-differential equation plays major roles in mathematical modeling of the real life phenomena with several fields such as engineering, physics, biology and natural sciences. Volterra integro-differential equation happen when any equation consists of the derivative and integral of the unknown function $y(x)$. Volterra integro-differential equation are usually difficult to solve analytically. Some numerical methods of ordinary differential equation have been extended to approximate the numerical solution of Volterra integro-differential equation. Numerical integration methods for Volterra integro-differential equation has been proposed by Day (1967). Linz (1969) extended theory of stability analysis for ordinary differential equation to the integro-differential equation. Then, he proposed the combination of numerical quadrature rule and interpolation scheme for solving the problem of Volterrra integro-differential equation.

The nonlinear integro-differential equation has been studied by Chang and Day (1978) and they analyzed the properties of the nonlinear integro-differential equation. The convergence of the cyclic multistep method has been developed by Mckee (1979). He derived higher order of the cyclic multistep method for Volterra integro differential equation and implemented the quadrature rule which consists of Simpson's rule and Weddle's rule for solving the integral term in VIDE. Yuan and Tang (1990) introduced implicit Runge-Kutta method for the nonlinear integro-differential equation. They had two advantages for using implicit Runge-Kutta method in order to solve the Volterra integro-differential equation which are the stability of the method and the accuracy of the numerical results. Shaw (2000) constructed a parallel algorithm with fourth order Adam-Bashforth-Moulton predictor-corrector method and Newton Gregory quadrature rule to approximate the solution for the nonlinear Volterra integro-differential equation.

Recently, some reseachers have been interested in applying the block method on Volterrra integro-differential equation. Mohamed and Majid (2015) introduced one-step block method for the linear problem of Volterra integro differential equation. Then they extended their work on Volterra integro-differential equation using multistep block method in Mohamed and Majid (2016). Baharum et al (2018) proposed the third order of diagonally implicit multistep block method to approximate the numerical solution of VIDE. In this paper, we propose the application of implicit multistep block method to solve the second kind of Volterra integro-differential equation of the form;

$$y'(x) = F\big(x, y(x), z(x)\big), \qquad 0 \le x \le a \tag{1}$$

where

$$z(x) = \int_0^x K(x,s)y(s)\,ds. \qquad y(0) = y_0 \tag{2}$$

Comparisons are made between the proposed method with the existing method in the literature review.

**Methodology**

Regarding Majid and Suleiman (2011), the interval $[a, b]$ is divided into series of block with each block containing two points as Figure 1.

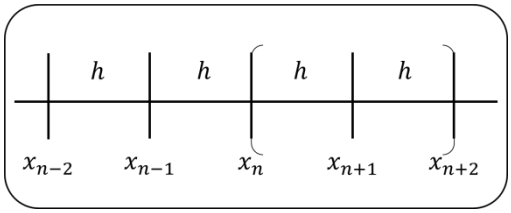


**Figure 1: Implicit multistep block method**

Equation $(1)$ will be integrated once over the interval $[x_n, x_{n+1}]$ and $[x_n, x_{n+2}]$ simultaneously with respect to $x$. Hence, the formulae of $y_{n+1}$ and $y_{n+2}$ can be determined as,

$$\int_{x_n}^{x_{n+i}} y'(x)\,dx = \int_{x_n}^{x_{n+i}} F\big(x, y(x), z(x)\big)\,dx,$$

$$y(x_{n+i}) - y(x_n) = \int_{x_n}^{x_{n+i}} F\big(x, y(x), z(x)\big)\,dx.$$

where $i = 1, 2$. The function $F\big(x, y(x), z(x)\big)$ will be approximated using the Lagrange interpolating polynomial of degree three where the interpolation points involved is four points ie $\{x_{n-2}, x_{n-1}, x_n, x_{n+1}\}$ for the first point $y_{n+1}$. Thus, taking $x = x_{n+1} + sh$, replacing $dx = hds$ and the range of the limit of integration is changed from $-1$ to $0$. The first point formula can be obtained by solving in **MAPLE** software. The formula of $y_{n+1}$ is obtained as follows,

$$y_{n+1} = y_n + h\left[\frac{1}{24}F_{n-2} - \frac{5}{24}F_{n-1} + \frac{19}{24}F_n + \frac{3}{8}F_{n+1}\right]. \quad (3)$$

However, the formula of the second point can be developed by using the Lagrange interpolating polynomial of degree three at points $\{x_{n-1}, x_n, x_{n+1}, x_{n+2}\}$. Replacing $x = x_{n+2} + sh$ and changing $dx = hds$. Then, the limit of integration will be replaced from $-2$ to $0$ and the second point formula will be obtained;

$$y_{n+2} = y_n + h\left[\frac{1}{3}F_n + \frac{3}{4}F_{n+1} + \frac{1}{3}F_{n+2}\right]. \quad (4)$$

The formula $(2)$ and $(3)$ can be rewritten in matrix form,

$$\begin{bmatrix} 0 & 0 & -1 & 1 & 0 \\ 0 & 0 & -1 & 0 & 1 \end{bmatrix} \begin{bmatrix} y_{n-2} \\ y_{n-1} \\ y_n \\ y_{n+1} \\ y_{n+2} \end{bmatrix} = h \begin{bmatrix} \frac{1}{24} & -\frac{5}{24} & \frac{19}{24} & \frac{3}{8} & 0 \\ 0 & 0 & \frac{1}{3} & \frac{4}{3} & \frac{1}{3} \end{bmatrix} \begin{bmatrix} F_{n-2} \\ F_{n-1} \\ F_n \\ F_{n+1} \\ F_{n+2} \end{bmatrix}$$

By applying similar procedure as the derivation of the corrector formulae, the predictor formulae can be developed. The predictor formulae is derived using the Lagrange interpolating polynomial of degree two and the order of the predictor formulae is one order less. According to Lambert (1973) the order of the corrector formulae can be identified and the coefficient of the error constant is determined as follows,

$$C_p = \sum_{j=0}^{k} \left( \frac{j^p \alpha_j}{p!} - \frac{j^{p-1}\beta_j}{(p-1)!} \right),$$

$$C_1 = \begin{bmatrix} 0 \\ 0 \end{bmatrix},$$

$$C_2 = \begin{bmatrix} 0 \\ 0 \end{bmatrix},$$

$$\vdots$$

$$C_5 = \begin{bmatrix} -\frac{19}{720} & -\frac{1}{90} \end{bmatrix}^T \neq 0.$$

Given $C_5 \neq 0$, then the derived method is of order four.

**Implementation**

Since $z(x)$ is the integral term in VIDE and cannot be evaluated explicitly, the numerical integration formula is adapted to the derived method for solving the integral term. The Newton-Cote quadrature formula which included Simpson's $1/3$ rule and composite Simpon's rule are appropriate is chosen to be adapted into the implicit multistep block method. Given that $n = 2, 4, 6, \ldots$, the composite Simpson's rule may be written as

$$z_{n+1} = \frac{h}{3}\sum_{i=0}^{n} \omega_i^s K(x_{n+1}, x_i, y_i) + \frac{h}{6}\left[K(x_{n+1}, x_n, y_n) + 4K\left(x_{n+1}, x_{n+\frac{1}{2}}, y_{n+\frac{1}{2}}\right) + K(x_{n+1}, x_{n+1}, y_{n+1})\right],$$

$$z_{n+2} = \frac{h}{3}\sum_{i=0}^{n+2} \omega_i^s K(x_{n+2}, x_i, y_i)$$

where $\omega_i^s$ are presented as the Simpson's rule weights which are $1,4,2,4, \ldots, 2,4,1$ and the

formula for $y_{n+\frac{1}{2}}$ can be generated from Lagrange interpolating polynomial at the points $\{x_{n-2}, x_{n-1}, x_n, x_{n+1}\}$. Therefore the formula for $y_{n+\frac{1}{2}}$ is

$$y_{n+\frac{1}{2}} = \frac{1}{16}y_{n-2} - \frac{5}{16}y_{n-1} + \frac{15}{16}y_n + \frac{5}{16}y_{n+1}.$$

**Stability region**

The stability region of the implicit multistep block method will be discussed in this section using the linear test equation of VIDE,

$$y' = \xi y(x) + \eta \int_0^x y(s)\ ds$$

where $\xi = \lambda + \mu$ and $\eta = -\lambda\mu$. The following equations represent the corresponding characteristics polynomial of the derived method and Simpson's $1/3$ rule.

1. Corrector formula for the first point

$$\rho_1(r) = r^3 - r^2, \qquad \sigma_1(r) = \frac{3}{8}r^3 + \frac{19}{24}r^2 - \frac{5}{24}r + \frac{1}{24}$$

2. Corrector formula for the second point

$$\rho_2(r) = r^4 - r^3, \qquad \sigma_2(r) = \frac{1}{3}r^4 + \frac{4}{3}r^3 + \frac{1}{3}r^2$$

3. Simpson's 1/3 rule

$$\tilde{\rho}(r) = r^2 - 1, \qquad \tilde{\sigma}(r) = \frac{1}{3}r^2 + \frac{4}{3}r + 1/3$$

The stability polynomial of these methods can be obtained after substituting the characteristic polynomial into this particular formula

$$\pi(r, h\xi, h^2\eta) = \breve{\rho}(r)[\rho(r) - h\xi\sigma(r)] - h^2\eta\breve{\sigma}(r)\sigma(r)$$

where $H_1 = h\xi$ and $H_2 = h^2\eta$. Hence, the stability polynomial of the developed method paired with the Simpson's rule is determined as,

$$\begin{aligned}\frac{2}{3}r^3H_1H_2 - \frac{1}{6}r^4H_1H_2 + \frac{1}{12}r^2H_1H_2 - \frac{2}{3}r^5H_1H_2 + \frac{1}{12}r^3H_2^2 - \frac{1}{72}r^2H_2^2 - \frac{5}{36}r^3H_2 + \frac{1}{72}r^2H_2 \\ - \frac{17}{72}r^6H_2 - \frac{131}{36}r^5H_2 + 4r^4H_2 + \frac{1}{72}r^6H_2^2 - \frac{11}{36}r^5H_2^2 + \frac{14}{9}r^4H_2^2 - \frac{5}{4}r^5H_1^2 \\ - \frac{3}{4}r^3H_1^2 - \frac{1}{8}r^2H_1^2 - \frac{2}{3}r^3H_1 - \frac{5}{24}r^2H_1 - \frac{17}{24}r^6H_1 + \frac{5}{4}r^4H_1 + \frac{1}{12}r^6H_1H_2 \\ + \frac{1}{8}r^6H_1^2 + \frac{1}{3}r^5H_1 + 2r^4H_1^2 + r^6 - 3r^5 + 3r^4 - r^3 = 0.\end{aligned}$$

By using **MAPLE** software, the stability region for the proposed methods can be illustrated and presented in the Figure 2.

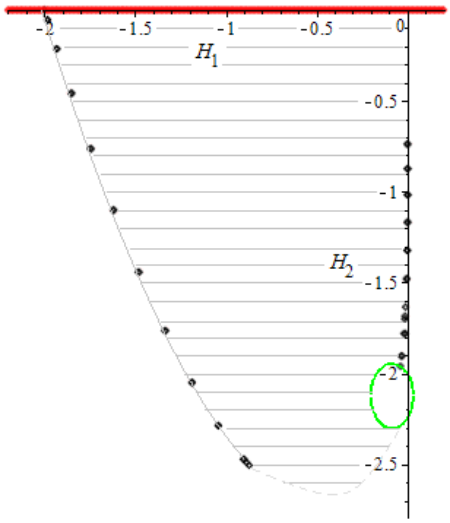


**Figure 2: Stability region for IMBM method in the H1, H2 plane.**

The stability region of these methods is $A$-stable since the region lies in the quarter plane $H_1 < 0$ and $H_2 < 0$.

**Results and Discussion**

The efficiency of the derived method, IMBM is compared with the existing methods by considering the following Problem 1 until Problem 4.

**Problem 1:** Linear VIDE

$$y'(x) = -\sin x - \cos x + \int_0^x 2\cos(x-s)\ y(s)\,ds,$$
$$y(0) = 1, \qquad 0 \le x \le 5.$$

Exact solution: $y(x) = \exp(-x)$.
Source: Chen and Zhang (2011)

**Problem 2:** Nonlinear VIDE

$$y'(x) = 2x - \frac{1}{2}\sin(x^4) + \int_0^x x^2 s\cos\big(x^2 y(s)\big)\,ds,$$
$$y(0) = 0, \qquad 0 \le x \le 2.$$

Exact solution: $y(x) = x^2$.
Source: Dehghan and Salehi (2012)

**Problem 3:** Nonlinear VIDE

$$y'(x) = x\exp\big(1 - y(x)\big) - \frac{1}{(1+x)^2} - x - \int_0^x \frac{x}{(1+s)^2}\exp\big(1 - y(s)\big)\,ds,$$
$$y(0) = 1, \qquad 0 \le x \le 4.$$

Exact solution: $y(x) = \frac{1}{1+x}$.
Source: Shaw (2000)

**Problem 4:** Nonlinear VIDE

$$y'(x) = \frac{4}{3}\exp\big(-y(x)\big) - \frac{1}{3}x^3 + \int_0^x \frac{4}{3x}s^2 \exp\big(y(s)\big)\ ds,$$
$$y(1) = 0, \qquad 1 \le x \le 2.$$

Exact solution: $y(x) = \ln(x)$.
Source: Mehdiyeva et al (2013)

These are notations that are applied in the following tables.

$h$ : Step size
ITN : Number of iterations
MAXE : Maximum error
TS : Total steps taken
TFC : Total function calls
ABM4 : Fourth order Adam-Bashforth-Moulton method with Simpson's rule.
2PBM4 : Two points multistep block method by Mohamed and Majid (2016) with Simpson's rule.
IMBM : Implicit Multistep Block Method with composite Simpson's rule.
The maximum error is defined as

$$MAXE = \max_{0 \le n \le N} |y(x_n) - y_n|$$

**Table 1: Numerical results for Problem 1**

| $h$ | Method | MAXE | TFC | TS | Time |
|---|---|---|---|---|---|
| $\frac{1}{4}$ | ABM4 | $5.4620(-04)$ | 88 | 20 | 0.0720 |
| | 2PBM4 | $4.3127(-03)$ | 64 | 11 | 0.0506 |
| | IMBM | $3.3729(-03)$ | 57 | 11 | 0.0070 |
| $\frac{1}{8}$ | ABM4 | $1.9899(-04)$ | 168 | 40 | 0.1617 |
| | 2PBM4 | $2.0203(-04)$ | 124 | 21 | 0.1096 |
| | IMBM | $7.5341(-05)$ | 117 | 21 | 0.0400 |
| $\frac{1}{16}$ | ABM4 | $2.8096(-05)$ | 328 | 80 | 0.2133 |
| | 2PBM4 | $1.8393(-05)$ | 244 | 41 | 0.2010 |
| | IMBM | $1.6808(-05)$ | 237 | 41 | 0.1040 |
| $\frac{1}{32}$ | ABM4 | $2.4801(-06)$ | 648 | 160 | 0.3328 |
| | 2PBM4 | $1.4924(-06)$ | 484 | 81 | 0.3026 |
| | IMBM | $1.4843(-07)$ | 477 | 81 | 0.1360 |

**Table 2: Numerical results for Problem 2**

| $h$ | Method | MAXE | TFC | TS | Time |
|---|---|---|---|---|---|
| $\frac{2}{9}$ | ABM4 | $4.0768(-02)$ | 45 | 8 | 0.0523 |
| | 2PBM4 | $1.0453(-01)$ | 26 | 6 | 0.0310 |
| | IMBM | $1.1208(-01)$ | 19 | 6 | 0.0050 |
| | ABM4 | $1.5832(-03)$ | 72 | 16 | 0.0823 |

| | | | | | |
|---|---|---|---|---|---|
| $\frac{2}{17}$ | 2PBM4 | $2.1837(-03)$ | 42 | 10 | 0.0471 |
| | IMBM | $8.2296(-03)$ | 35 | 10 | 0.0120 |
| $\frac{2}{33}$ | ABM4 | $1.1869(-04)$ | 141 | 32 | 0.1453 |
| | 2PBM4 | $1.1108(-04)$ | 74 | 18 | 0.0632 |
| | IMBM | $3.2810(-04)$ | 67 | 18 | 0.0160 |
| $\frac{2}{65}$ | ABM4 | $6.0167(-06)$ | 269 | 64 | 0.1987 |
| | 2PBM4 | $5.8611(-06)$ | 138 | 34 | 0.1566 |
| | IMBM | $1.6507(-05)$ | 131 | 34 | 0.0410 |

**Table 3: Numerical results for Problem 3**

| $h$ | Method | MAXE | TFC | TS | Time |
|---|---|---|---|---|---|
| $\frac{1}{40}$ | ABM4 | $1.9714(-07)$ | 648 | 160 | 0.3439 |
| | 2PBM4 | $3.6627(-07)$ | 484 | 81 | 0.2960 |
| | IMBM (ITN=3) | $7.9451(-07)$ | 477 | 81 | 0.0740 |
| | IMBM (ITN=4) | $4.2476(-08)$ | 635 | 81 | 0.0980 |
| $\frac{1}{80}$ | ABM4 | $1.3369(-08)$ | 1288 | 320 | 0.5554 |
| | 2PBM4 | $2.0834(-08)$ | 964 | 161 | 0.4999 |
| | IMBM (ITN=3) | $9.1816(-08)$ | 957 | 161 | 0.1980 |
| | IMBM (ITN=4) | $2.5564(-09)$ | 1275 | 161 | 0.2020 |
| $\frac{1}{160}$ | ABM4 | $8.7364(-10)$ | 2568 | 640 | 1.1720 |
| | 2PBM4 | $1.2376(-09)$ | 1924 | 321 | 0.8787 |
| | IMBM (ITN=3) | $1.0939(-08)$ | 1917 | 321 | 0.4350 |
| | IMBM (ITN=4) | $1.5749(-10)$ | 2555 | 321 | 0.4730 |
| $\frac{1}{320}$ | ABM4 | $5.5888(-11)$ | 5128 | 1280 | 1.8789 |
| | 2PBM4 | $7.5087(-11)$ | 3844 | 641 | 1.6850 |
| | IMBM (ITN=3) | $1.3338(-09)$ | 3837 | 641 | 1.2650 |
| | IMBM (ITN=4) | $9.7764(-12)$ | 5115 | 641 | 1.4000 |

**Table 4: Numerical results for Problem 4**

| $h$ | Method | MAXE | TFC | TS | Time |
|---|---|---|---|---|---|
| $\frac{1}{32}$ | ABM4 | $6.5536(-08)$ | 136 | 32 | 0.1325 |
| | 2PBM4 | $5.9812(-08)$ | 99 | 17 | 0.0940 |
| | IMBM (ITN=3) | $8.7625(-07)$ | 93 | 17 | 0.0070 |
| | IMBM (ITN=4) | $1.2868(-08)$ | 123 | 17 | 0.0230 |
| $\frac{1}{64}$ | ABM4 | $5.8346(-09)$ | 264 | 64 | 0.1974 |
| | 2PBM4 | $3.5212(-09)$ | 196 | 33 | 0.1753 |
| | IMBM (ITN=3) | $1.2333(-07)$ | 189 | 33 | 0.0260 |
| | IMBM (ITN=4) | $1.6238(-09)$ | 251 | 33 | 0.1080 |
| | ABM4 | $4.2190(-10)$ | 520 | 128 | 0.4003 |

| | | | | | |
|---|---|---|---|---|---|
| $\frac{1}{128}$ | 2PBM4 | $2.1345(-10)$ | 388 | 65 | 0.2810 |
| | IMBM (ITN=3) | $1.6320(-08)$ | 381 | 65 | 0.0720 |
| | IMBM (ITN=4) | $1.3081(-10)$ | 507 | 65 | 0.1670 |
| $\frac{1}{256}$ | ABM4 | $2.8199(-11)$ | 1032 | 256 | 0.6155 |
| | 2PBM4 | $1.3136(-11)$ | 772 | 129 | 0.4391 |
| | IMBM (ITN=3) | $2.0975(-09)$ | 765 | 129 | 0.1810 |
| | IMBM (ITN=4) | $9.1398(-12)$ | 1019 | 129 | 0.2060 |

The results shows the performance of the implicit multistep block method which has been derived earlier. This method is compared with two other methods which are ABM4 and 2PBM4 with the same order. In Table 1, the maximum error of IMBM is comparable compared to 2PBM4 and due to less number of total function calls and shortest execution time taken, IMBM is cheaper than ABM4 and 2PBM4 when solving the linear problem of VIDE in Problem 1.

Table 2 – 4 display the numerical results of the derived method when solving the nonlinear problem of VIDE. The results of ABM4 and 2PBM4 are slightly better compared to IMBM4 when the step size decreases. However, when the number of iteration increased, the IMBM4 is able to yield more accurate results than the other methods. The IMBM4 managed to reduce by almost half of the total steps taken of ABM4. The number of total function calls of IMBM4 at the fourth iteration is larger than 2PBM4 however, the execution time taken by IMBM4 at the fourth iteration is less than ABM4 and 2PBM4 at different step sizes. Thus, with IMBM4, the cost per step is much cheaper even with better accuracy.

## Conclusion

We have proposed the implicit multistep block method for the numerical solution of VIDE of the second kind. The implicit multistep block method have been adapted to solve the VIDE and further implemented in predictor-corrector scheme. From the numerical results, it is obviously shown that the proposed method is suitable to solve VIDE.


## Acknowledgements

This research was supported by the Ministry of Higher Education and Graduate Research Fund (GRF) from Universiti Putra Malaysia.


## References


Baharum, N. A., Majid, Z. A., & Senu, N. (2018). Solving Volterra integrodifferential equations via diagonally implicit multistep block method. *International Journal of Mathematics and Mathematical Sciences*, *2018*. https://doi.org/10.1155/2018/7392452

Chang, S. H. and Day, J. T. (1978). On the numerical solution of a certain nonlinear integro-differential equation. *Journal of Computational Physics*, *26*(2), 162–168.

Chen, H., & Zhang, C. (2011). Boundary value methods for Volterra integral and integro-differential equations. *Applied Mathematics and Computation*, *218*(6), 2619–2630.

https://doi.org/10.1016/j.amc.2011.08.001

Day, J. (1967). Note on the numerical solution of integro-differential equations. *The Computer Journal*, (1), 394–395. https://doi.org/10.1093/comjnl/9.4.394

Dehghan, M., & Salehi, R. (2012). The numerical solution of the non-linear integro-differential equations based on the meshless method. *Journal of Computational and Applied Mathematics*, *236*(9), 2367–2377. https://doi.org/10.1016/j.cam.2011.11.022

Lambert, J. D. (1973). *Computational methods in ordinary differential equations.* John Wiley and Son Ltd.

Linz, P. (1969). Linear multistep methods for Volterra integro-differential equations. *Journal of the Association for Computing Machinery*, *16*(2), 295–301. https://doi.org/10.1007/BF01399087

Majid, Z. A., & Suleiman, M. (2011). Predictor-corrector block iteration method for solving ordinary differential equations. *Sains Malaysiana*, *40*(6), 659–664.

Mckee, S. (1979). Cyclic multistep methods for solving Volterra integro-differential equations, *16*(1).

Mehdiyeva, G., Imanova, M., & Ibrahimov, V. (2013). The application of the hybrid method to solving the Volterra integro-differential equation, *I*(5), 3–7.

Mohamed, N. A., & Majid, Z. A. (2015). One-step block method for solving Volterra integro- differential equations. *AIP Conference Proceeding*. https://doi.org/10.1063/1.4932427

Mohamed, N. A., & Majid, Z. A. (2016). Multistep block method for solving volterra integro-differential equations. *Malaysian Journal of Mathematical Sciences*, *10*, 33–48.

Shaw, R. E. (2000). A parallel algorithm for nonlinear Volterra integro-differential equations. *In Proceeding of the 2000 Acm Symposium on Applied Computing*, 86–88.

Yuan, W and Tang, T. (1990). The numerical analysis of implicit Runge-Kutta methods for a certain nonlinear intgero-differential equation. *Mathematics of Computation*, *54*(189), 155–168.

# CHAPTER 6

# NUMERICAL COMPUTATION FOR SOLVING BOUNDARY VALUE PROBLEMS WITH ROBIN CONDITIONS


## Abstract

The aim of this study is to find the numerical solutions of second order linear and nonlinear boundary value problems (BVPs) with Robin boundary conditions. We implement the direct method of Adams Moulton of order four together with shooting technique to compute the approximate solutions. The missing guessing values are calculated using Newton's divided difference formula. All the formulas are verified by considering numerical examples. The numerical results are presented and compared with the exact solutions, and also with the solutions of the establish Runge-Kutta order four method. Our results provide an efficient performance and good accuracy in all cases.



*Keywords: Robin boundary conditions, shooting method, direct method, Newton's divided difference*


## Introduction

Many real life applications that related to science and engineering can be modelled using linear and nonlinear differential equations of two point boundary value problems (BVPs). Due to that, researchers are actively focusing on the investigation that involved the improvement of their method which contributes to high accuracy result. Some researchers obtained the numerical solution for second order BVPs using collocation framework including Sinc collocation method (Bialecki, 1991) and the combination with Haar wavelet (Kaur, Mittal, & Mishra 2011). Besides that, boundary value problems that deals with Dirichlet condition had been solved by Erdogan and Ozis (2011) and they had obtained the numerical result using a new kind of finite difference scheme. Later, studied by Lang and Xu (2012) present a new quantic B-spline that able to reduce computational cost and at the same time overcome the limitation occur in quadratic and cubic spline when solving BVPs with mixed conditions. Adomian decomposition method discussed in detail by Duan et al. (2013) that showed their interest in solving two point BVPs with analytic approximation solution and followed by the numerical simulation. The development of a new cubic Hermite collocation method for solving all three conditions, Dirichlet, Neumann and Robin had been considered in the study report by Ganaie, Arora, and Kukreja (2014). Again, Adomian decomposition method has been discussed by Rach et al. (2016) that highlight on solving multipoint and higher order BVPs with Robin conditions. Meanwhile, Omar (2016) solved directly second order BVPs with the implementation of conventional Taylor's approximation in deriving the approximation formula.

Numerous literatures gave more attention on solving the nonlinear BVPs compared to linear problems since nonlinear have the ability to model various phenomena in wide areas. One of the established techniques for solving nonlinear BVPs is shooting methods. Shooting methods are quite general and very straightforward in terms of problem analysis and preparation. Due to shooting behaviour that uses trial and error procedure, one attempt to get the approximate result as close as possible to the BVPs using systematic and some specific approach. Roberts and Shipman, (1967) suggested a continuation method to determine the initial guessing that possible to break out the cycle of guessing which normally occurs in the conventional shooting method. While Keller (1971) demonstrated that Newton's method gave a very powerful shooting procedure in theoretical and practical determination of missing initial condition and hence for solving the BVPs. This approach of guessing also implemented in Ha (2001) for solving nonlinear BVPs. Next, See et al. (2011) combined three iterative methods together with Newton's technique as an improvement to the iterative process in solving nonlinear problem with Dirichlet condition via shooting methods.

In this study, we are focus on solving second order BVPs subject to Robin conditions that can be written in general form as follows

$$y'' = f(x, y, y'), \quad a \le x \le b \tag{1}$$

with Robin boundary conditions

$$c_1 y'(a) + c_2 y(a) = \alpha \text{ and } c_3 y'(b) + c_4 y(b) = \beta \tag{2}$$

where $c_1 = c_2 = c_3 = c_4 \neq 0$ and $a, b, c_1, c_2, c_3, c_4, \alpha$ and $\beta$ are all constants. The BVPs as (1) will be solved using fourth order direct method via shooting technique with constant step size. The authors have used the formula derived in Majid et al. (2011) and motivated to extend their work by solving BVPs with Robin boundary conditions. In their study, they implement Newton's method as the iterative procedure to estimate the guessing values whilst in this study we will introduce Newton's interpolation technique.

## Material and Methods

The approximate solution of point $y_{n+1}$ at $x_{n+1}$ are obtained by integrating (1) once and twice. Then, to successfully evaluate the integral, the $f(x, y, y')$ term is replaced with Lagrange interpolation formulas where the number of the interpolating points chosen depend on the order of the predictor and corrector formula. In this study, we compute the solution of $y_{n+1}$ using the predictor and corrector formula as discussed in Majid et al. (2011) .

The predictor and corrector formulas of order four used is as follows

$$y'_{n+1} = y'_n + \frac{h}{12}(23 f_n - 16 f_{n-1} + 5 f_{n-2})$$
$$y_{n+1} = y_n + h y'_n + \frac{h^2}{24}(19 f_n - 10 f_{n-1} + 3 f_{n-2}). \quad (3)$$

$$y'_{n+1} = y'_n + \frac{h}{24}(9 f_{n+1} + 19 f_n - 5 f_{n-1} + f_{n-2})$$
$$y_{n+1} = y_n + h y'_n + \frac{h^2}{360}(38 f_{n+1} + 171 f_n - 36 f_{n-1} + 7 f_{n-2}). \quad (4)$$

Two additional values are required at the beginning of the calculation before continued with the multistep method procedure until the end of the interval. These starting values are obtained using one step method. This computation is adapted with shooting methods where the calculation must start with the idea of deciding the appropriate initial guess that result in "hit or miss" iterative process. For every new guessing, one step method will play a role again to give the starting values for the next new computation. All the calculation is done by developing the C programming code.

**Implementation of the shooting technique**

Let us now write (1) and (2) as

$$y'' = f(x, y, y') \text{ with } y'(a) + C_1 y(a) = V_1 \text{ and } y'(b) + C_2 y(b) = V_2 \quad (5)$$

where $C_1 = \frac{c_2}{c_1}, V_1 = \frac{\alpha}{c_1}, C_2 = \frac{c_4}{c_3}$ and $V_2 = \frac{\beta}{c_3}$.

In this study, we also represent the terminal condition as $g\left(y(b), y'(b)\right) = V_2$. Our aim in this shooting algorithm is to convert the Robin boundary value problems to two initial value problems (IVPs). Robin type required a set of initial guesses to initiate the calculation. Translate BVPs in (5) into two initial value problems (IVPs) as

$$y''_j = f(x, y_j, y'_j) \quad (6)$$

with conditions

$$\text{(i)} \quad y_0(a) = s_0, \qquad y_0'(a) = V_1 - C_1 y_0(a). \quad (7)$$

Compute the approximate solutions using the formula in (3) and (4). We obtained the first stopping condition as

$$\left| g\left(y_0(b), y'_0(b)\right) - V_2 \right| \le TOL. \quad (8)$$

If this is sufficiently close to the terminal condition, then the BVPs is solved. Otherwise, set

$$\text{(ii)} \quad y_1(a) = s_1, \qquad y_1'(a) = V_1 - C_1 y_1(a). \tag{9}$$

Repeat the entire process and obtained the second stopping condition

$$\left| g\left(y_1(b), y_1'(b)\right) - V_2 \right| \le TOL. \tag{10}$$

The starting values for $s_0$ and $s_1$ are chosen as 0 and 1 respectively based on the consideration in Robert (1979). This "hit and miss" iterative process is continued until we reached the $j^{th}$ stopping condition

$$\left| g\left(y_j(b), y_j'(b)\right) - V_2 \right| \le TOL. \tag{11}$$

The value of $y_j(a) = s_j$ can be updated by Newton's divided difference formula.

**Result and Discussion**

One linear and two nonlinear problems have been used as a tested problem to verify the accuracy and efficiency of DAM4R. The entire numerical examples used the step size of $h = 0.1, 0.05$ and $0.01$ with the $TOL = 10^{-5}$.

The following notations are used in the tables.

| | |
|---|---|
| MAXE | Maximum absolute error |
| AVE | Average absolute error |
| ITN | Total iteration of guessing values |
| TS | Total step at last iteration |
| FCN | Total function call |
| TIME | Computational times in seconds |
| *h* | Step size |
| DAM4R | Direct Adams Moulton method of order four with Robin conditions |
| RK4 | Runge-Kutta order four |
| MTD | Method |

**Problem 1** Given linear BVPs

$$y'' = y - 2\cos(x), \quad \frac{\pi}{2} \le x \le \pi$$

subject to $y'\left(\frac{\pi}{2}\right)+3y\left(\frac{\pi}{2}\right)=-1$ and $y'(\pi)+4y(\pi)=-4.$ (12)

The exact solution is $y(x)=\cos(x)$. Source : Islam and Shirin (2011).

**Problem 2** Given nonlinear BVPs

$$y''=-\frac{1}{8}(e^{-2y}+4(y')^2),\ 0\le x\le 1$$

subject to $-2y'(0)+y(0)=-1$ and $2y'(1)+y(1)=\frac{2}{3}+\log\left(\frac{3}{2}\right)$. (13)

The exact solution is $y(x)=\log\left(\frac{2+x}{2}\right)$. Source : Duan et al. (2013).

**Problem 3** Given nonlinear BVPs

$$y''=\frac{1}{2}e^{-x}(y^2+(y')^2),\ 0\le x\le 1$$

subject to $-y'(0)+y(0)=0$ and $y'(1)+y(1)=2e.$ (14)

The exact solution is $y(x)=e^x$. Source : Duan et al. (2013).

Table 1: Comparison of the numerical result for solving problem 1 with $\pi=3.141592654$

| MTD | *h* | MAXE | AVE | TS | FC | TIME | ITN |
|---|---|---|---|---|---|---|---|
| | 0.1 | 3.0066e-6 | 2.1851e-6 | 10 | 101 | 0.0203 | 3 |
| **DAM4R** | 0.05 | 4.8417e-7 | 1.2051e-7 | 20 | 49 | 0.0220 | 1 |
| | 0.01 | 1.5513e-9 | 5.5987e-10 | 100 | 114 | 0.0500 | 1 |
| | 0.1 | 2.1185e-6 | 7.6729e-7 | 10 | 240 | 0.0310 | 3 |
| **RK4** | 0.05 | 6.0277e-7 | 2.4430e-7 | 20 | 160 | 0.0230 | 1 |
| | 0.01 | 4.9887e-10 | 1.7028e-10 | 100 | 800 | 0.1567 | 1 |

Table 2: Comparison of the numerical result for solving problem 2

| MTD | *h* | MAXE | AVE | TS | FC | TIME | ITN |
|---|---|---|---|---|---|---|---|
| | 0.1 | 5.9272e-7 | 2.3282e-7 | 10 | 32 | 0.0160 | 1 |
| **DAM4R** | 0.05 | 1.1959e-9 | 7.3206e-10 | 20 | 34 | 0.0210 | 1 |
| | 0.01 | 5.5710e-12 | 2.0472e-12 | 100 | 114 | 0.0523 | 1 |
| | 0.1 | 8.6220e-8 | 5.8037e-8 | 10 | 80 | 0.0160 | 1 |
| **RK4** | 0.05 | 5.2899e-9 | 3.4351e-9 | 20 | 160 | 0.0310 | 1 |
| | 0.01 | 8.3330e-12 | 5.2482e-12 | 100 | 800 | 0.0577 | 1 |

Table 3: Comparison of the numerical result for solving problem 3

| MTD | *h* | MAXE | AVE | TS | FC | TIME | ITN |
|---|---|---|---|---|---|---|---|
| **DAM4R** | 0.1 | 7.9048e-7 | 6.5440e-7 | 10 | 56 | 0.0160 | 2 |
| | 0.05 | 6.4796e-7 | 1.9446e-7 | 20 | 64 | 0.0260 | 2 |
| | 0.01 | 1.1912e-9 | 3.3210e-10 | 100 | 228 | 0.0573 | 2 |
| **RK4** | 0.1 | 2.0701e-6 | 1.5806e-6 | 10 | 320 | 0.0260 | 4 |
| | 0.05 | 5.2405e-7 | 1.9199e-7 | 20 | 320 | 0.0234 | 2 |
| | 0.01 | 8.7853e-10 | 3.0406e-10 | 100 | 1600 | 0.0573 | 2 |

Table 1 display that MAXE for DAM4R are comparable with RK4. DAM4R also gave a superiority result in term of function calls and time computation. This output aligned with the nature of DAM4R algorithm that solved the second order BVPs directly. Among all tested problem, problem 2 gave the smallest MAXE for DAM4R and also comparable to RK4 as describe in Table 2. In addition, this result also illustrate the most efficient performance for DAM4R since the results converge rapidly with less execution time. Only one iteration is required for guessing value too sufficiently close to the end boundary for all step size. DAM4R achieved a better MAXE with less number of guessing at $h = 0.1$ than RK4 as stated in Table 3. We also observed that as the step size getting smaller, the MAXE, AVE as well as iteration for guessing decrease for both DAM4R and RK4 as shown in Tables 1 – 3.

## Conclusion

In this study, we have shown that the direct Adam Moulton formula of order four derived in Majid et al. (2011) for solving second order BVPs with Dirichlet and Neumann conditions able to be implement in solving Robin BVPs. The results also illustrate that Newton's interpolation formula is a good alternative in choosing the missing guessing values which give rapidly converge in order to satisfy the end boundary. Overall, the results of DAM4R show a good competitive performance compared to the exact value and the well-known Runge-Kutta order four method in all cases.

## Acknowledgements

The authors gratefully acknowledge the financial support received from Putra Grant (Project Code: GP-IPS/2018/9625100), Universiti Putra Malaysia (UPM) and SLAB Scholarship sponsored by the Ministry of Higher Education (MOHE), Malaysia.

## References


Bialecki, B. (1991). Sinc-Collection Methods for Two-Point Boundary Value Problems. *IMA Journal of Numerical Analysis,11*(3), 357-375.

Duan, J., Rach, R., Wazwaz, A., Chaolu, T., & Wang, Z. (2013). A new modified Adomian decomposition method and its multistage form for solving nonlinear boundary value problems with Robin boundary conditions. *Applied Mathematical Modelling,37*(20-21), 8687-8708.

Erdogan, U., & Ozis, T. (2011). A smart nonstandard finite difference scheme for second order nonlinear boundary value problems. *Journal of Computational Physics,230*(17), 6464-6474.

Ganaie, I. A., Arora, S., & Kukreja, V. K. (2014). Cubic Hermite Collocation Method for Solving Boundary Value Problems with Dirichlet, Neumann, and Robin Conditions. *International Journal of Engineering Mathematics,2014*, 1-8.

Ha, S. N. (2001). A nonlinear shooting method for two-point boundary value problems. *Computers & Mathematics with Applications,42*(10-11), 1411-1420.

Islam, M. S., & Shirin, A. (2011). Numerical Solutions of a Class of Second Order Boundary Value Problems on Using Bernoulli Polynomials. *Applied Mathematics,02*(09), 1059-1067.

Kaur, H., Mittal, R., & Mishra, V. (2011). Haar Wavelet Quasilinearization Approach for Solving Nonlinear Boundary Value Problems. *American Journal of Computational Mathematics,01*(03), 176-182.

Keller, H. B. (1971). Shooting and embedding for two-point boundary value problems. *Journal of Mathematical Analysis and Applications,36*(3), 598-610.

Lang, F., & Xu, X. (2012). Quintic B-spline collocation method for second order mixed boundary value problem. *Computer Physics Communications,183*(4), 913-921.

Majid, Z., See, P., & Suleiman, M. (2011). Solving Directly Two Point Non Linear Boundary Value Problems Using Direct Adams Moulton Method. *Journal of Mathematics and Statistics,7*(2), 124-128.

Omar, Z. (2016). Solving two-point second order boundary value problems using two-step block method with starting and non-starting values. *International Journal of Applied Engineering Research, 11(4),* 2407–2410.

Rach, R., Duan, J., & Wazwaz, A. (2016). Solution of Higher-Order, Multipoint, Nonlinear Boundary Value Problems with High-Order Robin-Type Boundary Conditions by the Adomian Decomposition Method. *Applied Mathematics & Information Sciences,10*(4), 1231-1242.

Roberts, C. E. (1979). *Ordinary differential equations: A computational approach*. Englewood Cliffs N.J.: Prentice-Hall.

Roberts, S., & Shipman, J. (1967). Continuation in shooting methods for two-point boundary value problems. *Journal of Mathematical Analysis and Applications,18*(1), 45-58.

Phang, P. S., Majid, Z. A., & Suleiman, M. (2011). Solving nonlinear two point boundary value problem using two step direct method (Menyelesaikan masalah nilai sempadan dua titik tak linear menggunakan kaedah langsung dua langkah). *Journal of Quality Measurement and Analysis*, *7*(1), 129-140.

# CHAPTER 7

# HYBRID ONE–STEP BLOCK METHOD WITH ONE-OFF STEP FOR SOLVING FIRST ORDER VOLTERRA INTEGRO-DIFFERENTIAL EQUATIONS


## Abstract

Numerical solutions of the first order linear and nonlinear Volterra integro-differential equation (VIDE) of second kind are discussed. The hybrid one-step block method with one-off step are derived using the Lagrange interpolating polynomial. VIDE is an equation which is the unknown function appears under the derivative and integral terms. Therefore, the hybrid one-step block method together with numerical quadrature rules are applied for solving the second kind of VIDE using constant step size. Two different approaches are proposed to solve for two cases where kernel equal one and kernel not equal one. Numerical results are given and the accuracy and efficiency of the schemes are discussed.



*Keywords: Volterra integro-differential equation, Lagrange interpolating polynomial, Hybrid one-step block method, Quadrature rule*


## Introduction

The linear and nonlinear integro-differential equations arise in many practical applications such as semiconductor devices, heat transfer and electrical circuit analysis. Many researchers have been working for solutions on VIDE problems as it plays an important role in real life problems. Day (1967) has presented numerical solution using quadrature rules for solving the linear integro-differential equations. In this paper, we consider the equation with difference kernels of the form Linz (1985) as

$$k(x,s) = k(xs). \tag{1}$$

The linear VIDE of the second kind is

$$y(x) = g(x) + \int_0^x k(x,s)y(s)ds. \tag{2}$$

Nonlinear VIDE, is

$$y(x) = g(x) + \int_0^x k(x,s)H(s,y(s))ds \tag{3}$$

under the conditions

i. $g(x)$ is a continuous function in $0 \leq x \leq X$.
ii. The kernel $K(x,s)$ is continuous in $0 \leq x \leq X$, $-\infty \leq y \leq \infty$.
iii. The kernel satisfies the Lipschitz condition.

$$|K(x,s,y1)K(x,s,y2)| \leq L|y1y2|$$

for all $0 \leq s \leq x \leq X$, and all $y1, y2$.

Wazwaz (2010), has used the variational iteration method (VIM) in solving the linear and nonlinear VIDE problems. Numerical results shown that the VIM method is suitable for solving the linear and nonlinear VIDE.

In recent years, several one-step methods had been applied to solve problems in VIDE of the second kind. Based on Filiz (2013a), the various methods such as Runge-Kutta, explicit and implicit Euler method have been used to solve VIDE for the ordinary differential equation (ODE) parts and quadrature rules for the integral parts. Filiz (2013b) have proposed a Runge-Kutta-Verner method and paired with Newton-Cotes quadrature rule to determine the numerical solution of nonlinear VIDE. The method has shown the applicability and efficiency in solving VIDE problems.

. Mohamed and Majid (2015) have presented a one-step block method to solve the linear VIDE problems. They have implemented the two-point block one-step method together with quadrature rules for solving VIDEs. The results indicate that the proposed block method is suitable to solve VIDEs. Therefore, we developed one-step method which is the two-point hybrid block one-step method to solve the ODE part and the composite Simpson's rule are adapted to solve the integral part of the VIDE problems.

**Derivation of Two-Point Hybrid Block One Step Method**

The two points, $y_{n+1}$ and $y_{n+2}$ are simultaneously found in a block. In the derivation of the corrector formulae, points $\{x_n, x_{n+1}, x_{n+\frac{3}{2}}, x_{n+2}\}$ are used by applying Lagrange interpolating polynomial. First, let $x_{n+1}$=$x_n + h$, therefore,

$$\int_{x_n}^{x_{n+1}} y' dx = \int_{x_n}^{x_{n+1}} F(x,y,z)dx,$$
$$y(x_{n+1}) - y(x_n) = \int_{x_n}^{x_{n+1}} F(x,y,z)dx. \quad (4)$$

$F(x,y,z)$ in (2) is replaced by applying Lagrange interpolating polynomial of order 4. Then taking $= \frac{x-x_{n+1}}{h}$ , $dx = hds$ and changing the limit of integration from -2 to -1 yield to

$$y_{n+1} = y_n + \frac{h}{6}\left(2F_n + 7F_{n+1} - 4F_{n+\frac{3}{2}} + F_{n+2}\right). \quad (5)$$

Now taking $x_{n+2} = x_{n+1} + h$ and the corrector formula is derived in the same manner. The integrating involved at the point from $x_{n+2}$ to $x_{n+1}$

$$\int_{x_{n+1}}^{x_{n+2}} y' dx = \int_{x_{n+1}}^{x_{n+2}} F(x,y,z)dx. \quad (6)$$

For the second corrector formulae, replace $dx = hds$ and change the limit of integration from -1 to 0. Solve equation (6) using MAPLE to obtain the formula as follows.

$$y_{n+2} = y_{n+1} + \frac{h}{6}\left(F_{n+1} + 4F_{n+\frac{3}{2}} + F_{n+2}\right). \quad (7)$$

Hence, the formulae of the two- point block method are

$y_{n+1} = y_n + \frac{h}{6}\left(2F_n + 7F_{n+1} - 4F_{n+\frac{3}{2}} + F_{n+2}\right)$ and

$$y_{n+2} = y_{n+1} + \frac{h}{6}\left(F_{n+1} + 4F_{n+\frac{3}{2}} + F_{n+2}\right). \quad (8)$$

The formula for the constants $C_q$ will apply to determine the order of this method. The general formula is defined as follows:

$$C_0 = \sum_{j=0}^{k} \alpha_j$$

$$C_1 = \sum_{j=0}^{k} j\alpha_j - \sum_{j=0}^{k} \beta_j - \sum_{j=1}^{k} \beta_{vj}$$

.

.

.

$C_q = \frac{1}{q!}[\sum_{j=0}^{k} j^q \alpha_j - q(\sum_{j=0}^{k} j^{q-1}\beta_j + \sum_{j=1}^{k} vj^{q-1}\beta_{vj})]$, where q= 2, 3,4, … (9)

Thus, the order of the method is four where the coefficient of error constant is

$$C_{p+1} = C_5 = \left[-\frac{31}{2880} - \frac{1}{2880}\right]^T \neq [0\ 0]^T. \quad (10)$$

Here the stability region of the method together with Simpson's rule is discussed and the method is applied to the test equation.

$$y'(x) = \xi y(x) + \eta \int_0^x y(t)dt, \quad (11)$$

where $\xi$ and $\eta$ are real constants. Therefore, from the combinations of the method the stability polynomial is obtained and from that we can plot the region of absolute stability.

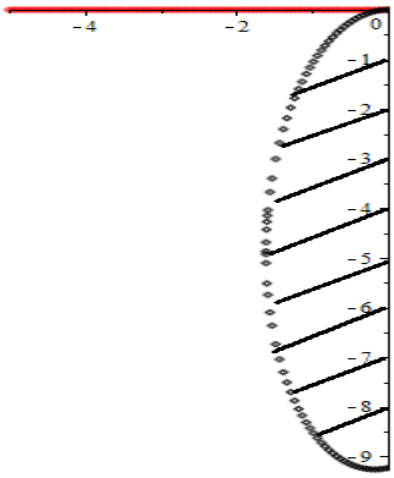


Figure 1. Stability region for hybrid block method.

Figure 1 shown the stability region for the method then the region of absolute stability lies inside the boundary.

**Implementation for Solving VIDEs**

We proposed two different type of methods as a predictor which is Euler's method and one-off step point. We will approximate $y_{n+1}$ and $y_{n+2}$ in Equation (8) by applied the block method to the differential part of VIDE. Similar technique is applied to generate the explicit method as a predictor.

$$y_{n+1}^{p} = y_n + \frac{h}{2}[F(x_n, y_n, z_n)] \quad (12)$$

$$y_{n+2}^{p} = y_{n+1} + \frac{h}{2}[F(x_{n+1}, y_{n+1}, z_{n+1})] \quad (13)$$

$$y_{n+\frac{3}{2}}^{p} = y_n + \frac{h}{8}[3F(x_n, y_n, z_n) + 9F(x_{n+1}, y_{n+1}, z_{n+1})] \quad (14)$$

$$y_{n+1}^{c} = y_n + \frac{h}{6}[2F(x_n, y_n, z_n) + 7F(x_{n+1}, y_{n+1}, z_{n+1}) - 4(F\left(x_{n+\frac{3}{2}}, y_{n+\frac{3}{2}}, z_{n+\frac{3}{2}}\right) + F(x_{n+2}, y_{n+2}, z_{n+2})] \quad (15)$$

$$y_{n+2}^{c} = y_{n+1} + \frac{h}{6}[F(x_{n+1}, y_{n+1}, z_{n+1}) + 4(F\left(x_{n+\frac{3}{2}}, y_{n+\frac{3}{2}}, z_{n+\frac{3}{2}}\right) + F(x_{n+2}, y_{n+2}, z_{n+2}). \quad (16)$$

Thus, to generate the values of $z_1$ and $z_2$ we used modified Simpson's $1/3$ and standard Simpson's $1/3$ respectively,

$$z_1 = z_0 + \frac{h}{3}\left[K(x_1, x_0, y_0) + 4K(x_1, x_{\frac{1}{2}}, y_{\frac{1}{2}}\right) + K(x_1, x_1, y_1)] \quad (17)$$

$$z_2 = z_0 + \frac{h}{3}[K(x_2, x_0, y_0) + 4K(x_2, x_1, y_1) + K(x_2, x_2, y_2)]. \quad (18)$$

Next, the values for $z_{n+1}$ and $z_{n+2}$ are calculated by applied composite Simpson's rule with interpolation schemes. Given $n = 2,4,6, \ldots$, we can formulate

$$z_{n+1} = \frac{h}{3}\sum_{i=0}^{n} \omega_i^s K(x_{n+1}, x_i, y_i) + \frac{h}{6}\left[K(x_{n+1}, x_n, y_n) + 4K\left(x_{n+1}, x_{n+\frac{1}{2}}, y_{n+\frac{1}{2}}\right) + K(x_{n+1}, x_{n+1}, y_{n+1})\right] \quad (19)$$

$$z_{n+2} = \frac{h}{3}\sum_{i=0}^{n+2} \omega_i^s K(x_{n+2}, x_i, y_i). \quad (20)$$

Here, $y_{n+\frac{1}{2}}$ is unknown value where is can be estimated using Lagrange interpolating polynomial at points $\{x_n, x_{n+1}, x_{n+2}\}$ and yield

$$y_{n+\frac{1}{2}} = y_n + \frac{h}{8}(3F_n + F_{n+1}). \quad (21)$$

**Numerical Result**

In this part, in order to validate the performance of the method, we solve four problems with different condition and we will compare the results with the existing method.

Problem 1

$y'(x) = 1 - \int_0^x y(x)ds \qquad y(0) = 0, \qquad 0 \le x \le 1$

Exact solution: $y(x) = \sin(x)$.
Source: Mohamed and Majid (2015).

Problem 2

$y'(x) = \frac{4}{3}e^{-y(x)} - \frac{1}{3}x^3 + \frac{4}{3}\int_1^x \frac{1}{x}s^2 e^{y(s)}ds \qquad y(1) = 0, \qquad 1 \le x \le 2$

Exact solution: $y(x) = \ln(x)$.
Source: Mehdiyeva et. al (2013).

Problem 3

$y_1'(x) = 1 + x + x^2 - y_2(x) - \int_0^x (y_1(s) + y_2(s))\,ds \qquad y_1(0) = 1,$

$y_2'(x) = 1 - x - x^2 + y_2(x) - \int_0^x (y_1(s) - y_2(s))\,d \qquad y_2(0) = -1.$

Exact solution: $y_1(x) = x + e^x$ and $y_2(x) = x - e^x$.
Source: Berenguer et. al (2013).

Problem 4

$$y_1'(x) = 2y_2(x) - \frac{1}{3}x^4 + \cos\left(y_1(x)\right) - 1 + \int_0^x (2s\sin\left(y_1(s)\right) + sxy_2(s))ds,$$

$$y_2'(x) = 1 - x\sin\left(y_2(x)\right) - \frac{1}{2}x^2\sin\left(y_1(x)\right) + \int_0^x (sx^2\cos\left(y_1(s)\right) + xcos(y_2(s)))ds,$$

$y_1(0) = 0$ and $y_2(0) = 0$.

Exact solution: $y_1(x) = x^2$and $y_2(x) = x$.
Source: Berenguer et. al (2013).

Table 1: Comparison between TPHB and RK4 for Problem 1

| METHOD | h | MAXE | TS | TFC | TIME(s) |
|---|---|---|---|---|---|
| TPHB | 0.025 | 2.1973E-07 | 20 | 120 | 0.0684 |
| | 0.0125 | 1.9761E-10 | 40 | 240 | 0.133 |
| | 0.00625 | 9.3579E-11 | 120 | 480 | 0.1913 |
| RK4 | 0.025 | 1.4271E-07 | 40 | 160 | 0.1398 |
| | 0.0125 | 1.7477E-08 | 80 | 320 | 0.1896 |
| | 0.00625 | 2.1622E-09 | 160 | 640 | 0.3338 |

Table 2: Comparison between TPHB and ABM4 for Problem 2

| METHOD | h | MAXE | TS | TFC | TIME(s) |
|---|---|---|---|---|---|
| TPHB | 0.03125 | 1.2976E-08 | 16 | 96 | 0.0952 |
| | 0.015625 | 7.9318E-09 | 32 | 192 | 0.1733 |
| | 0.0078125 | 9.1795E-11 | 64 | 384 | 0.2679 |
| ABM4 | 0.03125 | 6.5536E-08 | 32 | 136 | 0.3125 |
| | 0.015625 | 5.8346E-09 | 64 | 264 | 0.1974 |
| | 0.0078125 | 4.2190E-10 | 128 | 520 | 0.4003 |

Table 3: Comparison between VIM and TPHB for Problem 3

| x | VIM | | TPHB | |
|---|---|---|---|---|
| | y1 | y2 | y1 | y2 |
| 0 | 1 | -1 | 1 | -1 |
| 0.2 | 2.7480E-06 | 2.7480E-06 | 3.1317E-06 | 3.1297E-06 |
| 0.4 | 8.9999E-05 | 8.9999E-05 | 9.8759E-05 | 7.5974E-05 |
| 0.6 | 6.9492E-04 | 6.9492E-04 | 5.4976E-04 | 5.5019E-04 |
| 0.8 | 2.9578E-03 | 2.9578E-03 | 1.7953E-04 | 1.8091E-04 |
| 1 | 9.0556E-03 | 9.0556E-03 | 4.4545E-04 | 4.4499E-04 |
| TS | - | | 6 | |
| TFC | - | | 30 | |
| TIME(s) | - | | 0.01625 | |

Table 4: Comparison between VIM and TPHB for Problem 4

| x | VIM | | TPHB | |
|---|---|---|---|---|
| | y1 | y2 | y1 | y2 |
| 0 | 0 | 0 | 0 | 0 |
| 0.2 | 2.9592E-05 | 1.6362E-06 | 1.9763E-06 | 1.9971E-06 |
| 0.4 | 2.2480E-04 | 1.3064E-05 | 5.5549E-05 | 6.0917E-06 |
| 0.6 | 7.4203E-04 | 2.7894E-05 | 8.8879E-04 | 9.1919E-05 |
| 0.8 | 1.7055E-03 | 1.3135E-04 | 1.6937E-04 | 2.5859E-04 |
| 1 | 3.1011E-03 | 4.8173E-04 | 4.5179E-03 | 8.9497E-03 |
| TS | - | | 10 | |
| TFC | - | | 60 | |
| TIME(s) | - | | 0.0335 | |

$h$ Step size
TS Total of step
TFC Total function call
TIME(s) Execution time in seconds
MAXE Maximum error for the computed solution.
ABM4 Adam Bashforth of order 4 combined with approach in Case I and Case II.
TPHB Two-point hybrid block.
RK4 Runge-Kutta method of order 4 with Simpson 1/3 rule by Filiz (2013).
VIM Variational iteration method by Saberi, J. et. al (2008)

In this section, we discussed the numerical results that have been tabulated with different step sizes. The numerical result for Problem 1 presented that the TPHB method has performed better than RK4. It can be observed from the Table 1 where the maximum error for the TPHB is better than RK4. In terms of total steps, total function calls and execution time, we concluded that the TPHB is less costly than the RK4. Then, TPHB method is applied to solve kernel not equal one for the nonlinear problems and the results are shown in Table 2. When $h = 0.0078125$, the MAXE of TPHB is better than ABM4 and the number of function calls taken by TPHB is less than ABM4. The numerical results for problems 3 and 4 with $h = 0.2$ and $h = 0.1$ are presented in Table 3 and 4 respectively. We observed that the MAXE of TPHB is comparable compared to VIM.

## Conclusion

In this study, we proposed hybrid one-step block method with one-off step together with quadrature rules for solving linear and nonlinear VIDEs. We conclude that combination of the block method together with quadrature rules is appropriate for solving VIDEs. This proposed method is efficient and economically.

## Acknowledgements

This research was endorsed by Minister of Higher Education and Graduate Research Fund (GRF) from Universiti Putra Malaysia.

## References

Berenguer, M. I., Guillem A. I. G., and Galan, M. R. (2013). An Approximation Method for Solving Systems of Volterra Integro- Differential Equations. *Applied Numerical Mathematics,* 67, 126-135.

Burden, R. L. and Faires, J. D. (2005). Numerical Analysis 8th edition. Thomson.

Day, J. T. (1967). Note on the Numerical Solution of Integro-Differential Equations. *The Computer Journal*, 9:394–395.

Filiz, A. (2013). Fourth- Order Robust Numerical Method for Integro- Differential Equations. *Asian Journal of Fuzzy and Applied Mathematics*, 1(1), 28-33.

Filiz, A. (2013). Numerical Solution of a Non- linear Volterra Integro- Differential Equation via Runge- Kutta- Verner Method. *International Journal of Scientific and Research Publications*, 3, 9.

Ishak, F. and Ahmad, S. N. (2016). Development of Extended Trapezoidal Method for Numerical Soluiton of Volterra Integro- Differential Equations. *International Journal of Mathematics, Computational, Physical, Electrical and Computer Engineering*, 10(11), 52856.

Lambert, J. D. (1973). Computational Methods in Ordinary Differential Equations. John Wiley & Sons.

Lee, K. Y. and Ismail, F. (2015). Implicit Block Hybrid-Like Method for Solving System of First Order Ordinary Differential Equations. *Malaysia Journal of Science,* 34 (2), 192-198.

Linz, P. (1969). Linear Multistep Methods for Volterra Integro- Differential Equations. *Journal of the Association for Computing Machinery*, 16, 295-310.

Mehdiyeva, G., Imanova, M., and Ibrahimov, V. (2013). The Application of the Hybrid Method to Solving the Volterra Integro-Differential Equation. *Proceedings of the World Congress on Engineering* 2013., 1.

Makroglou, A. (1982). Hybrid Methods in the Numerical Solution of Volterra Integro-Differential Equations. *IMA Journal of Numerical Analysis*, 2, 21-35.

Mohamed, N. A. and Majid, Z. A. (2015). One-step Block Method for Solving Volterra Integro- Differential Equations. *In AIP Conference Proceedings,* 020018. AIP Publishing.

Saadati, R., Raftari, B., Adibi, H., Vaezpour, S. M., and Shakeri, S. (2008). A Comparison Between the Variational Iteration Method and Trapezoidal Rule for Solving Linear Integro-Differential Equations. *World Applied Sciences Journal*, 4(3):321–325.

Shampine, L. F. and Watts, H. (1969). Block Implicit One-Step Methods. *Math. Comp*., 23:731–740.

Wazwaz, A. M. (2010). The Variational Iteration Method for Solving Linear and Nonlinear Volterra Integral and Integro-Differential Equations. *International Journal of Computer Mathematics*, 87(5),1131-1141.

Wolkenfelt, P. H. M. (1982). The Construction of Reducible Quadrature Rules for Volterra Integral and Integro-Differential Equations. *IMA Journals of Numerical Analysis*, 2:131–152.

## CHAPTER 8

# DEVELOPMENT NEW TWO DERIVATIVE RUNGE-KUTTA-NYSTRöM METHOD FOR SOLVING $y'' = f(x, y, y')$


## Abstract

In this paper, we extend the classical Runge-Kutta-Nyström (RKN) methods for the general second order ordinary differential equations $y'' = f(x, y, y')$ to two derivative Runge-Kutta-Nyström methods (TDRKN) by including the third derivative of the solution that possess one evaluation of first derivative and many evaluations of second and third derivative per step. A two-stage explicit TDRKN method of order four is derived. The formulation used for the derivation of the new method is developed. The linear stability of the new method is also given. The experimental results for some problems are showed. The results obtained of numerical calculations showed that the new TDRKN method is more efficient than the standard explicit RKN methods for the general second order ordinary differential equations of the same algebraic order.



Keywords: Two Derivative Runge-Kutta-Nyström methods, Second Order Ordinary Differential Equations, Initial Value Problems.


## 1. Introduction

In this paper, consider the numerical integration of the initial value problem (IVPs) of second-order ODEs of the form:

$$y'' = f(x, y, y'), \quad y(x_0) = y_0 \quad , f: \mathcal{R} \times \mathcal{R}^n \times \mathcal{R}^n \to \mathcal{R}^n \tag{1}$$

This kind of problems arise in variety fields of applied science such as Kepler problems in quantum physics, celestial mechanics, Newton's second law in classical mechanics, LRC circuit in physics and concentration in chemical or biological problems so on, see ([1],[2],[3],[4],[14],[15]).

In recent decades, many authors have been proposed and developed several numerical methods for solving (1), for instance, A collocation approach which produces a family of order six continuous methods has been described for the approximate solution of problem (1) by Awoyemi [9]. Franco [11] constructed a type of adapted Runge-Kutta-Nyström methods (ARKN) for the numerical methods of nonstiff second order IVPs $y'' + \omega^2 y = f(x, y, y')$. Wu and Wang [6] constructed three novel multidimensional ARKN for oscillatory systems. Jator [10] derived a piecewise continuous hybrid third derivative approximation (CHTDA) that is defined for all values of the independent variable on the range of interest. You et al.[8] extended Runge-Kutta-Nyström methods (ERKN) to the integration of the general second-order differential equation in $\mathrm{y}'' + \mathrm{My} = \mathrm{f}(\mathrm{x}, \mathrm{y}, \mathrm{y}')$ where M is a positive semi-definite matrix containing implicitly the frequencies of the problem. Very recently, Chen et al. [12] extended classical RKN to two-derivative RKN methods involving the third derivative of the solution.

This paper is organized as follows. In section 2, we derived the new method of order four. The linear stability analysis of the TDRKN are discussed in section 3 and in section 4, the numerical experiment is given to show the accuracy and efficiency of the new method.

## 2. Derivation of method

In this part, a new method of two derivative Runge-Kutta-Nyström methods of order 4 is derived. For many problems in applications, the derivative the third derivative for (1) is known,

$$y^{(3)}\ (x) = \ g(x, y, y'\ ) = \ f_x + \ f_y y' + f_{y'} f\ , \qquad g: \mathcal{R} \times \mathcal{R}^n \times \mathcal{R}^n \to \mathcal{R}^n$$

A two derivative Runge-Kutta-Nyström methods obtained by using third derivative in classical Runge-Kutta-Nyström methods is given as follows:

$$y_{n+1} = y_n + hy_n' + h^2 \sum_{i=1}^{s} b_l k_i + h^3 \sum_{i=1}^{s} d_l k_i' \qquad (2)$$

$$y_{n+1}' = y_n' + h \sum_{i=1}^{s} e_l k_i + h^2 \sum_{i=1}^{s} g_l k_i'$$

$$k_i = f\left( x_n + c_i h, y_n + hy_n' + h^2 \sum_{j=1}^{s} b_l a_{i.j} + h^3 \sum_{j=1}^{s} d_l\, r_{i.j}, y_n' + h \sum_{j=1}^{s} e_l s_{i.j} + h^2 \sum_{j=1}^{s} g_l t_{i.j} \right)$$

$$k_i' = f\left( x_n + c_i h, y_n + hy_n' + h^2 \sum_{j=1}^{s} b_l a_{i.j} + h^3 \sum_{j=1}^{s} d_l\, r_{i.j}, y_n' + h \sum_{j=1}^{s} e_l s_{i.j} + h^2 \sum_{j=1}^{s} g_l t_{i.j} \right)$$

where $i = 1, \dots, s$ and $a_{i,j}\ , r_{i,j}\ , s_{i,j}\ , t_{i,j}\ , b_i\ b_i\ , d_i\ , e_i\ , g_i$ are real numbers.

An alternative expression of the scheme (2) is as follows:

$$y_{n+1} = y_n + hy'_n + h^2 \sum_{i=1}^{s} b_i f(x_n + c_i h, Y_i, Y'_i) + h^3 \sum_{i=1}^{s} d_i g(x_n + c_i h, Y_i, Y'_i) \quad (3)$$

$$y'_{n+1} = y'_n + h \sum_{i=1}^{s} e_i f\left(x_n + c_i h, Y_j, Y'_j\right) + h^2 \sum_{i=1}^{s} g_i g\left(x_n + c_i h, Y_j, Y'_j\right)$$

$$Y_i = y_n + hy'_n + h^2 \sum_{j=1}^{s} a_{i.j} f\left(x_n + c_i h, Y_j, Y'_j\right) + h^3 \sum_{j=1}^{s} r_{i.j}\, g\left(x_n + c_i h, Y_j, Y'_j\right)$$

$$Y'_i = y'_n + h \sum_{j=1}^{s} s_{i.j} f(x_n + c_i h, Y_i, Y'_i) + h^2 \sum_{j=1}^{s} t_{i.j}\, g\left(x_n + c_i h, Y_j, Y'_j\right)$$

We can rewrite (2) in Butcher tableau as follows: (see Chen et al. [12])

Table 1: Butcher tableau for TDRKN methods

| $C$ | $A$ | $R$ | $S$ | $T$ |
|---|---|---|---|---|
| | $b^T$ | $d^T$ | $e^T$ | $g^T$ |

Here, we consider $s = 2$.The simplifying condition for tow stage TDRKN methods are:

$$s_{21} = c_2, a_{21} = \frac{1}{2}c_2^2$$

From Chen et al.[12], the order conditions for two stage four order TDRKN can be given as follows:

$$b_1 + b_2 = \frac{1}{2}, e_1 + e_2 = 1, d_1 + d_2 + b_2 c_2 = \frac{1}{6}, g_1 + g_2 + e_2 c_2 = \frac{1}{2}, g_2 t_{21} = \frac{1}{24} \quad (4)$$

$$e_2 c_2^2 + 2g_2 c_2 = \frac{1}{3}, e_2 t_{21} + g_2 c_2 = \frac{1}{6}, b_2 c_2^2 + 2d_2 c_2 = \frac{1}{12}, b_2 t_{21} + d_2 c_2 = \frac{1}{24}$$

$$e_2 c_2^3 + 3g_2 c_2^2 = \frac{1}{4}, e_2 c_2 t_{21} + g_2 c_2^2 + g t_{21} = \frac{1}{8}, g_2 c_2^2 = \frac{1}{12}, e_2 r_{21} + g_2 t_{21} = \frac{1}{24}$$

By solving the system nonlinear in (4), we get a solution with two free parameters $b_2$ and $r_{21}$.

The choices $b_2 = \frac{1}{10}$ , $r_{21} = \frac{41}{1000}$ lead to the method with the coefficients:

$$c_2 = \frac{1}{2}, b_1 = \frac{2}{5}, d_1 = d_2 = \frac{7}{120}, e_1 = 1, e_2 = 0, g_1 = \frac{1}{6}, g_2 = \frac{1}{3}, s_{21} = \frac{1}{2},$$

$$a_{21} = \frac{1}{8}, t_{21} = \frac{1}{8}$$

Table 2: Butcher tableau for TDRKN2(4) method

| | | | | | | | | |
|---|---|---|---|---|---|---|---|---|
| 0 | 0 | 0 | 0 | 0 | 0 | 0 | 0 | 0 |
| $\frac{1}{2}$ | $\frac{1}{8}$ | 0 | $\frac{41}{1000}$ | 0 | $\frac{1}{2}$ | 0 | $\frac{1}{8}$ | 0 |
| | $\frac{2}{5}$ | $\frac{1}{10}$ | $\frac{7}{120}$ | $\frac{7}{120}$ | 1 | 0 | $\frac{1}{6}$ | $\frac{1}{3}$ |

## 3. Stability of the TDRKN4(2) Method

In this part, the linear stability of the TDRKN4(2) method is discussed. The following test equation will be used (see [5],[7],[12],[13] ).

$$y'' = -\omega^2 y + \varepsilon y' \tag{5}$$

Applying TDRKN methods (3) to test equation (5), we obtain

$$\begin{bmatrix} y_{n+1} \\ hy'_{n+1} \end{bmatrix} = M(v,z) \begin{bmatrix} y_n \\ hy'_n \end{bmatrix}$$

where

$$M(v,z) = \begin{bmatrix} m_{11} & m_{12} \\ m_{21} & m_{22} \end{bmatrix}$$

$m_{11} = 1 - v^2(b^T + zd^T)N_2^{-1}e - v^2(zb^T + (z^2 - v^2)d^T)N_1^{-1}(S + zT)N_2^{-1}e$
$m_{12} = 1 - v^2(b^T + zd^T)N_3 + (zb^T + (z^2 - v^2)d^T)(N_1^{-1}e - v^2N_1^{-1}(S + zT)N_3)$
$m_{21} = -v^2(e^T + zg^T)N_2^{-1}e - v^2(ze^T + (z^2 - v^2)g^T)N_1^{-1}(S + zT)N_2^{-1}e$
$m_{22} = 1 - v^2(e^T + zg^T)N_3 + (ze^T + (z^2 - v^2)g^T)(N_1^{-1}e - v^2N_1^{-1}(S + zT)N_3)$
$N_1 = I - zS - (z^2 - v^2)T$
$N_2 = I + v^2(A + zR) + v^2(zA + (z^2 - v^2)R)N_1^{-1}(S + zT)$
$N_3 = N_2^{-1}(C + (zA + (z^2 - v^2)R)N_1^{-1})e$

where $v = \omega h, z = \varepsilon h$, $\mathrm{M(v,z)}$ is called stability matrix. The stability region of TDRKN4(2) method is presented as follows:

$$S_R = \{(v;\ z) : \lambda_i(M) < 1;\ i = 1,2\}$$

$\lambda_i$ are eigenvalues of $M(v,z)$.

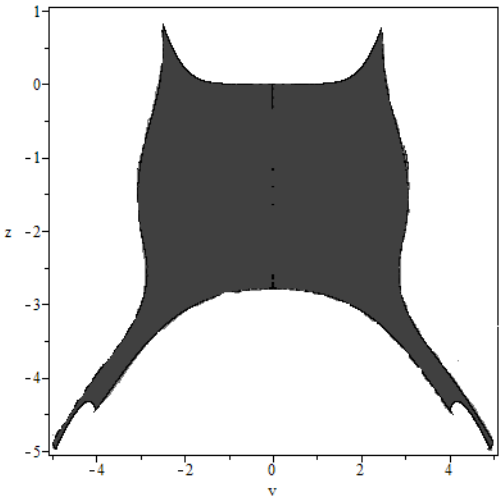


Figure 1: The absolute stability region of TDRKN4(2) method

## 4. Numerical Experiments

In this section, the effectiveness of the new method of order four tested on the some problems for comparison. The numerical methods used for comparison are given as follows:

TDRKN4(2):Two-stage fourth order two-derivative RKN method derived in this paper.
RKNG4: The classical four-stage fourth order RKN method derived in [2].
RK4: The classical four-stage fourth order RK method derived in [1].

Problem 1:

$$y'' = y' + cos(x), \qquad y(0) = -\frac{1}{2}, \qquad y'(0) = \frac{1}{2}, \qquad x_{end} = 10$$

The exact solution is:

$$y(x) = \frac{1}{2}(sin\,(x) - cos\,(x))$$

Problem 2:

$$y'' = \frac{1}{40}(10 - y)y', \qquad y(0) = 1, \qquad y'(0) = \frac{19}{80}, \qquad x_{end} = 10$$

The exact solution is: $y(x) = \frac{20}{1+19e^{\frac{-x}{4}}}$

Problem 3: [11]

$$y'' = -My + \frac{12\varepsilon}{5}Ky' + \varepsilon^2 L(x),$$

$$M = \begin{bmatrix} 13 & -12 \\ -12 & 13 \end{bmatrix}, \qquad K = \begin{bmatrix} 3 & 2 \\ -3 & -2 \end{bmatrix}, \qquad L = \begin{bmatrix} \frac{36}{5}\ sin\ (x)\ +\ 24\ sin\ (5\ x) \\ \frac{-24}{5}\ sin\ (x) - 36\ sin\ (5\ x) \end{bmatrix}$$

$$\varepsilon = 0.001, \quad y(0) = (\ \varepsilon, \varepsilon)^T, \qquad y'(0) = (-4,6)^T, \qquad x_{end} = 5$$

The exact solution is:

$$y(x) = \begin{bmatrix} sin\ (x) - \ sin\ (5\ x) + \varepsilon cos(x) \\ sin\ (x) + \ sin\ (5\ x) + \varepsilon cos(5x) \end{bmatrix}$$

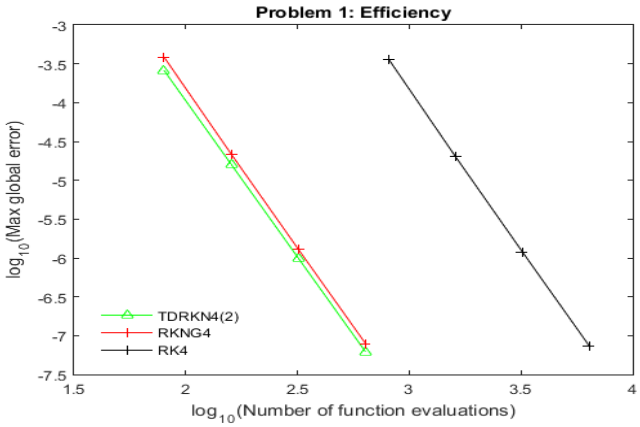


Figure 2:Efficiency curve for Problem 2 for $h\ = \frac{1}{2^i}\ , i\ =\ 1, 2, 3, 4$

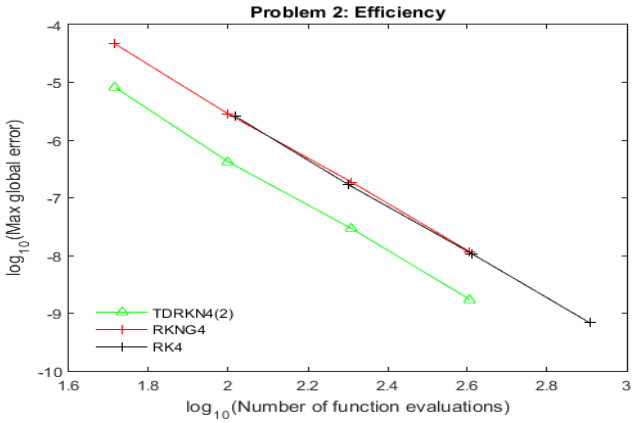


Figure 3:Efficiency curve for Problem 2 for $h\ = \frac{0.8}{2^i}, i\ =\ 0, 1, 2, 3$

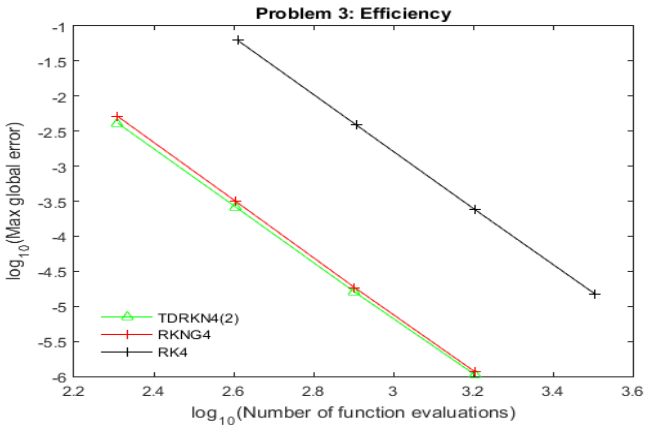


Figure 4:Efficiency curve for Problem 3 for $h = \frac{0.1}{2^i}, i = 0,1,2,3$

## 5. Discussion

In this section, the performance of the newly proposed method is examined by solving different test problems. From Figure 2, the numerical results show that the STDRKN4 method is comparable with RKNG4 and RK4 methods for all step sizes. In Figure 3, the numerical result show that the TDRKN4 method is less accurate when compared with the RK4 method for step size $h = 0.1$ and the TDRKN4 has less number of functions evaluations compared with RK4 method.
Meanwhile, the TDRKN4 method is slightly accurate than RKNG4 method for all step sizes. Figure 4, demonstrate the superiority of the TDRKN4 method over RK4 method for all step sizes. Also, TDRKN4 method has the same order of accuracy as RKNG4 method.

## 6. Conclusions

In this study, we develop a new TDRKN method for solving IVPs of second-order differential equations. In this context, we get higher order (four order) than the classical RKN methods with the same stage. So, an advantage of the TDRKN method is that they can reach higher order with fewer function evaluation (see figures 2,3,4).

## References

1. Dormand, J. R. (1996). Numerical methods for differential equations: a computational approach (Vol. 3). CRC Press.
2. E. Hairer, S. P. Norsett, G. Wanner. (2008). Solving Ordinary Differential Equations I: Nonstiff Problems, Springer-Verlag, Berlin
3. Kristensson, G. (2010). Second order differential equations: special functions and their classification. Springer Science & Business Media.
4. Holland, P. R. (1995). The quantum theory of motion: an account of the de Broglie-Bohm causal interpretation of quantum mechanics. Cambridge university press.

5. Gear, C. W. (1978). The stability of numerical methods for second order ordinary differential equations. SIAM Journal on Numerical Analysis, 15(1), 188-197.
6. Wu, X., & Wang, B. (2010). Multidimensional adapted Runge-Kutta-Nyström methods for oscillatory systems. Computer Physics Communications, 181(12), 1955-1962.
7. -Kutta-Nyström Chawla, M. M., & Sharma, S. R. (1985). Families of three-stage third order Runge methods for $y'' = f(x, y, y')$. The ANZIAM Journal, 26(3), 375-386.
8. You, X., Zhao, J., Yang, H., Fang, Y., & Wu, X. (2014). Order conditions for RKN methods solving general second-order oscillatory systems. *Numerical Algorithms*, *66*(1), 147-176
9. Awoyemi, D. O. (2001). A new sixth-order algorithm for general second order ordinary differential equations. International Journal of Computer Mathematics, 77(1), 117-124.
10. Jator, S. N. (2012). A continuous two-step method of order 8 with a block extension for $y'' = f(x, y, y')$. Applied Mathematics and Computation, 219(3), 781-791.
11. Franco, J. M. (2002). Runge–Kutta–Nyström methods adapted to the numerical integration of perturbed oscillators. Computer Physics Communications, 147(3), 770-787.
12. Chen, Z., Qiu, Z., Li, J., & You, X. (2015). Two-derivative Runge-Kutta-Nyström methods for second-order ordinary differential equations. Numerical Algorithms, 70(4), 897-927.
13. Senu, N. (2010). Runge-Kutta-Nyström methods for solving oscillatory problems , PhD Thesis, Department of Mathematics, Faculty of Science, 43400 UPM Serdang, Malaysia.
14. Lambert, J. D. (1991). Numerical methods for ordinary differential systems: the initial value problem. John Wiley & Sons, Inc.
15. Butcher, J. C. (2016). Numerical methods for ordinary differential equations. John Wiley & Sons.

# CHAPTER 9

# MHD BOUNDARY LAYER FLOW OF CARREAU FLUID OVER A STRETCHING SURFACE WITH SUCTION AND THERMAL RADIATION


## Abstract

Magnetohydrodynamics (MHD) flow of Carreau fluid over a non-linear stretching surface with suction and convective boundary condition is studied. Non-linear thermal radiation is taken into account in the heat transfer analysis. The governing partial differential equations are transformed into non-linear ordinary differential equations by using similarity variables and then solved numerically by using shooting method. The effect of non-dimensional parameters such as the suction parameter $s$, the power law index $n$, the radiation parameter $N_R$, the temperature ratio parameter $\theta_w$, the magnetic parameter $M$, the Prandtl number $Pr$ and the Biot number $\gamma$ on velocity, temperature, local skin friction and local Nusselt number are discussed and shown in table and graphs. It is found that suction causes both the fluid velocity and temperature to decrease and the presence of radiation also causes the fluid temperature to decrease.



***Keywords:*** *MHD, Carreau fluid, stretching surface, suction, thermal radiation*


## 1. Introduction

Non-Newtonian fluid is fluid that does not follow Newton's law of viscosity. The viscosity of non-Newtonian fluid depends on the shear rate. Analysis of non-Newtonian fluid has gain some attention due to its wide applications in industry and engineering. The common example of non-Newtonian fluid is pseudoplastic fluids which appear in the flow of plasma and blood, in extrusion of polymer sheets, emulsion coated sheets like photographic films, solutions and melts of high molecular weight polymers, etc. However, the rheological properties of these fluids cannot be explained by Navier-Stokes equations alone, therefore some rheological models have been presented such as the Carreau model, power law model, Ellis model, and Cross model. According to Irgens (2014), Carreau fluid was proposed by Carreau (1968) in his Ph.D. thesis from University of Wisconsin. Carreau fluid is a generalized Newtonian fluid where viscosity depends on shear rate. At low shear rate, Carreau fluid behaves as Newtonian fluid while at high shear rate it behaves as power law fluid. There have been numerous studies about Carreau fluid. A study on blood flow through tapered artery is done by Akbar & Nadeem (2014) in which the blood is considered as Carreau fluid.

The effect of induced magnetic field and heat transfer on peristaltic transport of Carreau fluid was studied by Hayat et al. (2011). Then, Vajravelu et al. (2013) studied the effect of velocity slip, temperature and concentration jump conditions on the MHD peristaltic transport of Carreau fluid. Akbar et al. (2014) discussed the MHD stagnation-point flow of Carreau fluid towards a permeable shrinking

sheet where dual solutions were obtained in this study. Later, Suneetha & Gangadhar (2015) studied the effect of thermal radiation on MHD stagnation-point flow of Carreau fluid over a shrinking surface and in this study, convective boundary condition was considered for heat transfer analysis. Further, Khan et al. (2016a) analyzed MHD stagnation-point flow and heat transfer of Carreau fluid over a stretching sheet. This study was also done by considering the convective boundary condition. Next, Khan et al. (2016b) studied the MHD flow of Carreau fluid over a stretching sheet with convective boundary condition in the presence of non-linear thermal radiation. The heat and mass transfer in MHD Carreau fluid with thermal radiation and cross diffusion is then studied by Machireddy & Naramgari (2016). The effects of multiple slip on MHD flow of Carreau fluid along wedge with chemical reaction is studied by Khan & Hashim (2016). On the other hand, Shah et al. (2017) discussed on MHD Carreau fluid slip flow over a porous stretching sheet with variable thickness and thermal conductivity with viscous dissipation and thermal radiation. Hashim et al. (2017) studied the stagnation-point flow of MHD Carreau fluid over a shrinking sheet in the presence of non-linear thermal radiation. Recently, Hayat et al. (2017) studied the boundary layer flow of MHD Carreau fluid in the presence of Newtonian heating, chemical reaction and thermal radiation.

Inspired by previous studies, this paper will study on the MHD flow of Carreau fluid with suction over a stretching sheet with convective boundary condition. The presence of non-linear thermal radiation is taken into account in the heat transfer analysis.

## 2. Mathematical Formulation

Consider a steady, laminar, two-dimensional boundary layer flow and heat transfer of an incompressible Carreau fluid over a stretching sheet with convective boundary condition. The flow is generated by non-linear stretching of the sheet resulting from the application of two equal and opposite forces. The Cartesian coordinates $x$ and $y$ are used such that $x$-axis is along the stretching sheet and $y$-axis is perpendicular to it. It is assumed that the flow of the fluid is confined to $y \geq 0$ as shown in Fig. 1. Magnetic field of strength $B_0$ is applied in the direction normal to the flow and the induced magnetic field is neglected by the assumption of small magnetic Reynolds number. Non-linear thermal radiation is taken into account in the heat transfer analysis.

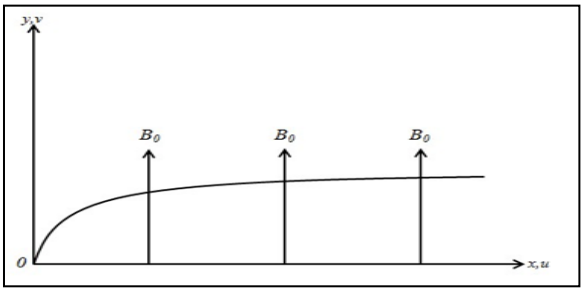


**Fig. 1.** Schematic diagram of the problem.

The governing equations of mass, momentum and energy for the subjected problems are as follows,

$$\frac{\partial u}{\partial x}+\frac{\partial v}{\partial y}=0 \tag{1}$$

$$u\frac{\partial u}{\partial x}+v\frac{\partial u}{\partial y}=\nu\frac{\partial^2 u}{\partial y^2}\left[1+\Gamma^2\left(\frac{\partial u}{\partial y}\right)^2\right]^{\frac{n-1}{2}}$$

$$+\nu(n-1)\Gamma^2\frac{\partial^2 u}{\partial y^2}\left(\frac{\partial u}{\partial y}\right)^2\left[1+\Gamma^2\left(\frac{\partial u}{\partial y}\right)^2\right]^{\frac{n-3}{2}}-\frac{\sigma B_0^2}{\rho}u \tag{2}$$

$$u\frac{\partial T}{\partial x}+v\frac{\partial T}{\partial y}=\alpha\frac{\partial^2 T}{\partial y^2}-\frac{1}{\rho c_p}\frac{\partial q_r}{\partial y} \tag{3}$$

with the boundary conditions

$$u=U_w(x)=bx^m,\qquad v=v_w,\qquad -k\frac{\partial T}{\partial y}=h_f\left(T_f-T\right)\quad \text{at}\quad y=0 \tag{4}$$

$$u\to 0,\qquad T\to T_\infty\quad \text{as}\quad y\to\infty \tag{5}$$

where $u$ and $v$ are the velocity components along the $x$ and $y$ directions respectively, $\rho$ is the fluid density, $\nu=\frac{\mu}{\rho}$ is the kinematic viscosity of the fluid, $\Gamma$ is the material constant called relaxation time, $\sigma$ is the electrical conductivity of the fluid, $n$ is the power law index, $T$ is the fluid temperature, $q_r$ is the radiative heat flux, $\alpha=\frac{k}{\rho c_p}$ is the thermal diffusivity with $c_p$ represents the specific heat and $k$ represents thermal conductivity of the fluid, $U_w(x)$ is the non-linear velocity with positive real number parameters, $b$ and $m$ that are related to stretching speed, $v_w$ is the mass transfer velocity, $h_f$ is the convective heat transfer coefficient, $T_f$ is the convective fluid temperature below the moving sheet and $T_\infty$ is the ambient fluid temperature.

Power law index, $n$ is used to determine the fluid behaviour. When the power law index $n=1$, it describes the fluid as Newtonian fluid. On the other hand, if $n$ is in the range of $0<n<1$, the fluid is said to be shear-thinning fluid and when $n>1$, the fluid is described as shear-thickening fluid. Based on Khan et al. (2016b), the radiative heat flux expression in Eq. (3) can be simplified using the Rosseland approximation,

$$q_r=-\frac{4\sigma^*}{3k^*}\frac{\partial T^4}{\partial y} \tag{6}$$

where $\sigma^*$ is the Stefan-Boltzmann constant and $k^*$ is the mean absorption coefficient. In considering the boundary layer flow over a horizontal flat plate, Eq. (6) can also be written as:

$$q_r=-\frac{16\sigma^*}{3k^*}T^3\frac{\partial T}{\partial y} \tag{7}$$

By substituting Eq. (7) into Eq. (3), we obtain,

$$u\frac{\partial T}{\partial x}+v\frac{\partial T}{\partial y}=\frac{\partial}{\partial y}\left[\left(\alpha+\frac{16\sigma^* T^3}{3k^*\rho c_p}\right)\frac{\partial T}{\partial y}\right] \tag{8}$$

Next, we introduce the following dimensionless variables to simplify the mathematical analysis using similarity transformations,

$$\psi(x,y)=\sqrt{\frac{2\nu b}{m+1}}x^{\frac{m+1}{2}}f(\eta),\qquad \eta=y\sqrt{\frac{b(m+1)}{2\nu}}x^{\frac{m-1}{2}},\qquad \theta(\eta)=\frac{T-T_\infty}{T_f-T_\infty} \quad (9)$$

where $\eta$ is the similarity variable and $\psi$ is the stream function given by

$$u=\frac{\partial\psi}{\partial y}\qquad \text{and}\qquad v=-\frac{\partial\psi}{\partial x} \quad (10)$$

From Eq. (9), we obtain

$$T=T_\infty[1+(\theta_w-1)\theta]\qquad \text{with}\qquad \theta_w=\frac{T_f}{T_\infty} \quad (11)$$

where $\theta_w>1$ is the temperature ratio parameter.

By substituting Eq. (9) – (11) into Eq. (1), (2), (4), (5) and (8), we obtain

$$[1+nWe^2(f'')^2][1+We^2(f'')^2]^{\frac{n-3}{2}}f'''+ff''-\left(\frac{2m}{m+1}\right)(f')^2-M^2f'=0 \quad (12)$$

$$\theta''+Prf\theta'+\frac{4}{3N_R}\frac{d}{d\eta}[(1+(\theta_w-1)\theta)^3\theta']=0 \quad (13)$$

$$f(0)=s,\qquad f'(0)=1,\qquad \theta'(0)=-\gamma[1-\theta(0)]\qquad \text{at}\qquad \eta=0 \quad (14)$$

$$f'(\infty)\to 0,\qquad \theta(\infty)\to 0\qquad \text{as}\qquad \eta\to 0 \quad (15)$$

where the prime represents ordinary derivative with respect to $\eta$.

In the above equation, the local Weissenberg number, $We^2=\frac{b^3(m+1)\Gamma^2x^{3m-1}}{2\nu}$, the magnetic parameter, $M^2=\frac{2\sigma B_0^2}{\rho b(m+1)x^{m-1}}$, the Prandtl number, $Pr=\frac{\mu c_p}{k}$, the non-linear radiation parameter, $N_R=\frac{kk^*}{4\sigma^*T_\infty^3}$ and the local Biot number, $\gamma=\frac{h_f}{k}\sqrt{\frac{2\nu}{b(m+1)}}x^{\frac{1-m}{2}}$. The mass transfer parameter is $s=-v_w\left(\sqrt{\frac{2}{\nu b(m+1)}}x^{\frac{1-m}{2}}\right)$ where $s>0$ for suction and $s<0$ for injection.

The local skin friction coefficient, $C_{fx}$ and the local Nusselt number, $Nu_x$ are given as follows

$$C_{fx}=\frac{\tau_w}{\rho U_w^2(x)},\qquad Nu_x=\frac{xq_w}{k(T_f-T_\infty)} \quad (16)$$

where $\tau_w$ is the wall shear stress and $q_w$ is the wall heat transfer given by

$$\tau_w=\eta_0\frac{\partial u}{\partial y}\left[1+\Gamma^2\left(\frac{\partial u}{\partial y}\right)^2\right]^{\frac{n-1}{2}}\Bigg|_{y=0},\qquad q_w=-k\left(\frac{\partial T}{\partial y}\right)_w+(q_r)_w \quad (17)$$

Substituting Eq. (17) into Eq. (16), we obtain

$$Re^{1/2}C_{fx}=\sqrt{\frac{m+1}{2}}f''(0)\left[1+We^2\left(f''(0)\right)^2\right]^{\frac{n-1}{2}} \quad (18)$$

$$Re^{-1/2}Nu_x=-\sqrt{\frac{m+1}{2}}\theta'(0)\left[1+\frac{4}{3N_R}[1+(\theta_w-1)\theta(0)]^3\right] \quad (19)$$

where $Re=\frac{bx^{m+1}}{\nu}$ is the local Reynolds number.

## 3. Results and Discussion

The non-linear ordinary differential equations in Eq. (12) and Eq. (13) subject to the boundary conditions (14) and (15) are solved numerically by using shooting method. The accuracy of the results is then validated by comparing the obtained results with the published results of Khan et al. (2016b). The results are found to be in excellent agreement as shown in Table 1. In current work, the numerical computations are done for various values of different parameters such as the suction parameter $s$, the power law index $n$, the radiation parameter $N_R$, the temperature ratio parameter $\theta_w$, the magnetic parameter $M$, the Prandtl number $Pr$ and the Biot number $\gamma$. As shown in Table 1, the magnitude of skin friction, $\left|Re^{1/2}C_{fx}\right|$ is larger in shear-thickening fluid compared to shear-thinning fluid. Besides that, the magnitude of skin friction are noted to increase as suction, $s$ and magnetic field, $M$ increase. This shows that the magnitude of the wall shear stress becomes bigger in the presence of suction and magnetic field. On the other hand, the local Nusselt number, $Re^{-1/2}Nu_x$ increases as suction parameter increases and drops in the presence of magnetic field. This indicates that strong magnetic field cause the heat transfer rate to be low.

**Table 1.** Values of the local skin friction $Re^{1/2}C_{fx}$ and local Nusselt number $Re^{-1/2}Nu_x$ for various $s, n$ and $M$ when $We = 2.0, Pr = 1.5, N_R = 1.0, \theta_w = 1.5, \gamma = 0.3$ and $m = 1.5$ are fixed.

| | | Khan et al. (2016b) | | | | Present Work | | | |
|---|---|---|---|---|---|---|---|---|---|
| $s$ | $M$ | $Re^{1/2}C_{fx}$ | | $Re^{-1/2}Nu_x$ | | $Re^{1/2}C_{fx}$ | | $Re^{-1/2}Nu_x$ | |
| | | $n = 0.5$ | $n = 1.5$ | $n = 0.5$ | $n = 1.5$ | $n = 0.5$ | $n = 1.5$ | $n = 0.5$ | $n = 1.5$ |
| 0 | 0.0 | -0.976815 | -1.345810 | 0.585077 | 0.613299 | -0.976815313 | -1.345803403 | 0.5850848794 | 0.6132870287 |
| | 0.5 | -1.057526 | -1.503946 | 0.565682 | 0.604028 | -1.057525483 | -1.503939381 | 0.5656770253 | 0.6040259460 |
| | 1.0 | -1.248588 | -1.918569 | 0.513053 | 0.579931 | -1.248576757 | -1.918552479 | 0.5131265403 | 0.5799214527 |
| 1 | 0.0 | - | - | - | - | -1.573984257 | -2.071448289 | 0.7037868742 | 0.7146529888 |
| | 0.5 | - | - | - | - | -1.647219540 | -2.219090906 | 0.7020684494 | 0.7138851187 |
| | 1.0 | - | - | - | - | -1.824302871 | -2.614341401 | 0.6982639891 | 0.7117744181 |
| 2 | 0.0 | - | - | - | - | -2.448630233 | -2.964784438 | 0.7431971906 | 0.7469205180 |
| | 0.5 | - | - | - | - | -2.500584263 | -3.092346078 | 0.7430922037 | 0.7467568847 |
| | 1.0 | - | - | - | - | -2.634510420 | -3.445822689 | 0.7427380320 | 0.7465746403 |
| 3 | 0.0 | - | - | - | - | -3.467001222 | -3.946967718 | 0.7583392762 | 0.7597571380 |
| | 0.5 | - | - | - | - | -3.501136581 | -4.056735323 | 0.7582327878 | 0.7597423250 |
| | 1.0 | - | - | - | - | -3.594470379 | -4.368177671 | 0.7581870877 | 0.7596830341 |
| 4 | 0.0 | - | - | - | - | -4.540149433 | -4.975366216 | 0.7654269701 | 0.7661278676 |
| | 0.5 | - | - | - | - | -4.563428644 | -5.071227374 | 0.7654203670 | 0.7661148681 |
| | 1.0 | - | - | - | - | -4.629166048 | -5.347576538 | 0.7654137638 | 0.7661083662 |

The effect of the suction parameter $s$ on the fluid velocity and temperature are shown in Fig. 2 and Fig. 3 respectively. $M > 0$ indicates the case of hydromagnetic flow while $M = 0$ indicates the hydrodynamic flow. Based on Fig. 2, it can be seen that as the suction parameter, $s$ increases, the fluid velocity, $f'(\eta)$ decreases. In the presence of magnetic field where $M > 0$, the velocity curves are nearer to the surface. This indicates that the fluid velocity is lower and the momentum boundary layer thickness is smaller in the presence of magnetic field. In Fig. 3, suction causes the fluid temperature, $\theta(\eta)$ to decrease. It can also be seen in Fig. 3 that the temperature curves become further from

the surface when magnetic field is applied to the fluid. Thus, the temperature is higher and the thermal boundary layer thickness is bigger in the presence of magnetic field. These results can be explained by the presence of Lorentz force in the flow. According to Lok et al. (2011), Lorentz force is a drag-like force that is produced when magnetic field is applied to an electrically conducting fluid. Therefore, the increase in magnetic parameter will results to a stronger Lorentz force. This force provides resistance against the flow velocity which then induces the temperature field and cause the fluid temperature to increase.

Next, Fig. 4 shows the effect of the radiation parameter, $N_R$ on the fluid temperature, $\theta(\eta)$ in the presence and absence of suction. The temperature and thermal boundary layer thickness decreases as the radiation parameter increases. As we discussed before, the presence of suction reduces the fluid temperature. In Fig. 5, the large temperature ratio parameter, where $\theta_w > 1$ indicates that the wall temperature, $T_f$ is higher than the ambient fluid temperature, $T_\infty$. As a result, the temperature of the fluid rises. The thermal boundary layer thickness becomes larger as the temperature ratio parameter increases. However, it can be noticed that the thermal boundary layer thickness reduces significantly when suction is applied.

Then, the influence of local Biot number, $\gamma$ on the dimensionless temperature is illustrated in Fig. 6. If the local Biot number, $\gamma$ is larger than 0.1, it implies that heat convection occur between the stretching sheet and the fluid. This will eventually increase the temperature of the fluid. The thermal boundary layer thickness becomes thicker as the local Biot number increases. When suction is applied, the thermal boundary layer thickness becomes thinner. Last but not least, Fig. 7 shows the effect of Prandtl number, $Pr$ on the temperature in the presence and absence of suction. The small value of Prandtl number indicates that the fluid has high thermal conductivity. Therefore, the smaller the value of Prandtl number, the higher the fluid temperature. This can be observed from Fig. 7 where the thermal boundary layer thickness becomes thicker with small Prandtl number. As expected, the thermal boundary layer thickness becomes thinner when suction is applied.

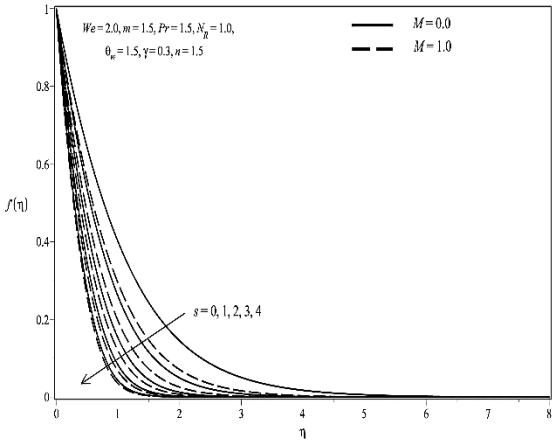


**Fig. 2. Effect of the suction parameter $s$ on the dimensionless velocity $f'(\eta)$.**

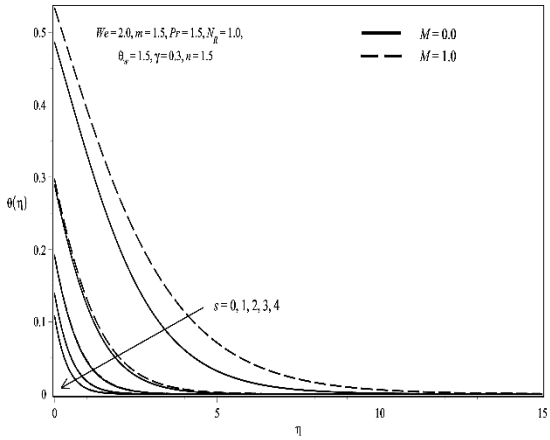


**Fig. 3. Effect of the suction parameter $s$ on the dimensionless temperature $\theta(\eta)$.**

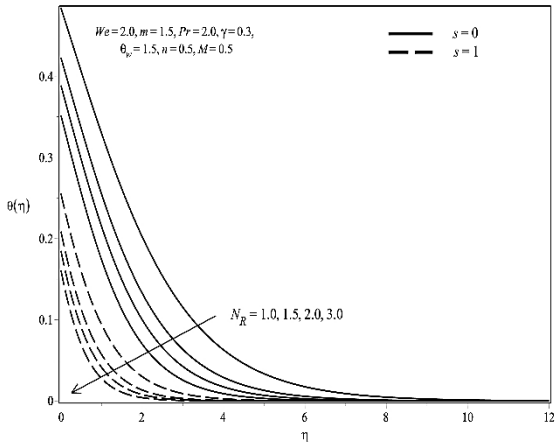


**Fig. 4. Effect of the radiation parameter $N_R$ on the dimensionless temperature $\theta(\eta)$.**

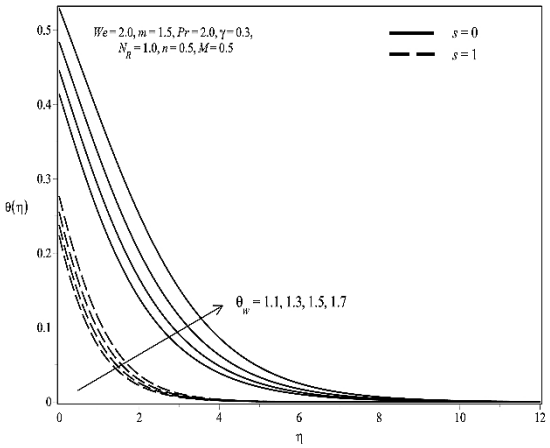


**Fig. 5. Effect of the temperature ratio parameter $\theta_w$ on the dimensionless temperature $\theta(\eta)$.**

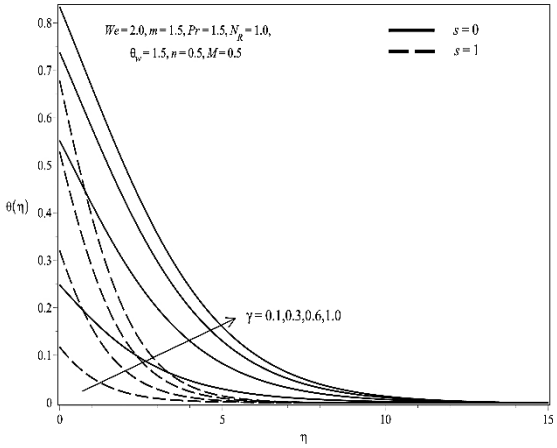


**Fig. 6. Effect of the Biot number $\gamma$ on the dimensionless temperature $\theta(\eta)$.**

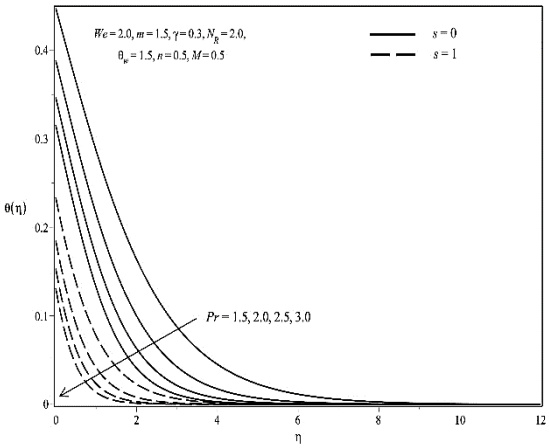


**Fig. 7. Effect of the Prandtl number $Pr$ on the dimensionless temperature $\theta(\eta)$.**

## 4. Conclusion

The MHD flow of Carreau fluid with suction over a non-linear stretching sheet with the presence of non-linear thermal radiation is investigated. Convective boundary condition is applied for heat transfer analysis. Rosseland approximation is used to simplify the radiative heat flux expression. The governing boundary layer equations along with the boundary conditions are transformed using the similarity variables before being solved numerically by using shooting method.

It is found that the presence of magnetic field causes the fluid velocity to decrease and the temperature to increase while the presence of suction reduces the fluid velocity and temperature. As radiation parameter increases, the temperature of the fluid decreases. The large value of local Biot number corresponds to high heat transfer rate between the sheet and the fluid causes the fluid temperature to increase.

Acknowledgement

The authors gratefully acknowledged the financial support received in the form of Putra Grant with grant number 9570600 from Universiti Putra Malaysia.

References

Akbar, N., Nadeem, S., Haq, R., & Ye, S. (2014). MHD stagnation point flow of Carreau fluid toward a permeable shrinking sheet: Dual solutions. *Ain Shams Engineering Journal*, 5(4), 1233 – 1239.

Carreau, P.J. (1968). (PhD thesis). University of Wisconsin.

Akbar, N., & Nadeem, S. (2014). Carreau fluid model for blood flow through a tapered artery with a stenosis. *Ain Shams Engineering Journal*, 5(4), 1307 – 1316.

Hashim, Khan, M., & Alshomrani, A. (2017). Numerical simulation for flow and heat transfer to Carreau fluid with magnetic field effect: Dual nature study. *Journal of Magnetism and Magnetic Materials*, 443, 13 – 21.

Hayat, T., Saleem, N., Asghar, S., Alhothuali, M., & Alhomaidan, A. (2011). Influence of induced magnetic field and heat transfer on peristaltic transport of a Carreau fluid. *Communications in Nonlinear Science and Numerical Simulation*, 16(9), 3559 – 3577.

Hayat, T., Ullah, I., Ahmad, B., & Alsaedi, A. (2017). Radiative flow of Carreau liquid in presence of Newtonian heating and chemical reaction. *Results in Physics*, 7, 715 – 722.

Irgens, F. (2014). Generalized Newtonian Fluids. In *Rheology and non-Newtonian Fluids* (pp. 113 – 124). Springer International Publishing.

Khan, M., & Hashim. (2016). Effects of multiple slip on flow of magneto-Carreau fluid along wedge with chemically reactive species. *Neural Computing and Applications*.

Khan, M., Hashim, & Alshomrani, A. (2016a). MHD stagnation-point flow of a Carreau fluid and heat transfer in the presence of convective boundary conditions. *PLOS ONE*, 11(6), 1 – 22.

Khan, M., Hashim, Hussain, M., & Azam, M. (2016b). Magnetohydrodynamic flow of Carreau fluid over a convectively heated surface in the presence of non-linear radiation. *Journal of Magnetism and Magnetic Materials*, 412, 63 – 68.

Lok, Y., Ishak, A., & Pop, I. (2011). MHD stagnation point flow with suction towards a shrinking sheet. *Sains Malaysiana*, 40(10), 1179 – 1186.

Machireddy, G., & Naramgari, S. (2016). Heat and mass transfer in radiative MHD Carreau fluid with cross diffusion. *Ain Shams Engineering Journal*.

Suneetha, S., & Gangadhar, K. (2015). Thermal radiation effect on MHD stagnation point flow of a Carreau fluid with convective boundary condition. *Open Science Journal of Mathematics and Application*, 3(5), 121–127.

Shah, R., Abbas, T., Idrees, M., & Ullah, M. (2017). MHD Carreau fluid slip flow over a porous stretching sheet with viscous dissipation and variable thermal conductivity. *Boundary Value Problems*, 2017(1).

Vajravelu, K., Sreenadh, S., & Saravana, R. (2013). Combined influence of velocity slip, temperature and concentration jump conditions on MHD peristaltic transport of a Carreau fluid in a non-uniform channel. *Applied Mathematics and Computation*, 225, 656 – 676.

# CHAPTER 10

# HEAT TRANSFER CHARACTERISTICS OF MHD STAGNATION-POINT FLOW OF CARREAU FLUID OVER A SHRINKING SHEET


## Abstract

In this paper, the problem of the magnetohydrodynamic (MHD) stagnation-point flow and heat transfer Carreau fluid toward a permeable shrinking sheet is studied. The governing boundary layer equations are transformed into a set of ordinary differential equation using the local similarity approach and then is solved numerically via the shooting method. Numerical results for different values of governing parameters on the heat transfer characteristics are presented and discussed. In this study, the existence of dual solutions of the problem is observed. It is also found that for various values of Prandtl number, the boundary layer separation occurs at the same turning point.



*Keywords: Boundary layer, Carreau fluid, Dual solutions, Magnetohydrodynamic*


## Introduction

A stagnation-point flow is a point in a flow field where the local velocity of the fluid is zero. A study on magnetohydrodynamic (MHD) stagnation-point flow has many important applications in engineering. For example in metallurgical, drawing, annealing, and tinning of copper wires processes, involve the cooling of continuous strips by drawing them through a quiescent fluid (Ali et al., 2011). Hiemenz (1911) studied a two-dimensional flow of a fluid near a stagnation-point in boundary layer flow. Other researchers extended the stagnation-point flow problem in various ways. For instance, Nazar et al. (2004) studied an unsteady two-dimensional stagnation-point flow of an incompressible viscous fluid over a flat deformable sheet and Ali et al. (2011, 2014) investigated the problems of mixed convection stagnation-point flow on a vertical stretching sheet with induced magnetic field and external magnetic field, respectively.

In non-Newtonian fluid, Sadeghy et al. (2006) investigated the problem of two-dimensional stagnation-point flow of viscoelastic fluids theoretically. The steady MHD mixed convection flow of a viscoelastic fluid in the vicinity of two-dimensional stagnation-point flow with magnetic field has been investigated by Kumari and Nath (2009). Both studies assumed that the fluid obeys the upper-convected Maxwell model. In micropolar fluid, Ishak et al. (2008) studied the problem of MHD flow towards a stagnation-point on a vertical surface.

In this present paper, we extend the work done by Akhbar et al. (2014) by obtaining the heat transfer characteristics where Akhbar et al. (2014) studied the dual solutions of MHD stagnation-point flow of Carreau fluid toward a permeable shrinking sheet problem.

Carreau fluid is a type of generalized Newtonian fluid. At low shear rate Carreau fluids behaves as a Newtonian fluid when the power law index, $n=1$ and at high shear rate as power law fluid. For $n<1$, the Carreau fluid gives pseudoplastic that is non-Newtonian, or shear-thinning fluids have a lower apparent viscosity at higher shear rates and for $n>1$ the Carreau fluid behaves as Dilatant which is non-Newtonian, or shear-thickening fluids increase in apparent viscosity at higher shear rates (Akhbar & Nadeem, 2014).

**Problem formulation**

Consider a two-dimensional stagnation-point flow of an incompressible Carreau fluid over a wall coinciding with plane $y=0$, the flow is being confined to $y>0$. The flow is generated due to the linear stretching. Extra stress tensor for Carreau fluid is

$$\bar{\tau}_{ij}=\eta_0\left[1+\frac{(n-1)}{2}(\Gamma\bar{\gamma})\bar{\gamma}_{ij}\right], \tag{1}$$

in which $\bar{\tau}_{ij}$ is the extra stress tensor, $\eta_0$ is the zero shear rate viscosity, $\Gamma$ is the time constant, $n$ is the power law index and $\bar{\gamma}$ is defined as

$$\bar{\gamma}=\sqrt{\frac{1}{2}\sum_i\sum_j\bar{\gamma}_{ij}\bar{\gamma}_{ji}}=\sqrt{\frac{1}{2}\Pi}, \tag{2}$$

where $\Pi$ is the second invariant strain tensor.

We assumed that the magnetic Reynolds number is small, so that the induced magnetic field is negligible. Under the assumption along with the Boussinesq and boundary layer approximations, the basic equations of the problem can be written as follows:

$$\frac{\partial u}{\partial x}+\frac{\partial v}{\partial y}=0, \tag{3}$$

$$u\frac{\partial u}{\partial x}+v\frac{\partial u}{\partial y}=\nu\frac{\partial^2 u}{\partial y^2}+\nu\frac{3(n-1)\Gamma^2}{2}\left(\frac{\partial u}{\partial x}\right)^2\frac{\partial^2 u}{\partial y^2}+\frac{\sigma}{B_0^2}(u_e-u)+u_e\frac{\partial u_e}{\partial x}, \tag{4}$$

$$u\frac{\partial T}{\partial x}+v\frac{\partial T}{\partial y}=\alpha\frac{\partial^2 T}{\partial y^2}, \tag{5}$$

where $u$ and $v$ are the velocity components along the $x-$ and $y-$axes, respectively, $T$ is the fluid temperature, $\nu$ is kinematic viscosity, $\sigma$ is the electrical conductivity and $\rho$ is the density. It is noticed that for power law index $n=1$ of the problem reduced to the case of Newtonian fluid while for $n>1$ phenomena remains for non-Newtonian fluid. In which $b>0$ is constant, we assume that $u_w(x)=ax$ and $u_e(x)=bx$ are the velocities near and away from the wall respectively.

The boundary conditions for Eqs. (3)-(5) are

$$u=u_w(x),\quad v=v_w(x),\quad T=T_w\ \text{ at } y=0$$

$$u \to u_e(x) = bx, \quad T \to T_\infty \text{ as } y \to \infty. \tag{6}$$

We introduce the following similarity transformations:

$$\eta = \left(\frac{b}{\upsilon}\right)^{1/2} y, \ \psi(x,y) = (b\upsilon)^{1/2} x f(\eta), \quad \theta(\eta) = \frac{T - T_\infty}{T_w - T_\infty}, \tag{7}$$

where $\eta$ is the similarity variable and $\psi$ is the stream function which is defined as $u = \partial\psi / \partial y$ and $v = -\partial\psi / \partial x$, hence Eq. (3) is satisfied.

Substituting Eq. (7) into Eqs. (4) and (5), we obtain the following similarity or ordinary nonlinear differential equations:

$$f''' - (f')^2 + ff'' + 1 + \frac{3(n-1)We^2}{2} f'''(f'')^2 + M^2(1 - f') = 0, \tag{8}$$

$$\frac{1}{\Pr}\theta'' + f\theta' = 0, \tag{9}$$

and the boundary conditions (6) reduced to

$$f(0) = s, \ f'(0) = \lambda, \ \theta(0) = 1,$$
$$f'(\infty) = 1, \ \theta(\infty) = 0, \tag{10}$$

where $s$ is the suction/injection parameter, $We^2 = \frac{b^3 x^2 \Gamma^2}{\nu}$ is the Weissenberg number, $M^2 = \frac{\sigma B_0^2}{\rho b}$ is the magnetic or Hartmann (1937) number, $\Pr = \frac{\nu}{\alpha}$ is the Prandtl number and $\lambda = \frac{a}{b}$ is the stretching or shrinking parameter. It is worth mentioning that $s = 0$ is impermeable case, $s > 0$ corresponds to suction case and $s < 0$ corresponds to injection case $\lambda > 0$ is the stretching case and $\lambda < 0$ is the shrinking case.

In this study, the physical quantities of interest are the skin friction coefficient $C_{fx}$ and also the local Nusselt number $Nu_x$, which are defined as

$$C_{fx} = \frac{\tau_w}{\rho u_e^2}, \ Nu_x = \frac{x q_w}{k(T_w - T_\infty)}, \tag{11}$$

where $\tau_w$ is the surface shear stress in the direction of $y$, while $q_w$ is the surface heat flux, which are given by:

$$\tau_w = \mu\left(\frac{\partial u}{\partial y}\right)_{y=0}, \ q_w = -k\left(\frac{\partial T}{\partial y}\right)_{y=0}, \tag{12}$$

with $\mu$ and $k$ being the dynamic viscosity and thermal conductivity of the fluid, respectively. Using Eq. (7), we obtain:

$$\sqrt{\mathrm{Re}}\, c_f = \left[ f''(0) + \frac{(n-1)We^2}{2} (f''(0))^3 \right], \quad -\theta'(0) = \mathrm{Re}^{-1/2}\, Nu, \tag{13}$$

where $\mathrm{Re}_x = \dfrac{u_e x}{\nu}$ is the Reynolds number.

## Results and Discussion

Equations (8)-(10) have been solved numerically using the shooting method built in Maple software, described by Meade et al. (1996). The results of the skin friction coefficient for stretching and shrinking sheets are compared with previously published results for validation purposes, as shown in Tables 1 and 2, respectively. The comparisons found to be in excellent agreement. Table 2 shows the numerical results for the first (upper branch) and second (lower branch) solutions of the problem. The dual solutions found to exist for a certain range of $\lambda$. The skin friction coefficient decreases with $\lambda$ for the first solution, however, it shows opposite effect for the second solution.

Table 1: Comparison of the values of the skin friction coefficient (with $M = 0$) for stretching sheet with different values of $\lambda$ when $n = 1, s = 0, We = 0$ and Pr = 0.72

| $\lambda$ | Present results | Akhbar et al. (2014) | Mahapatra & Nandy (2013) | Wang (2008) | Lok et al. (2006) |
|---|---|---|---|---|---|
| 0.0 | 1.2326 | 1.2326 | 1.2326 | 1.2326 | - |
| 0.1 | 1.1466 | 1.1466 | 1.1466 | 1.1466 | - |
| 0.2 | 1.0511 | 1.0511 | 1.0511 | 1.0511 | - |
| 0.5 | 0.7133 | 0.7133 | 0.7133 | 0.7133 | 0.7133 |
| 1.0 | - | 0 | 0 | 0 | - |
| 2.0 | –1.8873 | –1.8873 | –1.8873 | –1.8873 | –1.8873 |
| 5.0 | –10.2647 | –10.2647 | –10.2647 | –10.2647 | –10.2647 |

Table 2: Comparison of the values of coefficient of the skin friction (with $M = 0$) for shrinking sheet with different values of λ when $n = 1, s = 0, We = 0$ and Pr = 0.72

| $\lambda$ | Present results | | Akhbar et al. (2014) | | Mahapatra & Nandy (2013) | |
|---|---|---|---|---|---|---|
| | First solution | Second solution | First solution | Second solution | First solution | Second solution |
| -0.25 | 1.4022 | - | 1.4022 | - | 1.4022 | - |
| -0.50 | 1.4957 | - | 1.4956 | - | 1.14957 | - |
| -0.75 | 1.4893 | - | 1.4893 | - | 1.4893 | - |
| -1.15 | 1.0822 | 0.1167 | 1.0822 | 0.1167 | 1.0822 | 0.1167 |
| -1.20 | 0.9325 | 0.2336 | 0.9325 | 0.2336 | 0.9324 | 0.2336 |

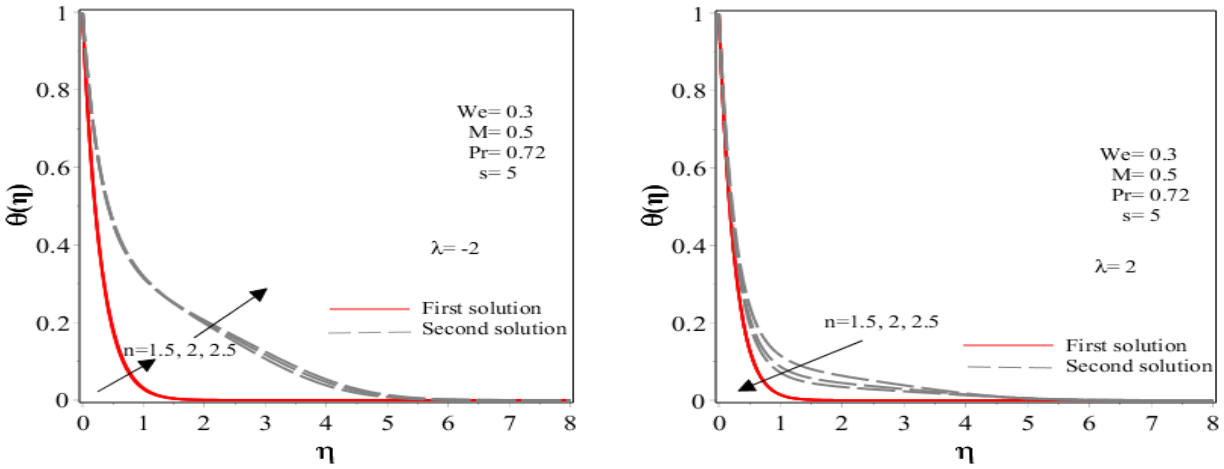


(a) (b)

Figure 1: Effects of power law index $n$ on temperature profile when (a) $\lambda = -2$ and (b) $\lambda = 2$

Figures 1(a) and (b) illustrate the effects of power law index, *n* on the temperature profile when $\lambda = -2$ (shrinking case) and $\lambda = 2$ (stretching case), respectively. Figures 1(a) and 1(b) show the dual profiles for both shrinking and stretching cases, thus admit the existence of the dual nature of solutions. From Fig. 1(a), when the sheet is shrunk, the temperature profiles increase with *n* for both solutions, however Fig. 1(b) shows opposite effect occurs for stretching case.

Figures 2 displays the temperature profiles for various values of *s* when other parameters are fixed. The temperature profiles for the first and second solutions decreases with suction parameter, *s*. Physically, suction increases the surface shear stress, hence it increases the temperature gradient. All the temperature profiles satisfy the boundary conditions (10).

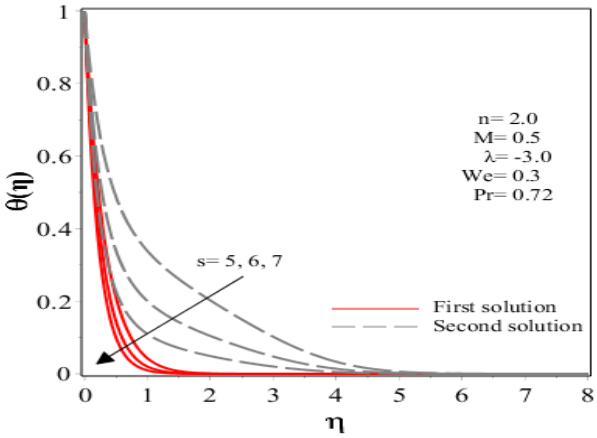


Figure 2: Effects of suction parameter *s* on temperature profile when $\lambda = -3$

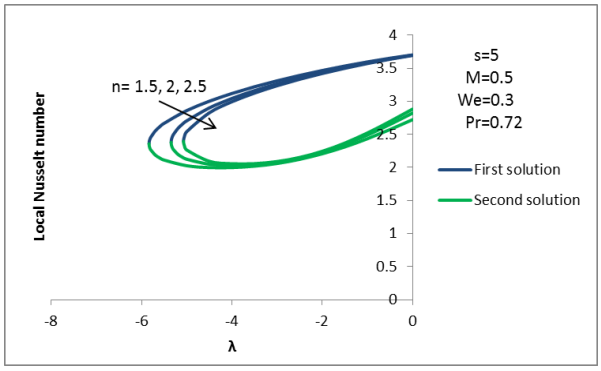


Figure 3: Variation of the local Nusselt number with $n$ and $\lambda$

Figure 3 shows the effects of $n$ and $\lambda$ on the local Nusselt number. Both the first solution and second solution show decreasing behavior for increasing values of power law index $n$. It is seen from Fig. 4 that there exist dual solutions for $\lambda_c < \lambda < 0$, where $\lambda_c$ is the critical value (turning point). No solution is found for $\lambda > |\lambda_c|$, therefore at $\lambda = \lambda_c$, boundary layer starts to separate from the surface. It is found that $\lambda_c$ is reduces with $n$, where for $n =$ 1.5, 2 and 2.5 the critical values $\lambda_c$ are –5.8348, –5.3459 and –5.0711, respectively. Thus, larger values of power law index enhance the boundary layer separation because the shear-thickening fluids increase in apparent viscosity at higher shear rates.

Figure 4 illustrates the effects of $s$ and $\lambda$ on the local Nusselt number, and dual solutions are also exist. The critical values for different values of suction parameter, $s =$ 5, 6 and 7 are –5.3459, –6.1763 and –6.9895, respectively. Thus, this shows that the suction parameter delays the boundary layer separation. As the values of the suction parameter, $s$ increase, a further increases in the local Nusselt number for both first and second solutions due to decreases in the temperature gradient at the plate surface.

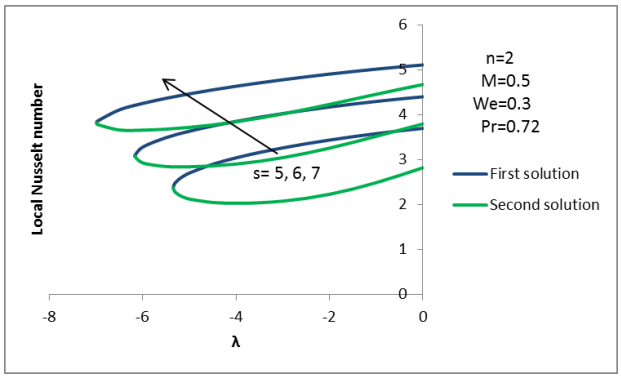


Figure 4: Variation of the local Nusselt number with $s$ and $\lambda$

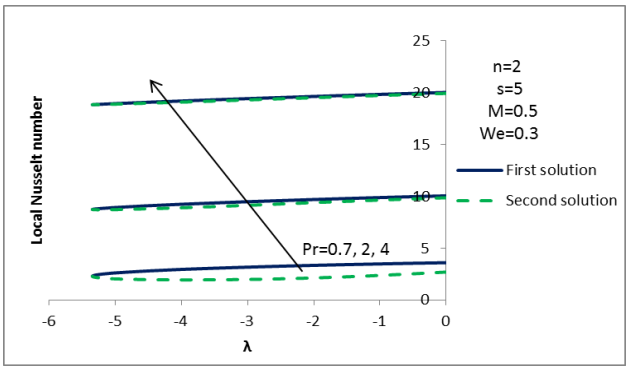


Figure 5: Variation of the local Nusselt number with λ and Pr

The effects of the Prandtl number, Pr and $\lambda$ on the local Nusselt number are shown in Figure 5, where the local Nusselt number increases when the value of Pr and $\lambda$ increases. Figure 5 also displays the dual solutions, with the critical value for all Pr = 0.7, 2 and 4 occurs at the same value, namely, $\lambda_c = -5.3459$..

## Conclusion

A numerical study is performed for the problem of stagnation-point flow and heat transfer of Carreau fluid toward a permeable sheet with the presence of magnetic field. For heat transfer characteristics, it is found that dual solutions exist. It is also observed that the power law index enhances the boundary layer separation, however the suction parameter delays the boundary layer separation. The boundary layer separation occurs at the same turning point for various values of Prandtl number.

## Acknowledgement

The authors gratefully acknowledge the financial support received in the form of a fundamental research grant (FRGS) from the Ministry of Higher Education, Malaysia.

## References

Akhbar, N.S. and Nadeem, S. 2014. Carreau fluid model for blood flow through a tapered artery with a stenosis. *Ain Shams Eng. J*. 5:1307–1316.

Akhbar, N.S., Nadeem, S., Rizwan Ul Haq and Shiwei, Y. 2014. MHD stagnation point flow of Carreau fluid toward a permeable shrinking sheet: Dual solutions. *Ain Shams Eng. J*. 5:1233-1239.

Ali, F.M., Nazar, R., Arifin, N.M. & Pop, I. 2011. MHD mixed convection boundary layer flow towards a stagnation point on a vertical surface with induced magnetic field. *ASME J. Heat Transf.* 133(2): 022502-1 – 022502-6.

Ali, F.M., Nazar, R., Arifin, N.M. & Pop, I. 2014. Mixed convection stagnation-point flow on a vertical stretching sheet with external magnetic field. *Appl. Math. Mech.* 35(2):155-166

Hartmann, J. (1937), Theory of the laminar flow of an electrically conducting liquid in a homogeneous magnetic field, *Mat. Fys. Medd. K. Dan. Vidensk. Selsk*., 15:1-28.

Hiemenz K. 1911. Die Grenzschicht an einem in den gleichfo¨ rmigen Flu¨ essigkeitsstrom eingetauchten geraden Kreiszylinder. Ding Polym J;321.

Ishak, A., Nazar, R., and Pop, I. (2008), Magnetohydrodynamic (MHD) flow of a micropolar fluid towards a stagnation point on a vertical surface, *Comp. Math. Appl*., 56:3188-3194.

Kumari, M. and Nath, G. 2009. Steady mixed convection stagnation-point flow of upper convected Maxwell fluids with magnetic field. *Int. J. Non-Linear Mech*. 44:1048-1055.

Lok, Y.Y., Amin, N and Pop, I. 2006. Non-orthogonal stagnation point flow towards a stretching sheet. *Int. J. Non-Linear Mech*. 41:622-627.

Mahapatra, T.R. and Nandy. 2013. Stability of dual solutions in stagnation point flow and heat transfer over a porous shrinking sheet with thermal radiation. *Meccanica.* 48:23–32.

Meade, D.B., Haran, B.S., and White, R. E. 1996. The Shooting technique for the solution two-point boundary value problems. *Maple Tech*. 3:85–93.

Nazar, R., Amin, N., Filip, D. and Pop, I. 2004. Unsteady boundary layer flow in the region of the stagnation-point on a stretching sheet*. Int. J. Eng. Sci*. 42:1241–1253.

Sadeghy, K., Hajibeygib, H., Taghavi, S.M. 2006. Stagnation-point flow of upper-convected Maxwell fluids. *Int. J. Non-Linear Mech*. 41:1242-1247.

Wang, C.Y. 2008. Stagnation flow towards a shrinking sheet. *Int. J. Non-Linear Mech*. 43:377-382.